Anisotropic flow and correlations at the MPD experiment

P. Parfenov (JINR, NRNU MEPhI) for the MPD Collaboration

XXXVI International Workshop on High Energy Physics
“Strong Interactions: Experiment, Theory, Phenomenology
23-25 July 2024

The work has been supported by the Ministry of Science and Higher Education of the Russian Federation, Project "Fundamental and applied research at the NICA megascience experimental complex" № FSWU-2024-0024

Relativistic heavy-ion collisions

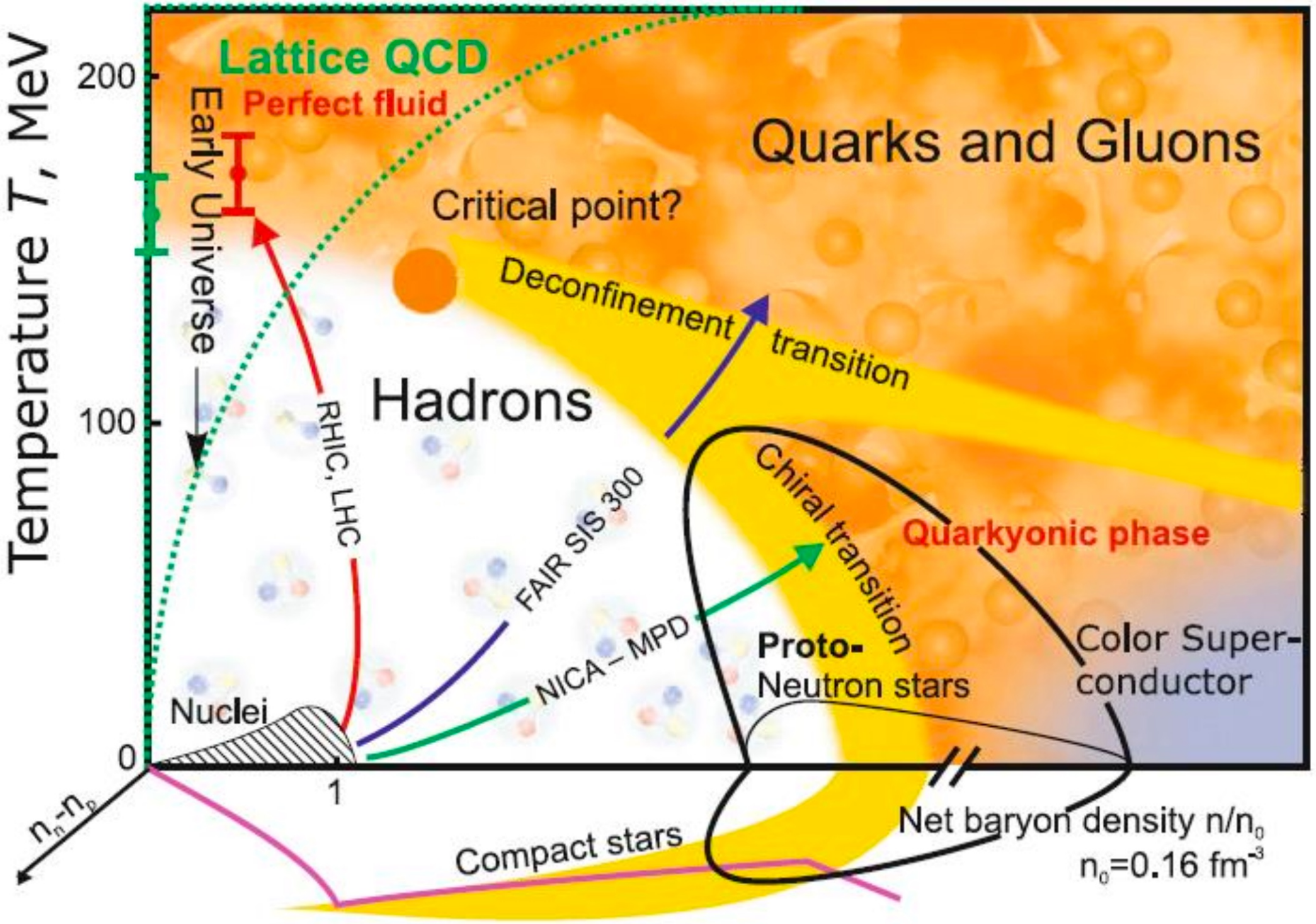

Relativistic heavy-ion collisions allows us to study QCD phase diagram

➢ **High beam energies ($\sqrt{s_{NN}} > 100\ GeV$):**

- High T, $\mu_B \approx 0$
- Evolution of the early Universe

➢ **Low beam energies ($\sqrt{s_{NN}} \sim 10\ GeV$):**

- Intermediate T, high μ_B
- Inner study of the compact stars

MPD and BM@N will study QCD matter at extreme μ_B

Several future (CBM) and ongoing (NA61/SHINE, STAR) experiments cover the same beam energy range

EOS for high baryon density matter

The binding energy per nucleon: $E_A(\rho,\delta) = \boxed{E_A(\rho,0)} + \boxed{E_{sym}(\rho)}\delta^2 + O(\delta^4)$

Isospin asymmetry:

$\delta = (\rho_n - \rho_p)/\rho$

Symmetric matter

Symmetry energy

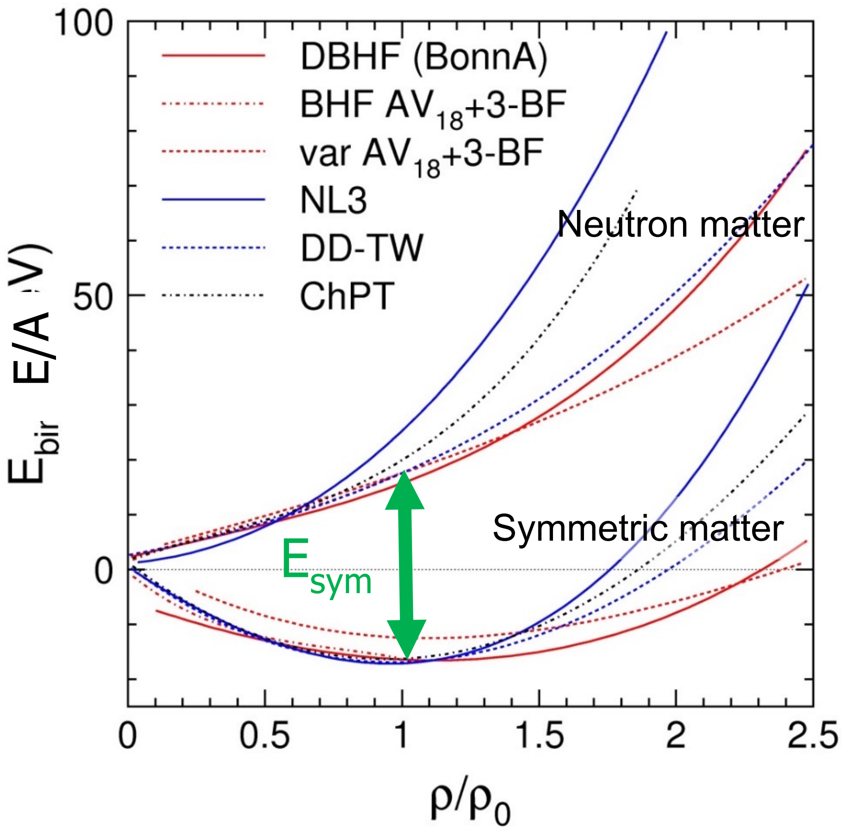

Ch. Fuchs and H.H. Wolter, EPJA 30 (2006) 5

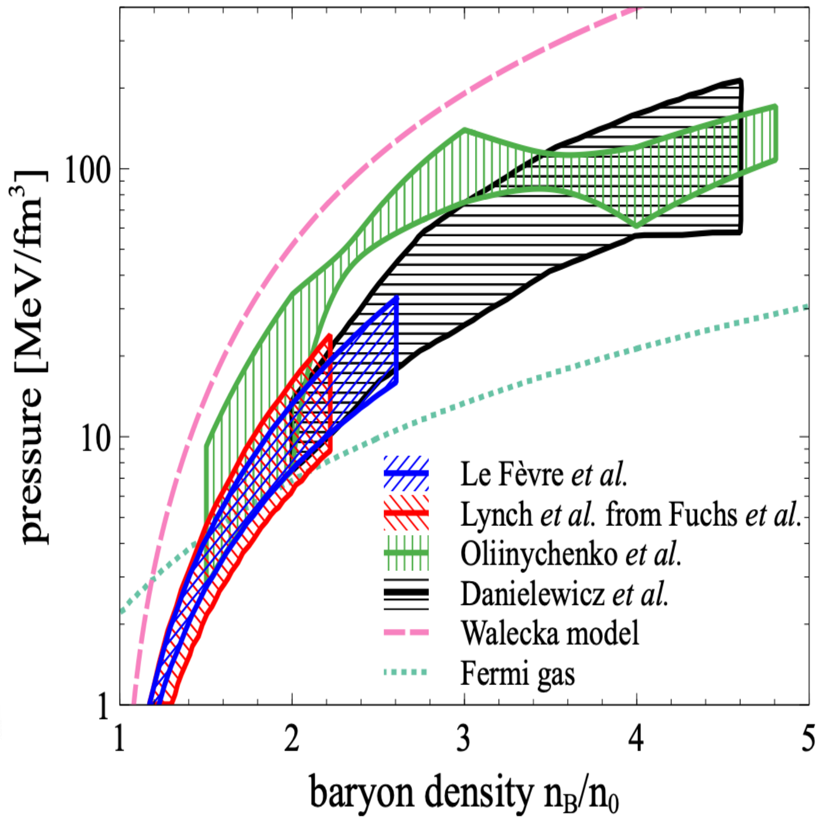

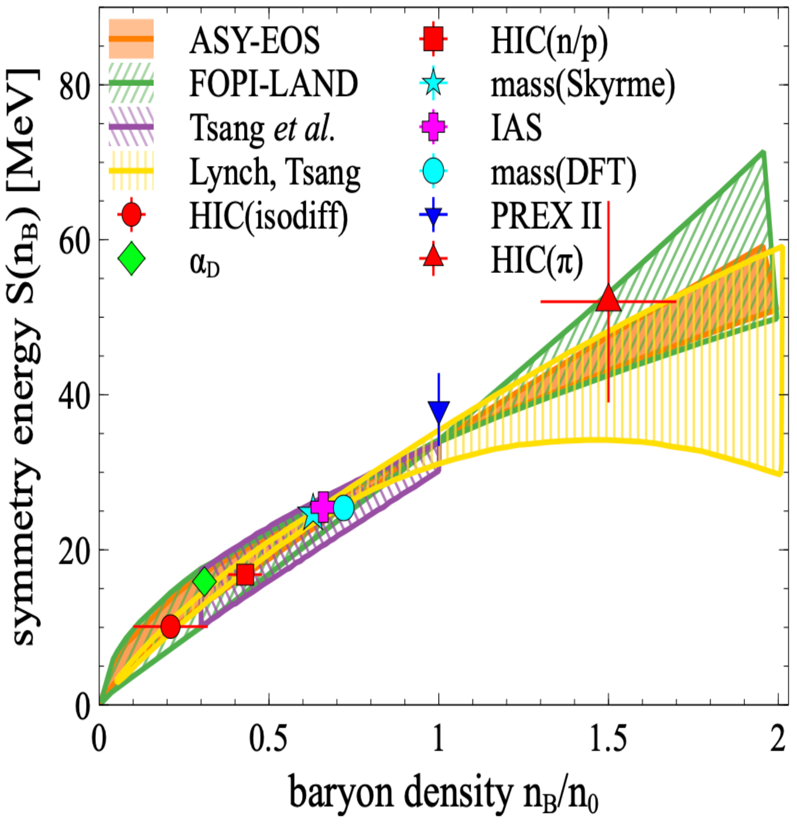

A. Sorensen et. al., Prog.Part.Nucl.Phys. 134 (2024) 104080

New data is needed to further constrain transport models with hadronic d.o.f.

Anisotropic flow

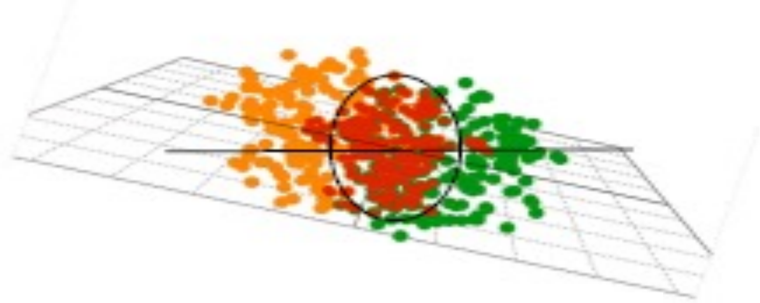

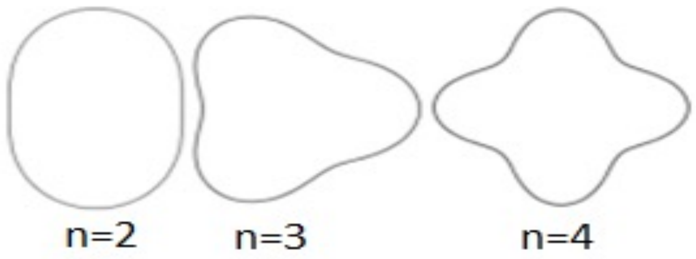

$$\epsilon_n = \sqrt{\frac{\langle r^n \cos n\phi \rangle + \langle r^n \sin n\phi \rangle}{\langle r^n \rangle}}$$

$$\frac{dN}{d\phi} \propto \left(1 + 2\sum_{n=1} v_n \cos\left[n\left(\phi - \Psi_n\right)\right]\right)$$

$$v_n = \langle \cos[n(\phi - \Psi_{RP})] \rangle$$

Initial eccentricity (and its attendant fluctuations) ε_n drive momentum anisotropy v_n with specific viscous modulation

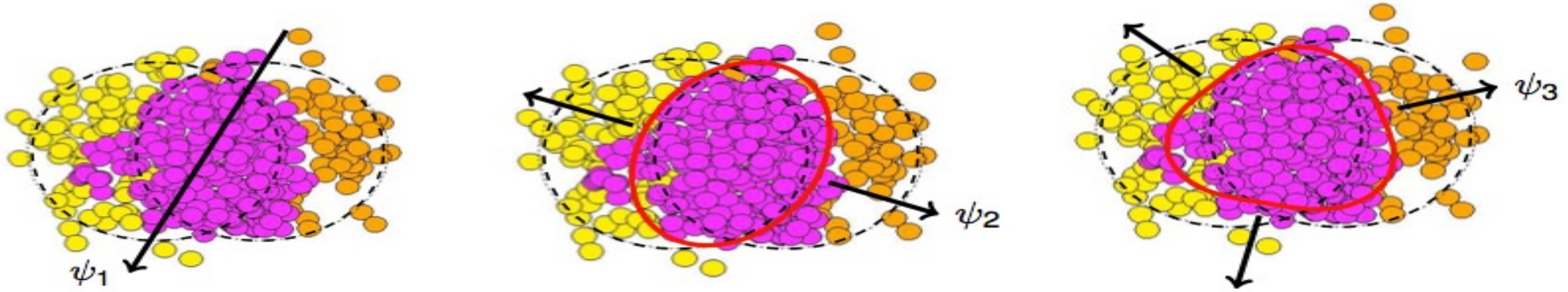

v_2 - elliptic flow

v_3 - triangular flow

Anisotropic flow at LHC/RHIC

Gale, Jeon, et al., Phys. Rev. Lett. 110, 012302

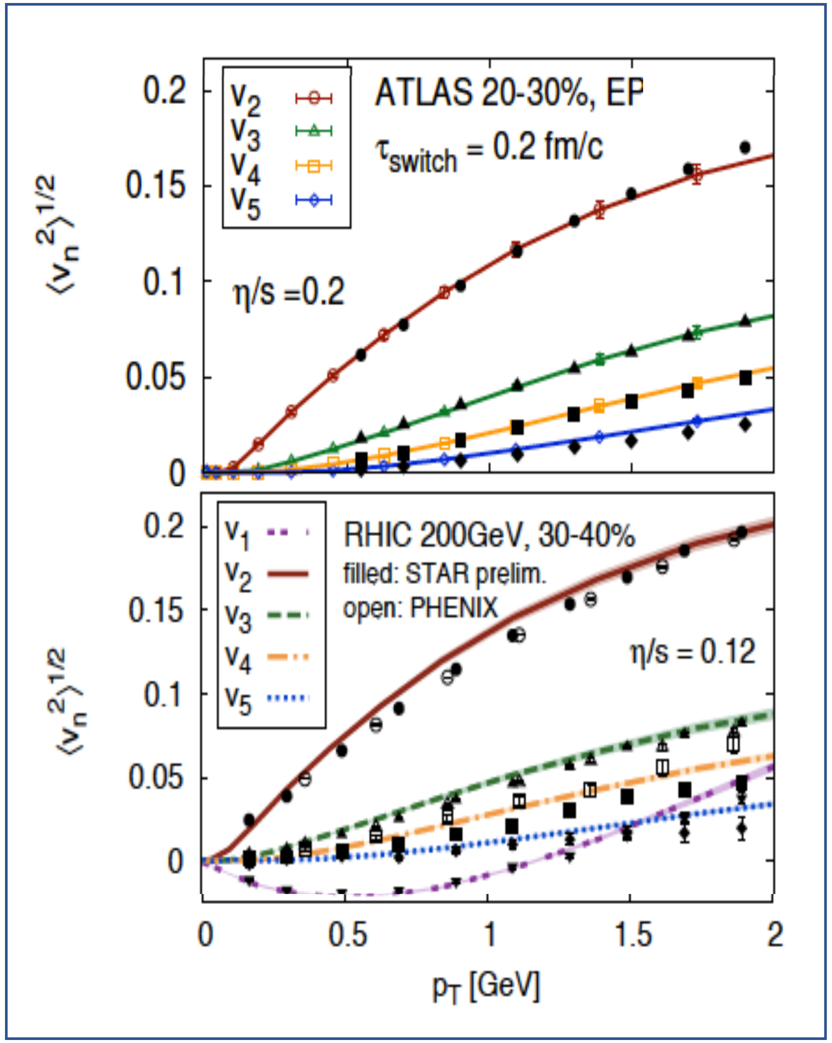

STAR PRL118 (2017) 212301

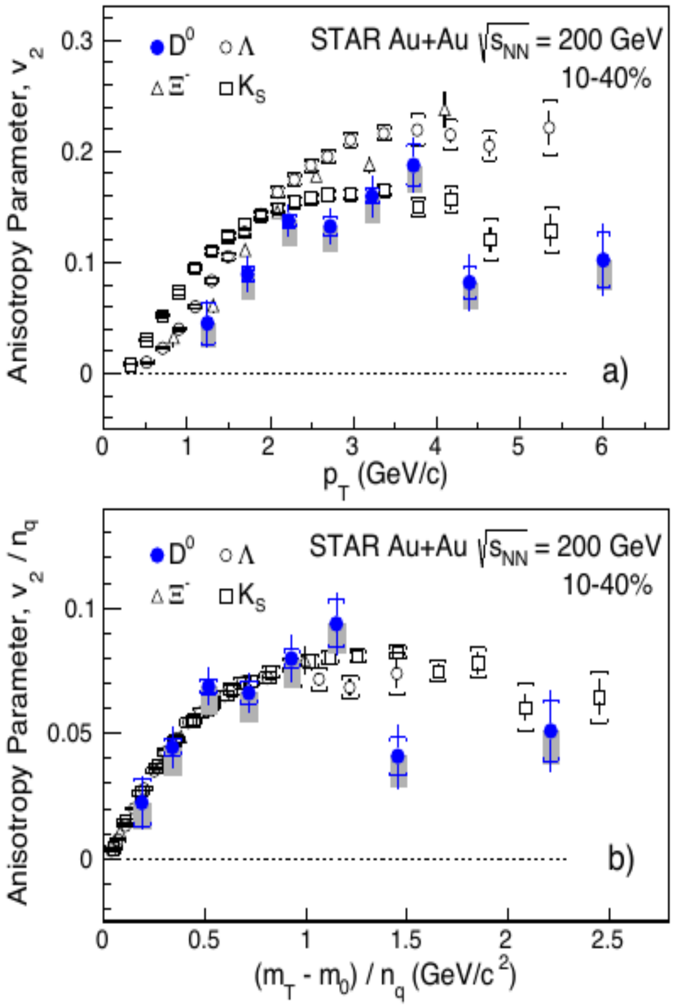

$v_n(p_T, \textbf{Centrality})$ - sensitive to the early stages of the collision

Important constrain for transport properties and EOS (η/s, ζ/s, etc.)

v_n of identified hadrons:

- **Mass ordering at p_T<2 GeV/c** (hydrodynamic flow, hadron rescattering)
- **Baryon/meson grouping at p_T>2 GeV/c** (recombination/coalescence) Number of constituent quark (NCQ) scaling

Hybrid models for anisotropic flow at RHIC/LHC

1. UrQMD + 3D viscous hydro model vHLLE+UrQMD

Iurii Karpenko, Comput. Phys. Commun. 185 (2014), 3016
https://github.com/yukarpenko/vhlle
Parameters: from Iu. A. Karpenko, P. Huovinen, H. Petersen, M. Bleicher, Phys. Rev. C91 (2015) no.6, 064901 – good description of STAR BES results for v_2 of inclusive charged hadrons (7.7-62.4 GeV)

Initial conditions: model UrQMD
QGP phase: 3D viscous hydro (vHLLE) with crossover EOS (XPT)
Hadronic phase: model UrQMD

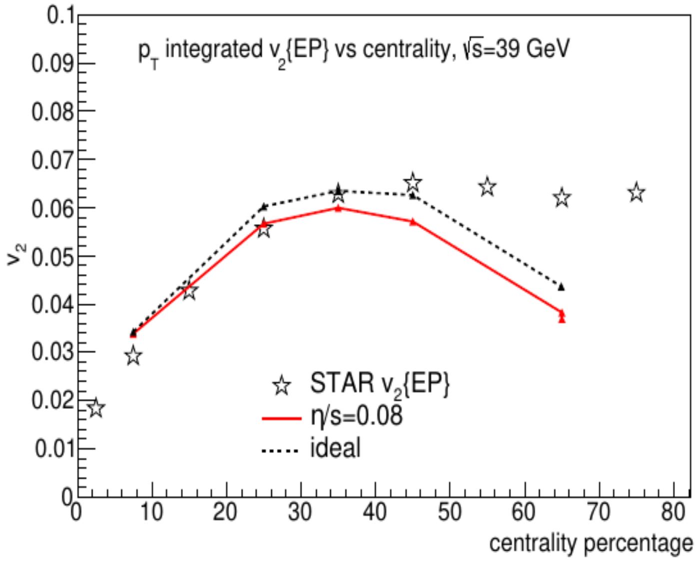

2. A Multi-Phase Transport model (AMPT) for high-energy nuclear collisions

The main source code (Zi-Wei Lin):
https://myweb.ecu.edu/linz/ampt/v1.26t9b/v2.26t9b

Initial conditions: model HIJING
QGP phase: Zhang's parton cascade for modeling partonic scatterings
Hadronic phase: model ART

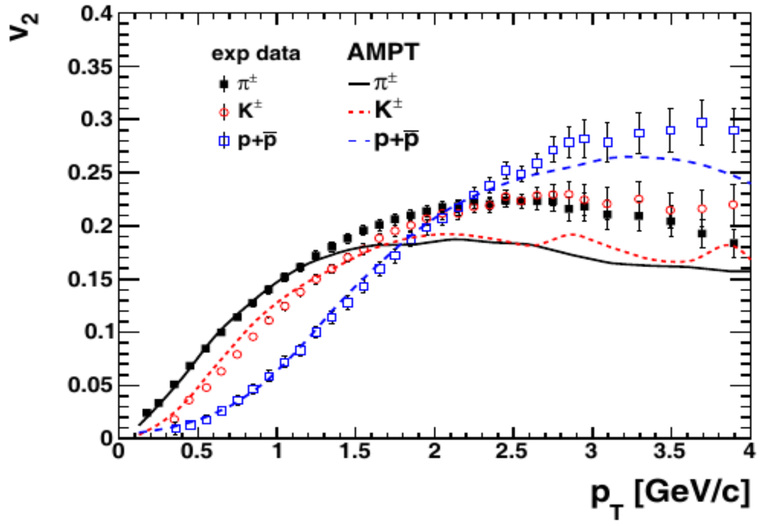

Z.W. Lin, C. M. Ko, B.A. Li, B. Zhang and S. Pal: Physical Review C 72, 064901 (2005).

vHLLE+UrQMD: Elliptic and triangular flow in Au+Au collisions at 200 GeV

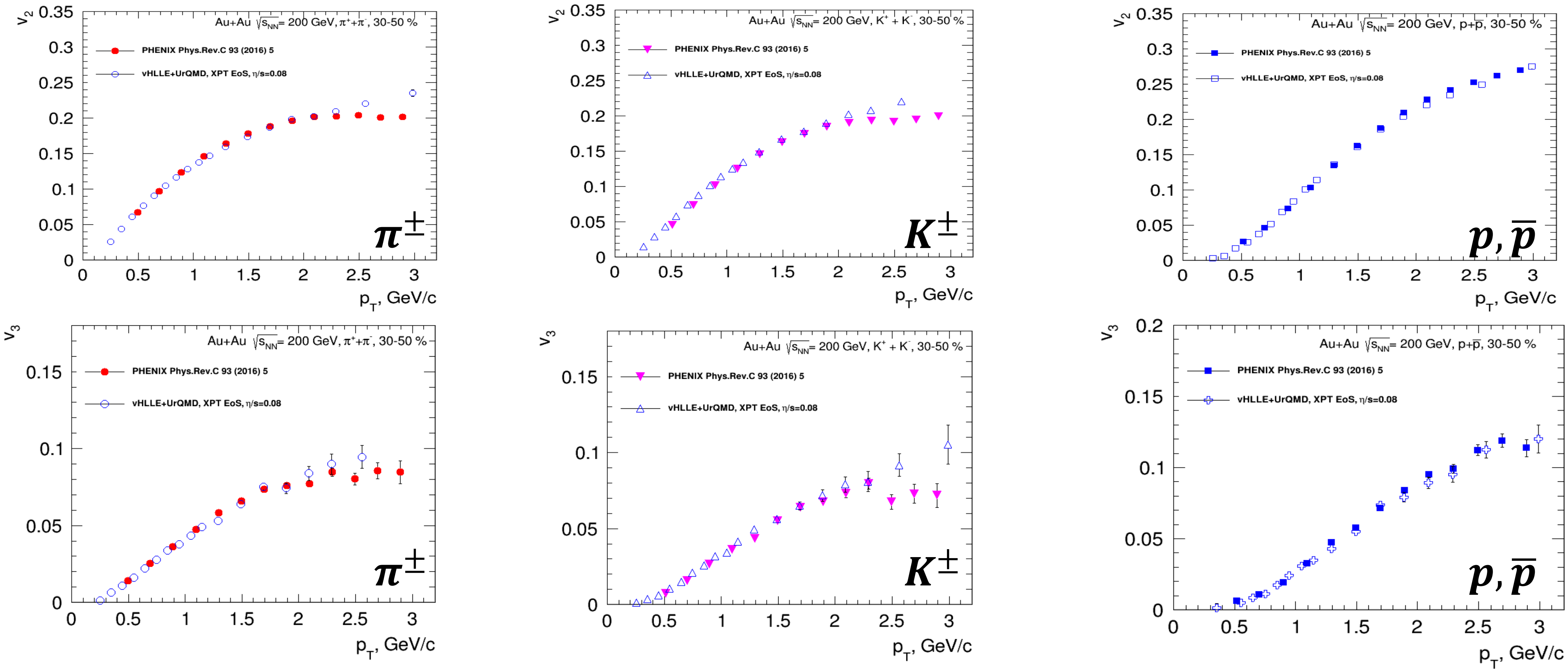

3D hydro model vHHLE + UrQMD (XPT EOS), $\eta/s = 0.08$ + param from Iu.A. Karpenko, P. Huovinen, H. Petersen, M. Bleicher , Phys.Rev. C91 (2015) no.6, 064901

Reasonable agreement between results of vHLLE+UrQMD model and published PHENIX data

Elliptic flow at NICA energies: Models vs. Data comparison

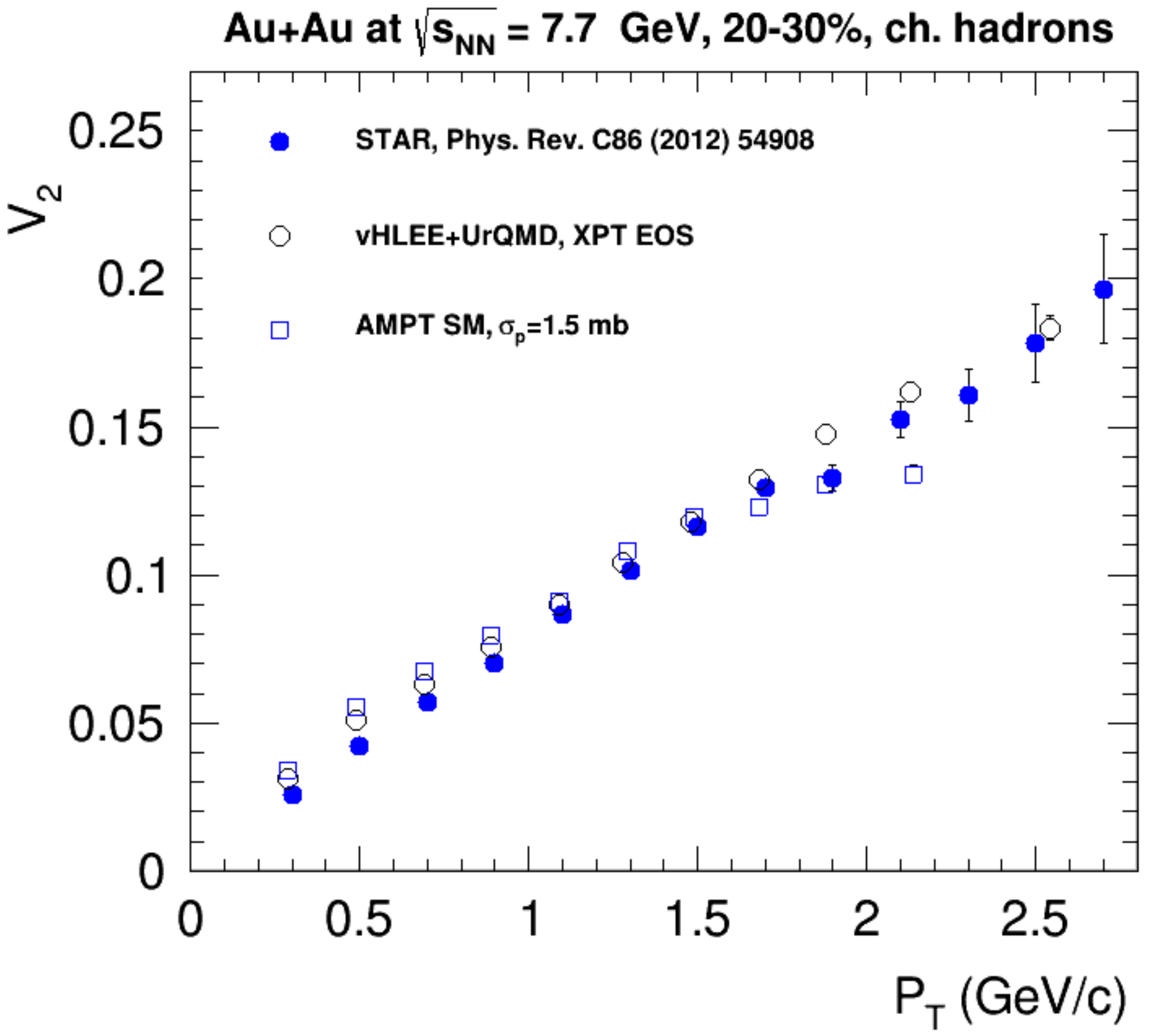

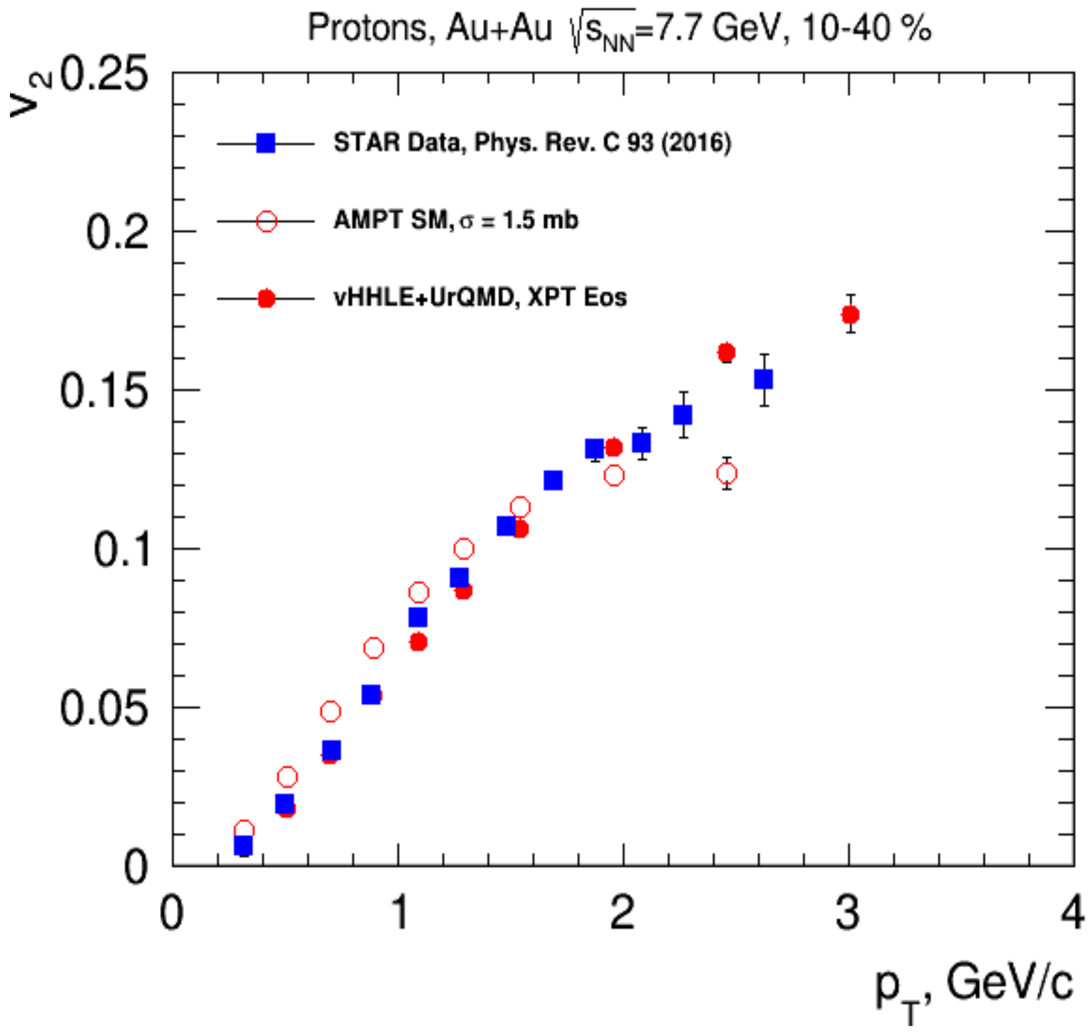

Good agreement between vHLLE+UrQMD ($\eta/s = 0.2$, XPT EOS), AMPT models and STAR data for $\sqrt{s_{NN}} \geq$7.7 GeV

Elliptic flow at NICA energies: Models vs. Data comparison

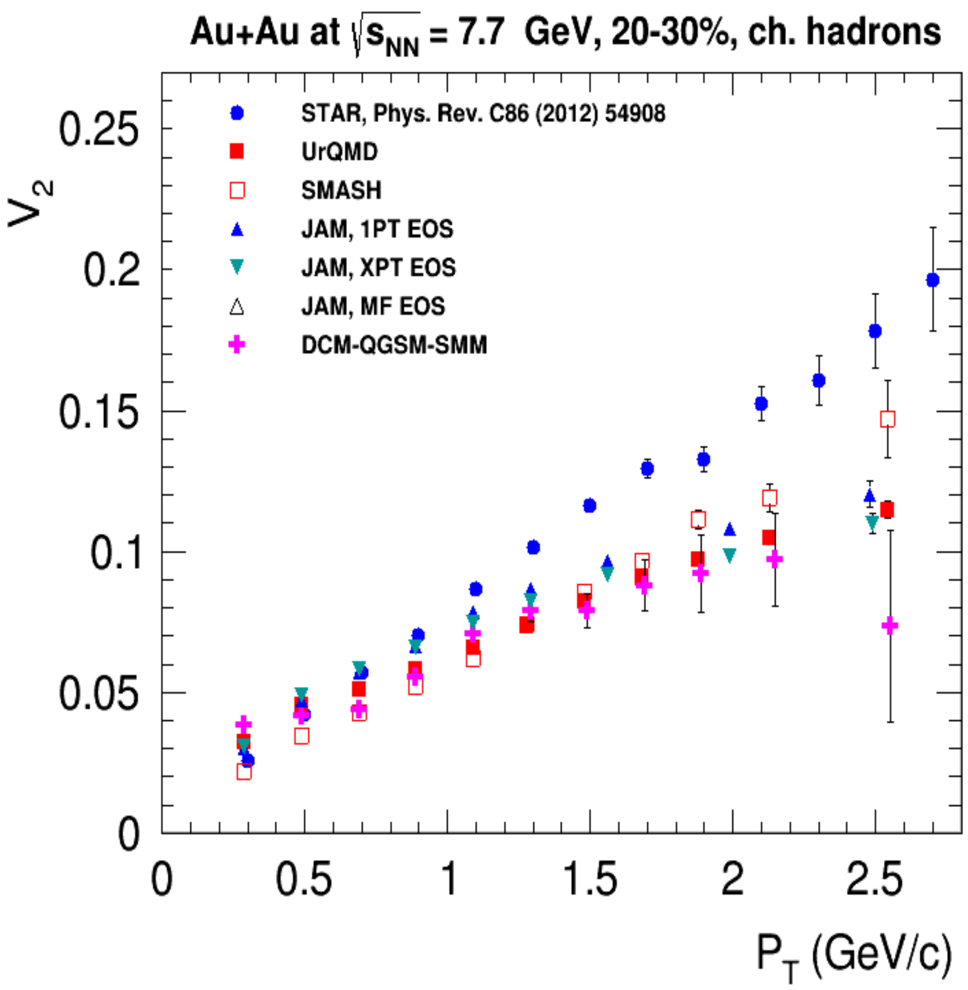

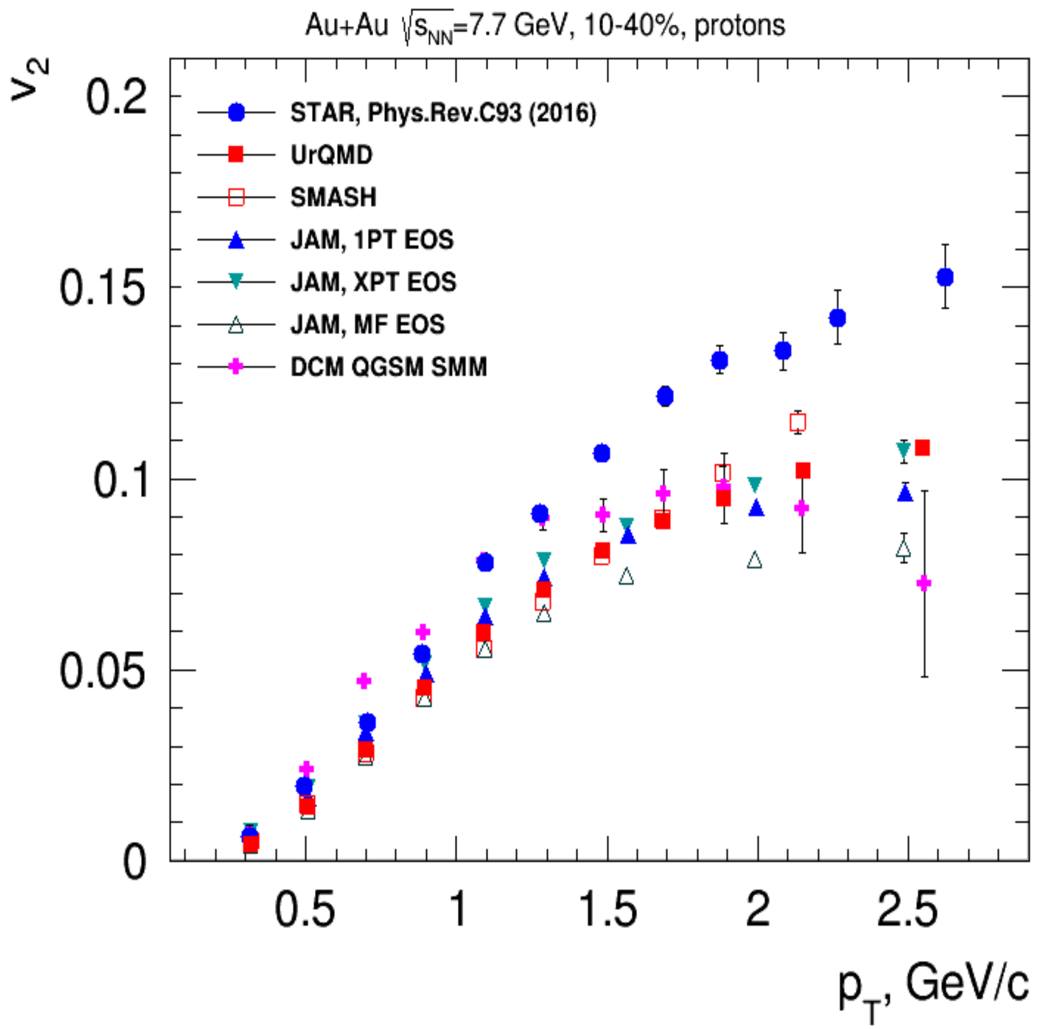

Pure String/Hadronic Cascade models give smaller v_2 signal compared to STAR data for $\sqrt{s_{NN}}$ ≥7.7 GeV

$v_{1,2}(y)$ in Au+Au $\sqrt{s_{NN}}$=3 GeV: model vs. STAR data

A. Sorensen et. al., Prog.Part.Nucl.Phys. 134 (2024) 104080

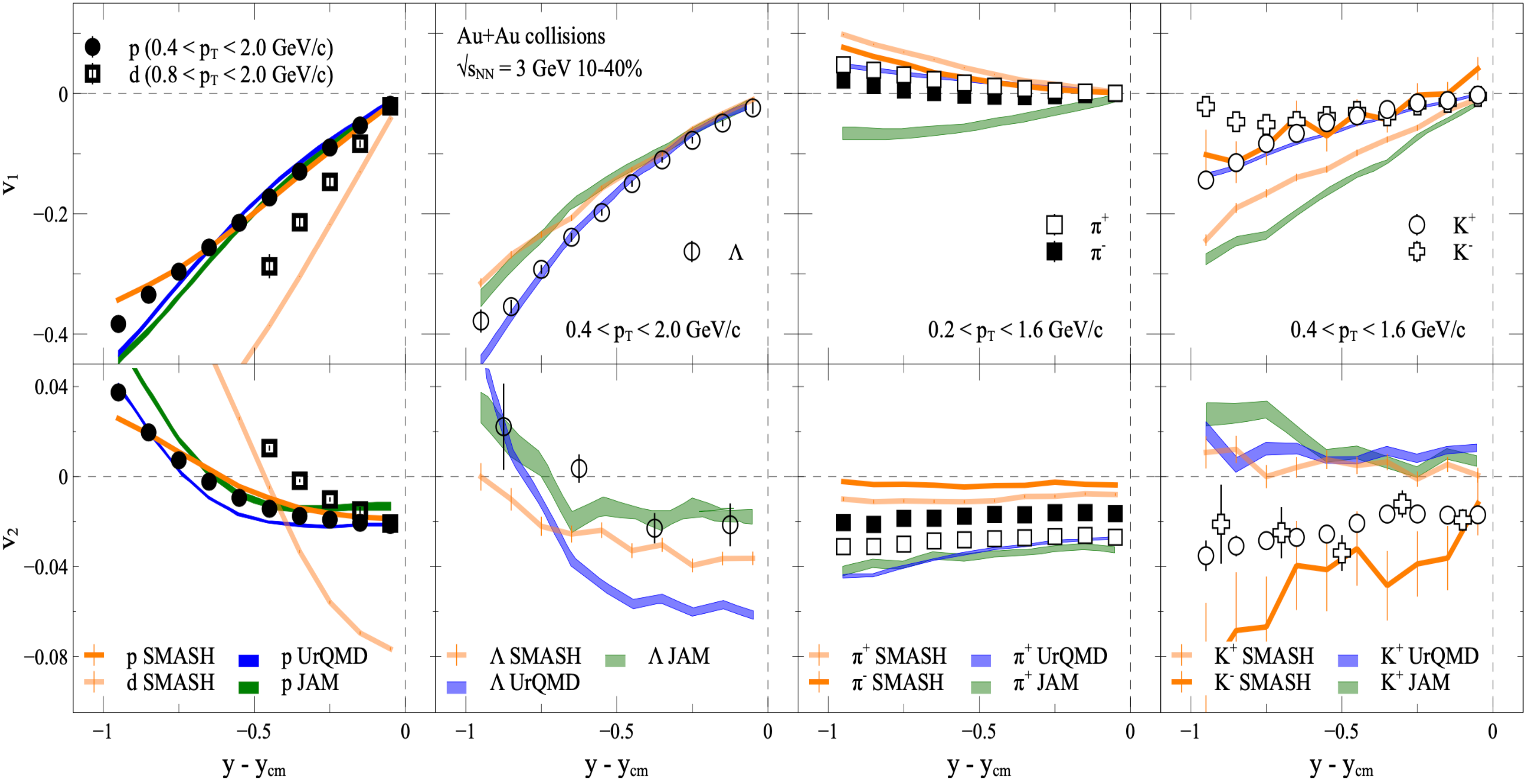

Model description of v_n:

- Good overall agreement for v_n of protons
- v_n of light nuclei is not described
- v_n of Λ is not well described
  - **nucleon-hyperon** and **hyperon-hyperon** interactions
- Light mesons (π,K) are not described
  - No mean-field for mesons

Models have a huge room for improvement in terms of describing v_n

Why do we need new measurements at BM@N and MPD?

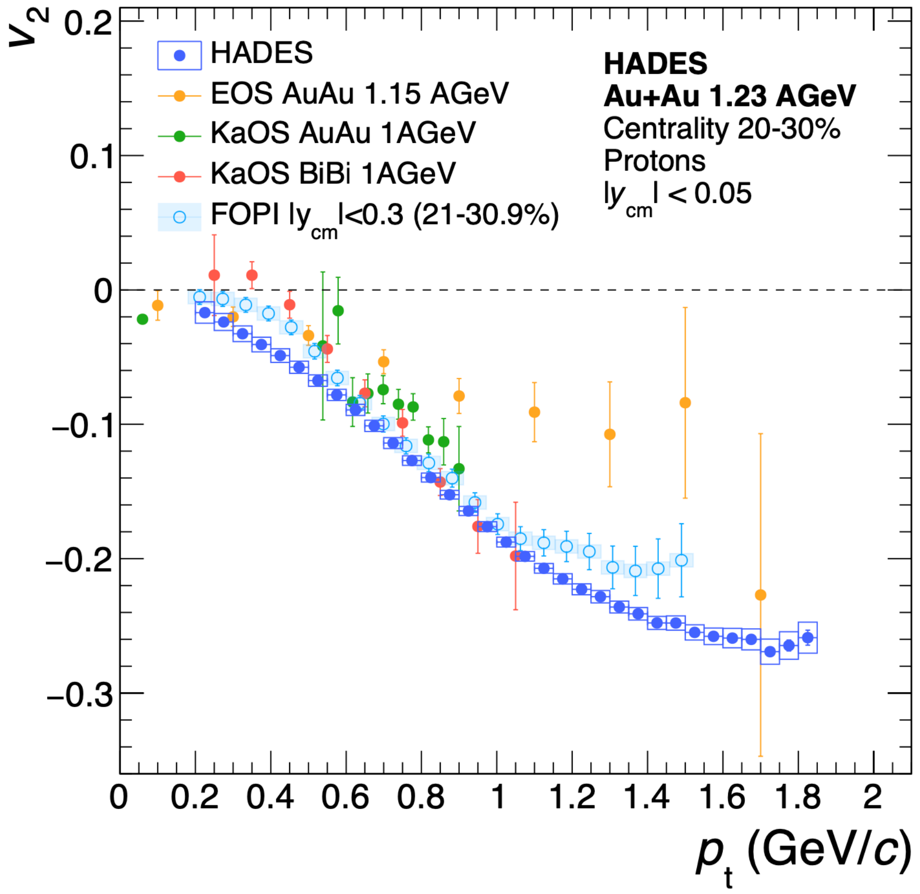

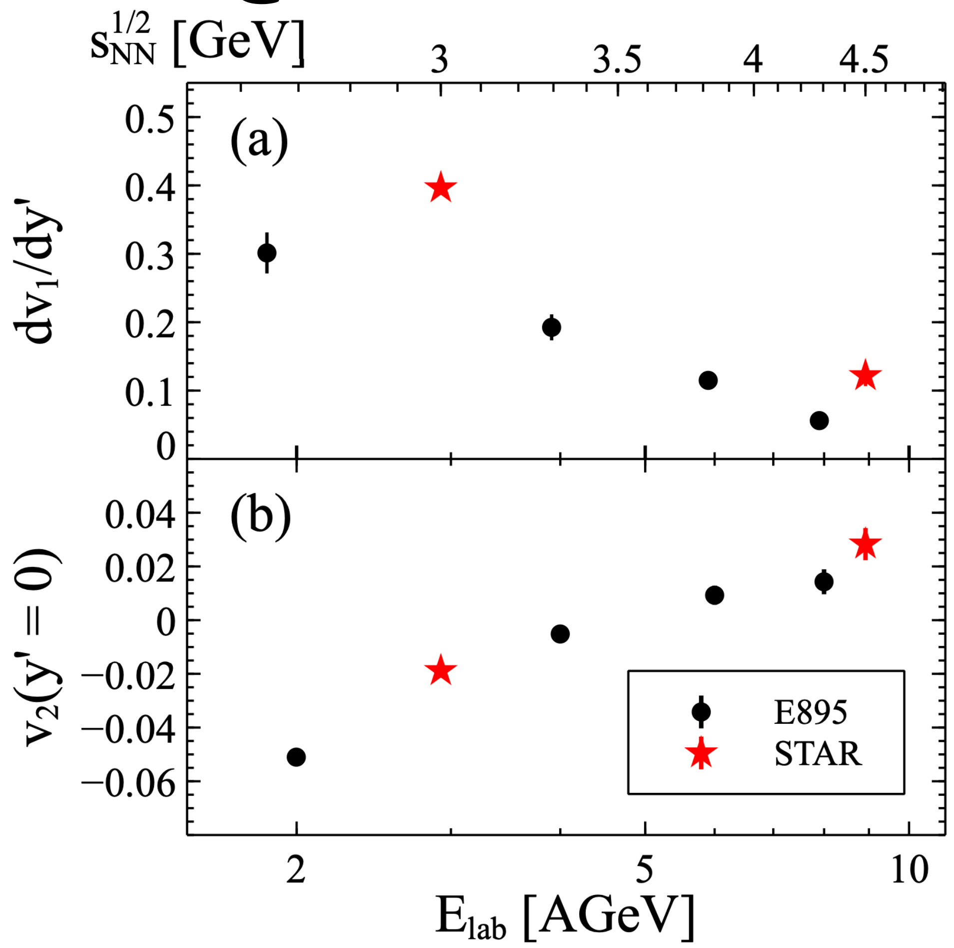

- The main source of existing systematic errors in v_n measurements is the difference between results from different experiments (for example, FOPI and HADES, E895 and STAR)
- New data from the future BM@N ($\sqrt{s_{NN}}$=2.3-3.3 GeV) and MPD ($\sqrt{s_{NN}}$=4-11 GeV) experiments will provide more detailed and robust v_n measurements

Sensitivity of the collective flow to the EOS

P. Danielewicz, R. Lacey, W.G. Lynch, Science 298 (2002) 1592

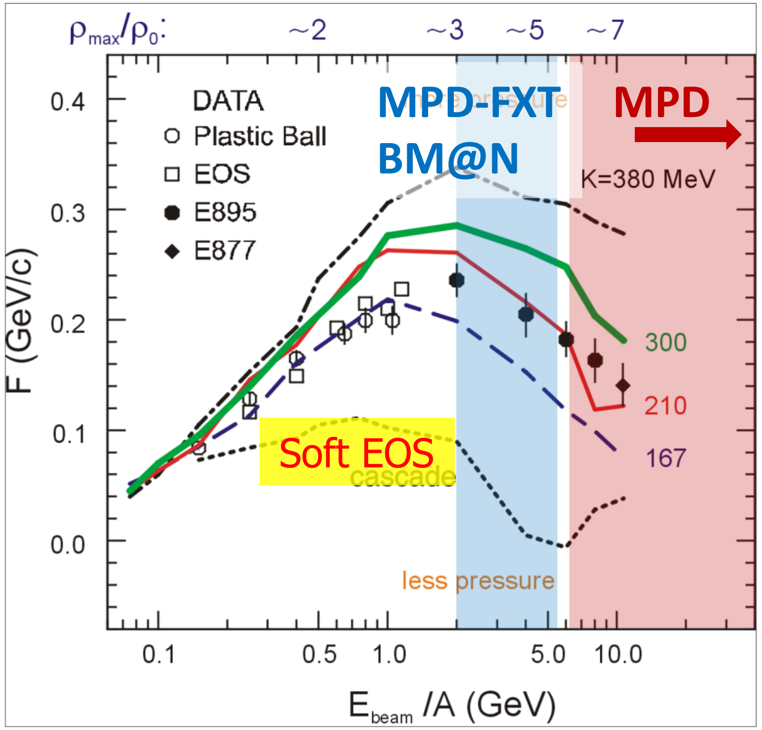

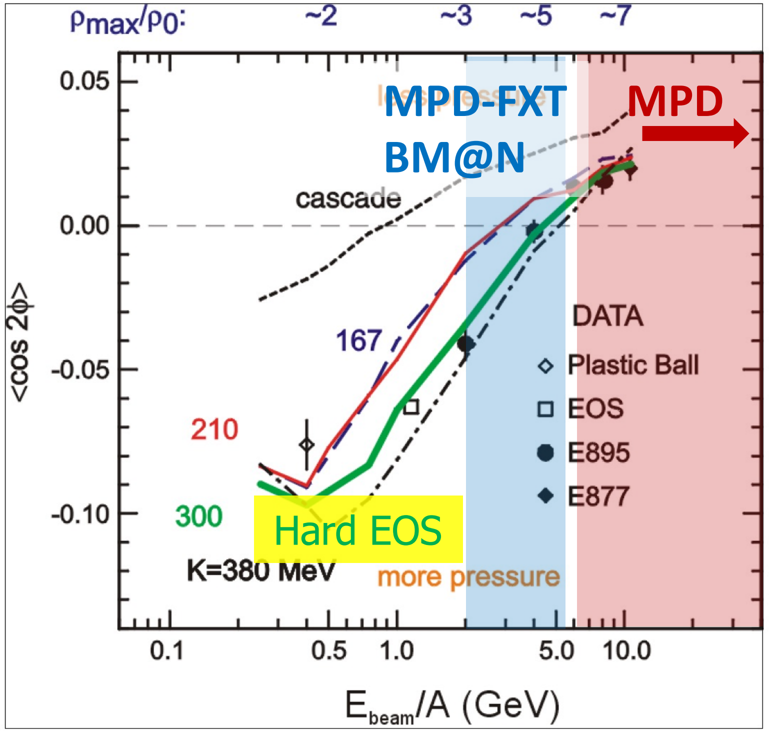

$$F = \frac{d\langle p_x/A\rangle}{d(y/y_{cm})}\bigg|_{y/y_{cm}=1}$$

$$v_2 \equiv \langle \cos(2(\varphi - \Psi_{RP}))\rangle$$

EoS extraction: define incompressibility

$$K_0 = 9\rho^2 \frac{\partial^2(E_A)}{\partial\rho^2}$$

Discrepancy in the interpretation:

- v_1 suggests soft EoS (K_0≈210 MeV)
- v_2 suggests hard EoS (K_0≈380 MeV)

New measurements using new data and modern analysis techniques might address this discrepancy

Additional measurements are essential to clarify the previous results

Global hyperon polarization

- w.r.t. reaction plane (RP)
- Emerges in HIC due to the system angular momentum
- Measured through the weak decay:

$$\frac{\mathrm{d}N}{\mathrm{d}\cos\theta^*} = \frac{1}{2}(1 + \alpha_\mathrm{H}|\vec{P}_\mathrm{H}|\cos\theta^*)$$

- * — denotes hyperon rest frame
- θ^* — angle between the decay particle(proton) and polarization direction
- $\alpha_\Lambda \simeq -\alpha_{\bar{\Lambda}} \simeq 0.732$ - hyperon decay constant

$$\Lambda \to p + \pi^-$$

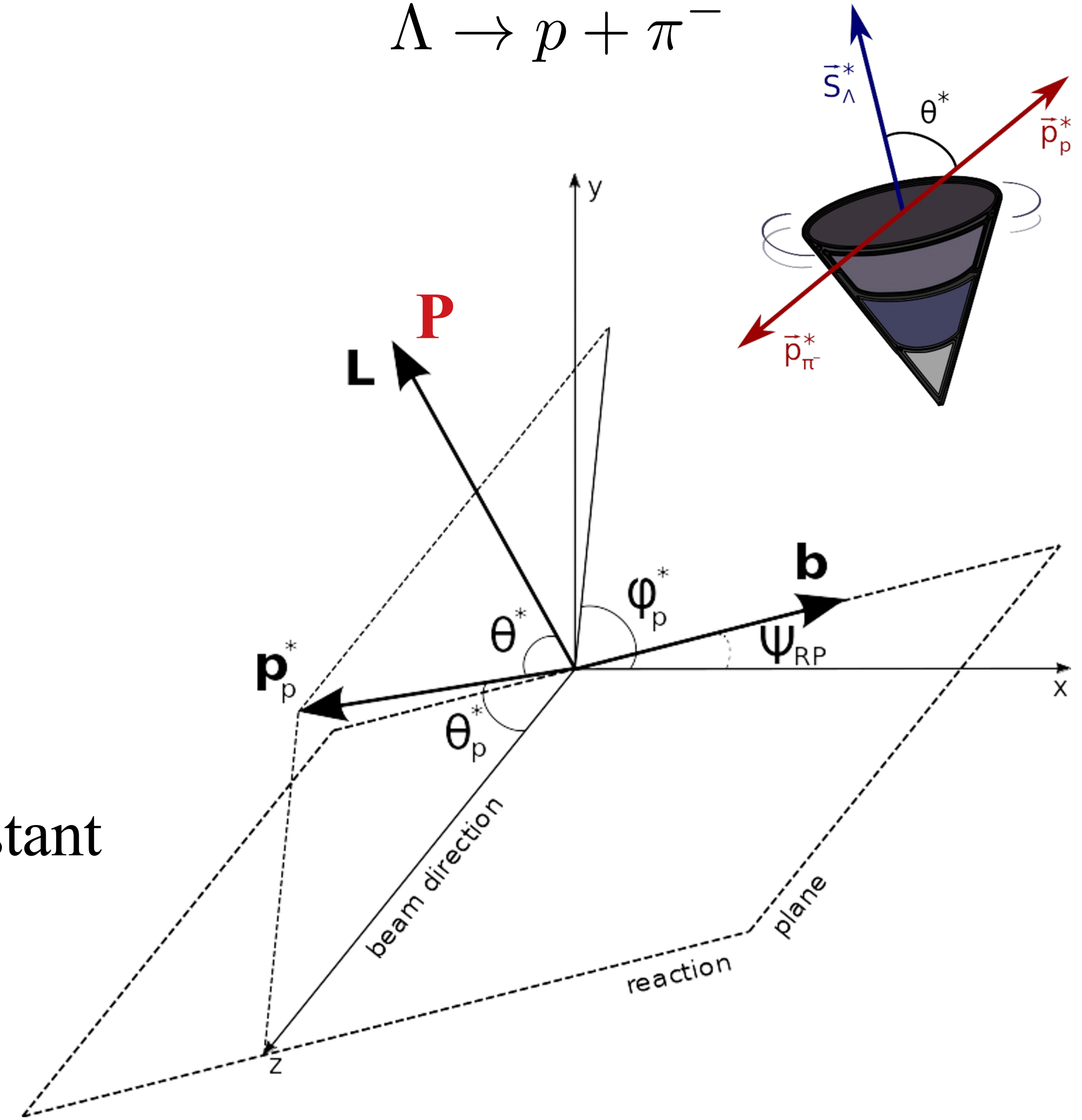

Global Polarization at Nuclotron-NICA energies

- Predicted and observed global polarization signals rise as the collision energy is reduced:

  NICA energy range will provide new insight

- $\Lambda(\bar{\Lambda})$ - splitting of global polarization
- Comparison of models, detailed study of energy and kinematical dependences, improving precision
- Probing the vortical structure using various observables

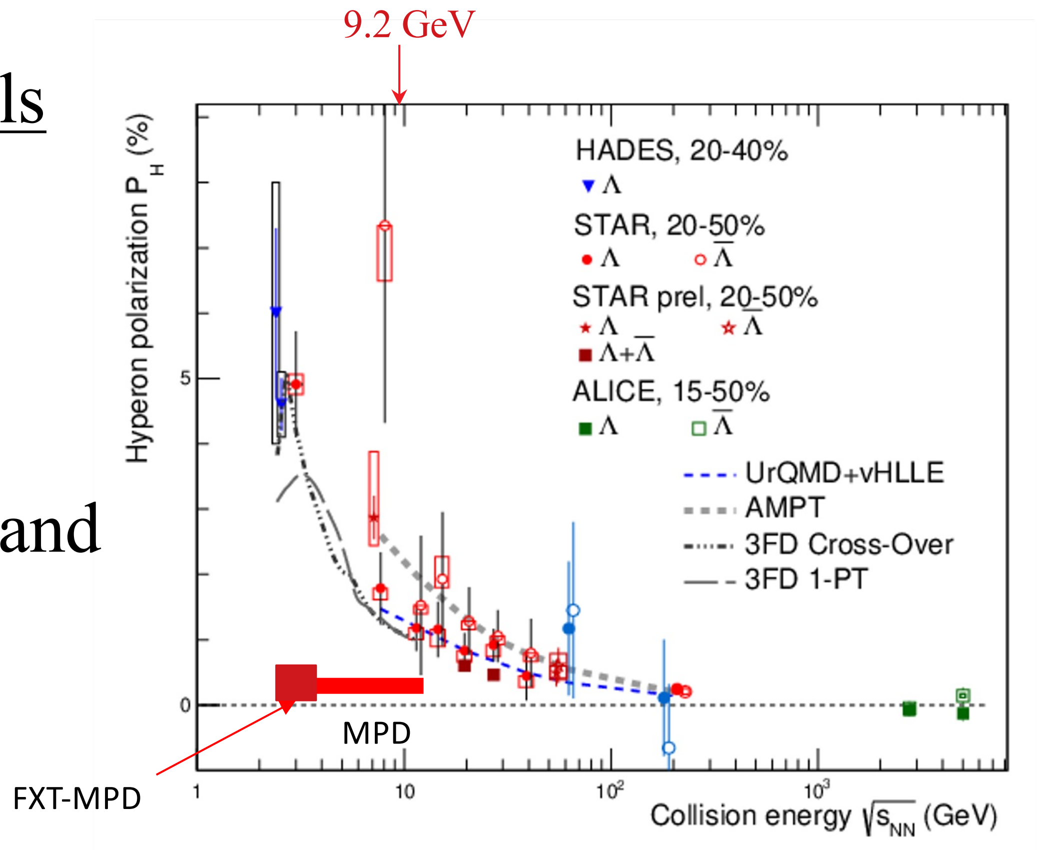

S. Singha, EPJ Web Conf. 276 (2023) 06012

J. Adam et al. (STAR Collaboration), Phys. Rev. C 98, 014910 (2018)
O. Teryaev and R. Usubov, Phys. Rev. C 92, 014906 (2015)

Hypernuclei

Hypernuclei are nuclei containing at least one hyperon:

- **nucleon-hyperon (NY)** and **hyperon-hyperon (YY)** interactions are poorly studied compared to nucleon-nucleon (NN) interactions
    - To study EOS we need to have better define NY and YY potentials
- Study of hypernuclei might help us with that

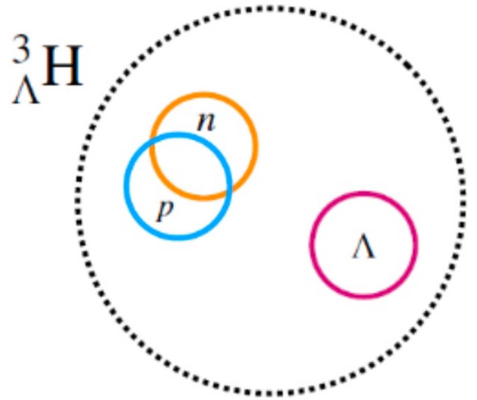

A. Andronic et al, PLB 697 (2011) 203

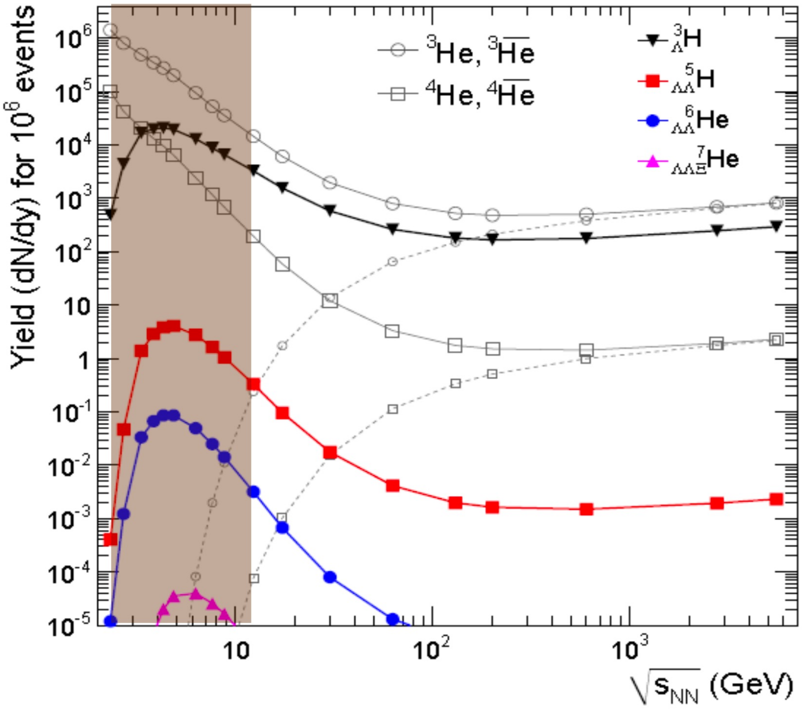

- Few data on the production of hypernuclei in heavy-ion collisions
- Available data leaves space for various model predictions (thermal, coalescence, hybrid)
- Thermal model predicts an enhanced production of (hyper)nuclei within the NICA energy range
- Further and deeper investigations of the hypernuclei formation mechanisms require additional measurements (beam energy and system size scans)

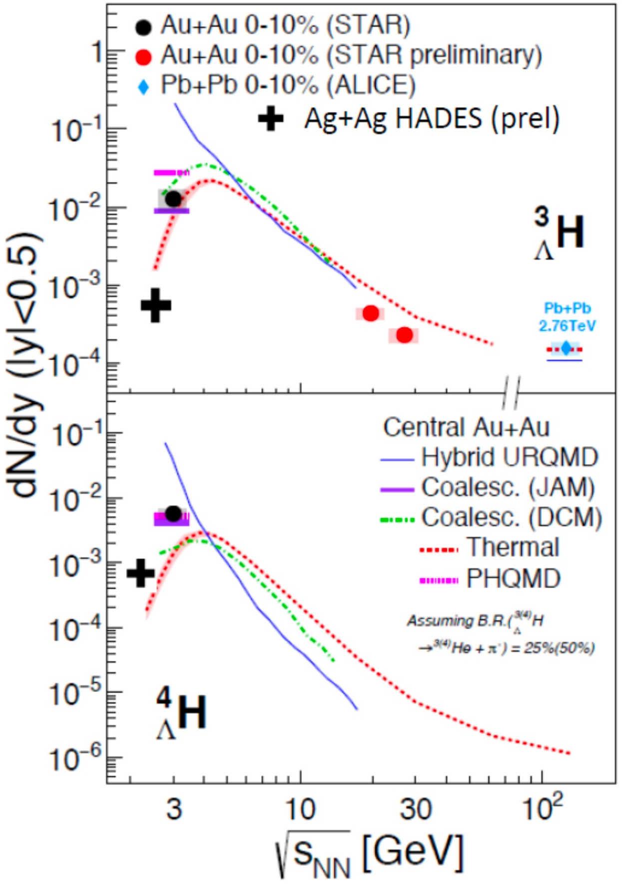

NICA Project

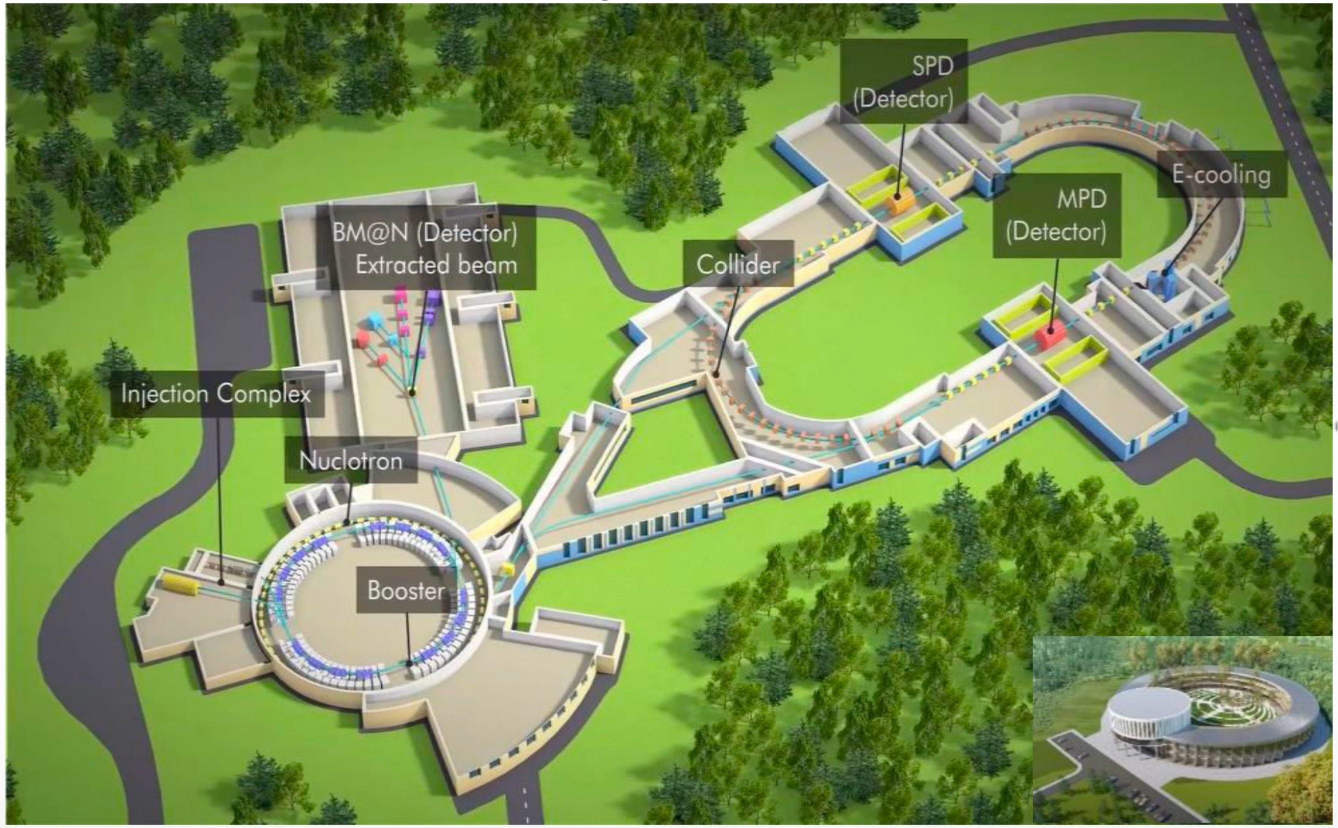

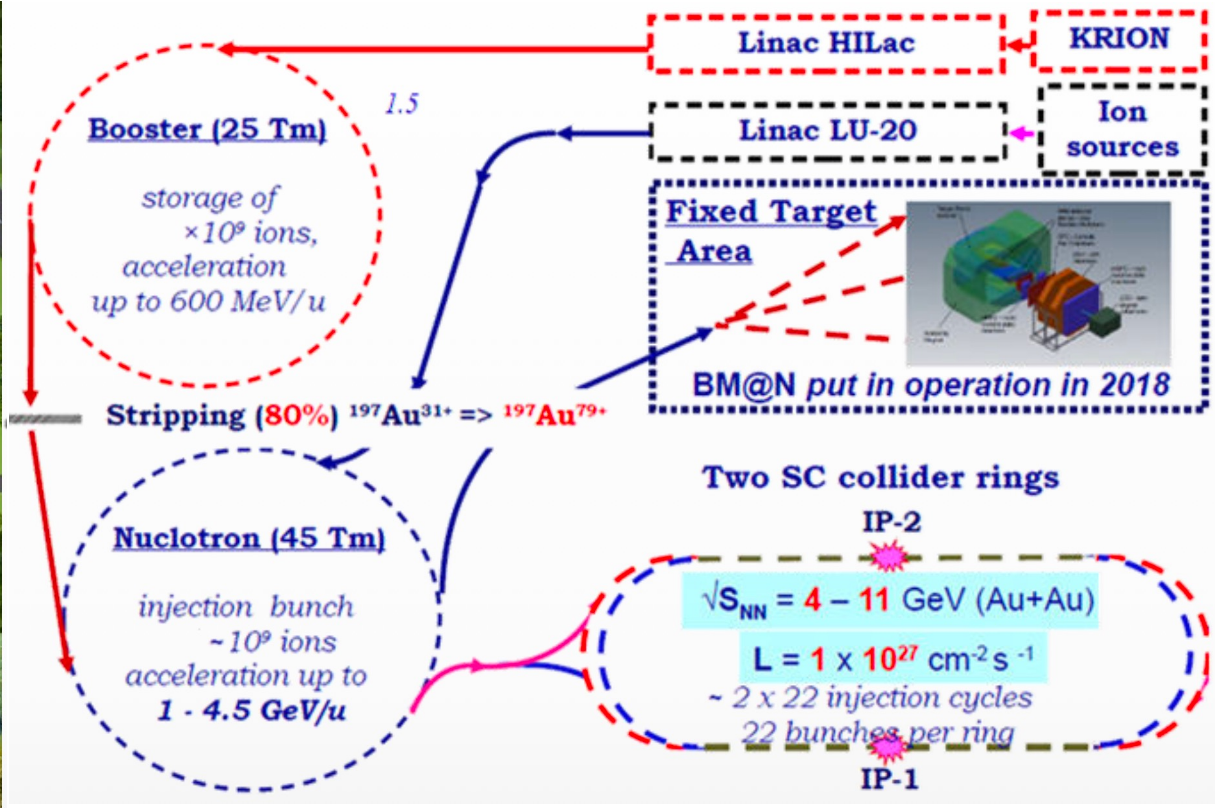

- **The first megascience project in Russia, which is approaching its full commissioning:**
  - **Baryonic matter at Nuclotron (BM@N) –** already running in the fixed-target mode
  - **Multi-Purpose Detector (MPD) –** start of operation in 2025
  - **Spin Physics Detector (SPD) –** operating on polarized deuterons later on

MPD experiment at NICA

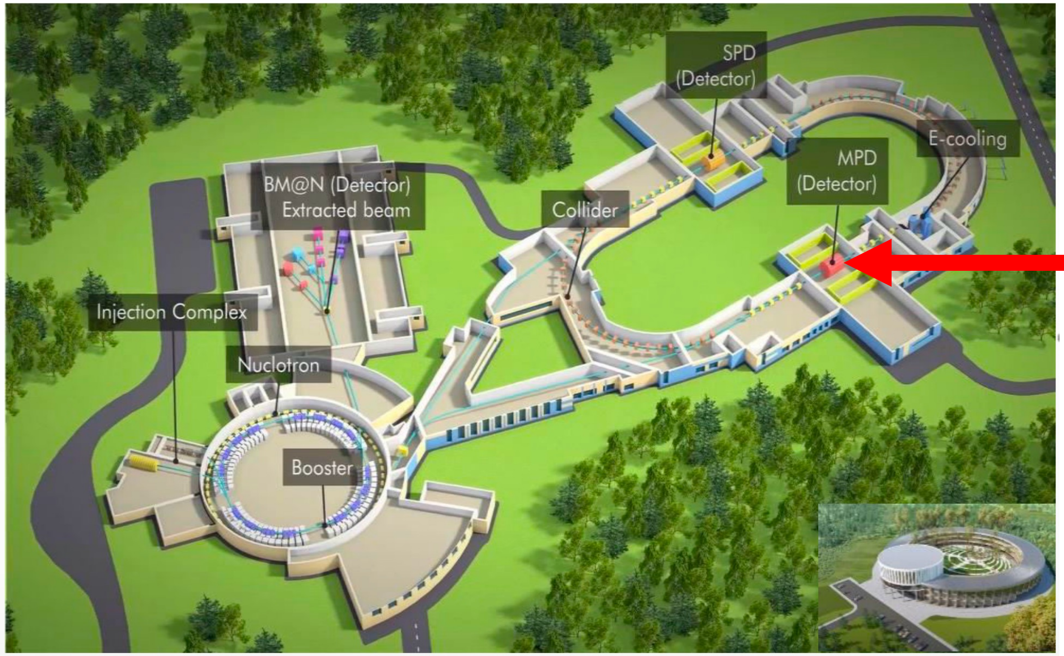

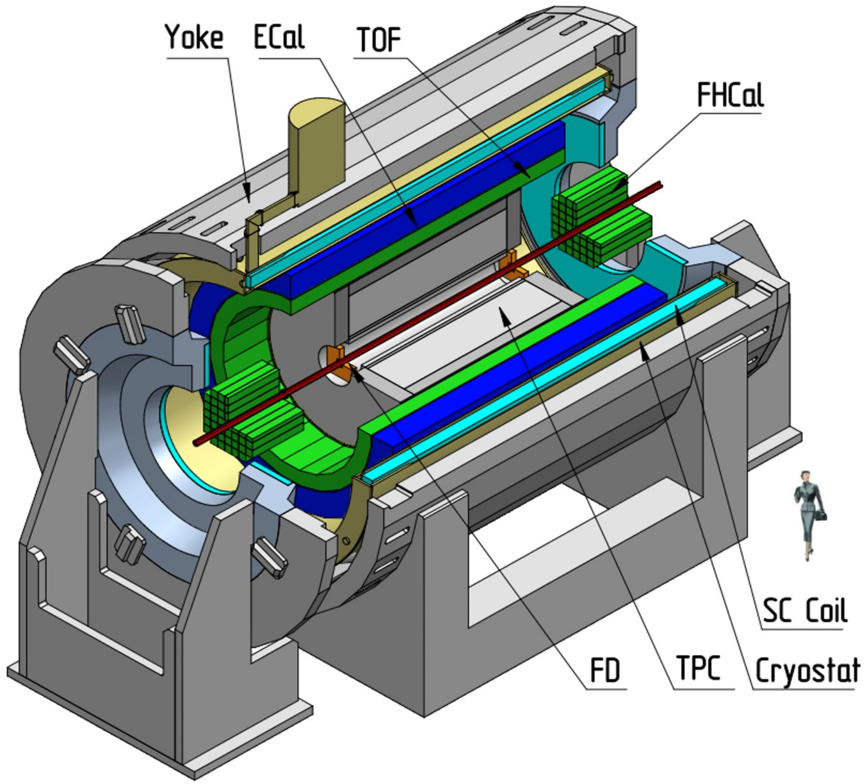

One of the two experiments at NICA collider to study heavy-ion collisions at $\sqrt{s_{NN}}$ = 2.4-11 GeV

Main subsystems:

- **TPC** ($|\Delta\varphi| < 2\pi, |\eta| \leq 1.6$): charged particle tracking + momentum reconstruction + dE/dx identification
- **TOF** ($|\Delta\varphi| < 2\pi, |\eta| \leq 1.6$): charged particle identification
- **EMC** ($|\Delta\varphi| < 2\pi, 2.9 < |\eta| < 3.3$): energy and PID for $\gamma/e^{\pm}$ + charged particle identification (limited ability)
- **FHCal** ($|\Delta\varphi| < 2\pi, 2 < |\eta| < 5$) and **FFD** ($|\Delta\varphi| < 2\pi, 2.9 < |\eta| < 3.3$): event triggering + event geometry + T_0
- **ITS**: secondary vertex reconstruction for heavy-flavor decays (considered for later runs)

MPD – fixed-target mode

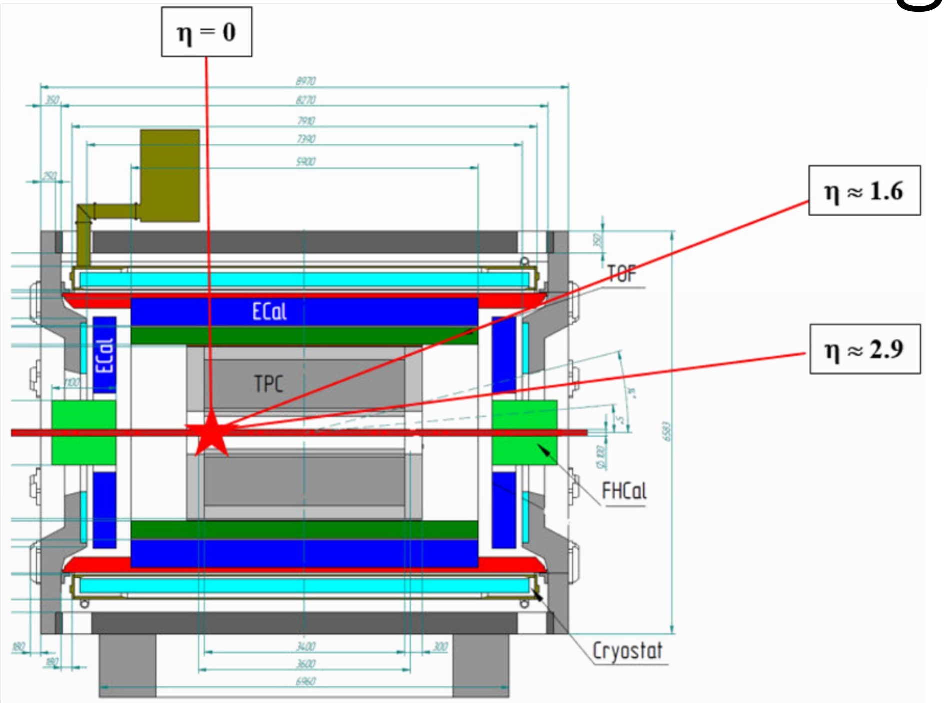

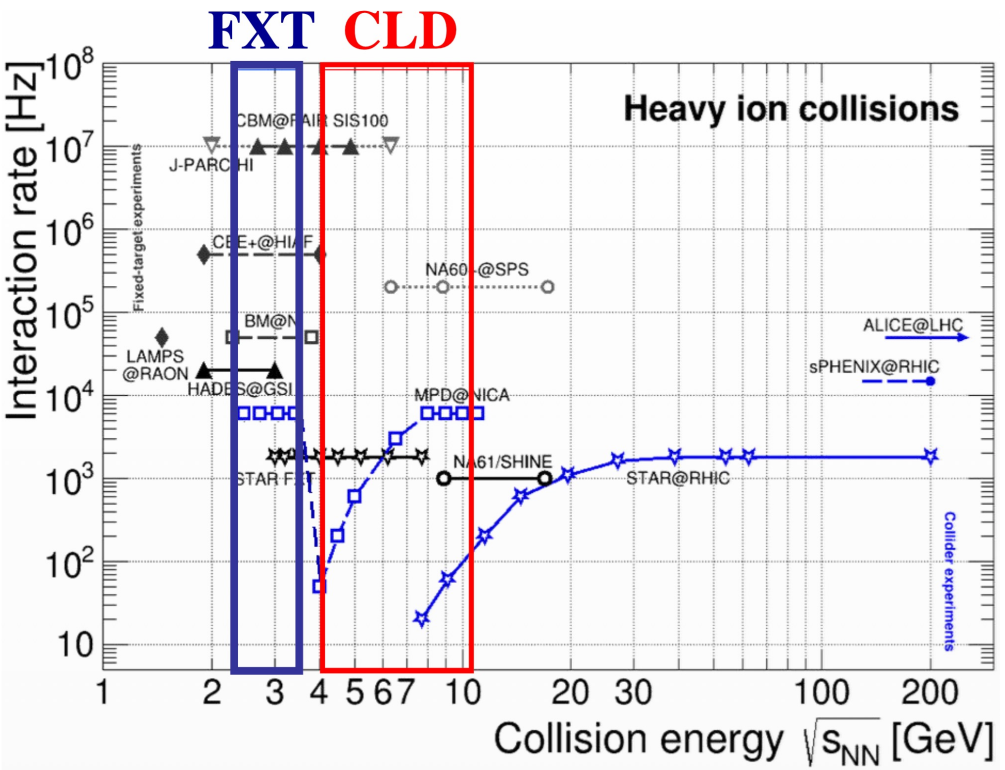

- **Collider mode (MPD-CLD):** two beams, $\sqrt{s_{NN}}$ = 4-11 GeV
- **Fixed-target mode (MPD-FXT):** one beam, thin (~50-100 μm) wire close to the edge of the central barrel:
  - Extends energy range of the MPD to $\sqrt{s_{NN}}$ = 2.4-3.5 GeV – overlap with HADES, BM@N, and CBM
  - Allows to maintain high interaction rate at lower beam energies compared to MPD-CLD
- **Expected beams at the first year(s) of operation:**
  - MPD-CLD: Xe+Xe at $\sqrt{s_{NN}} \sim 7$ GeV, reduced luminosity (~50 Hz interaction rate)
  - MPD-FXT: Xe+W at $\sqrt{s_{NN}} \sim 3$ GeV

MPD subsystem status (I)

Magnet and cryogenics

- Test cooling performed to 70°K in February-March
- Start of cooling to LHe and magnetic field measurements in the second half of the 2024

TPC – central tracker

- TPC cylinders, central membrane, service wheels, readout chambers, gas system - ready
- Final vessel assembly expected to be finished by the end of the year

MPD subsystem status (II)

Support structure

- Carbon fiber support frame delivered and ready for installation

ECAL

Half-sector at different stages of assembly

- 83% of the calorimeters will be ready in 2024
- The remaining modules will be produced (delays with fiber supply)

MPD subsystem status (III)

TOF

- 28 modules are produced and ready for installation

FHCal

- FHCal assembled on the platform and ready to be installed

FFD

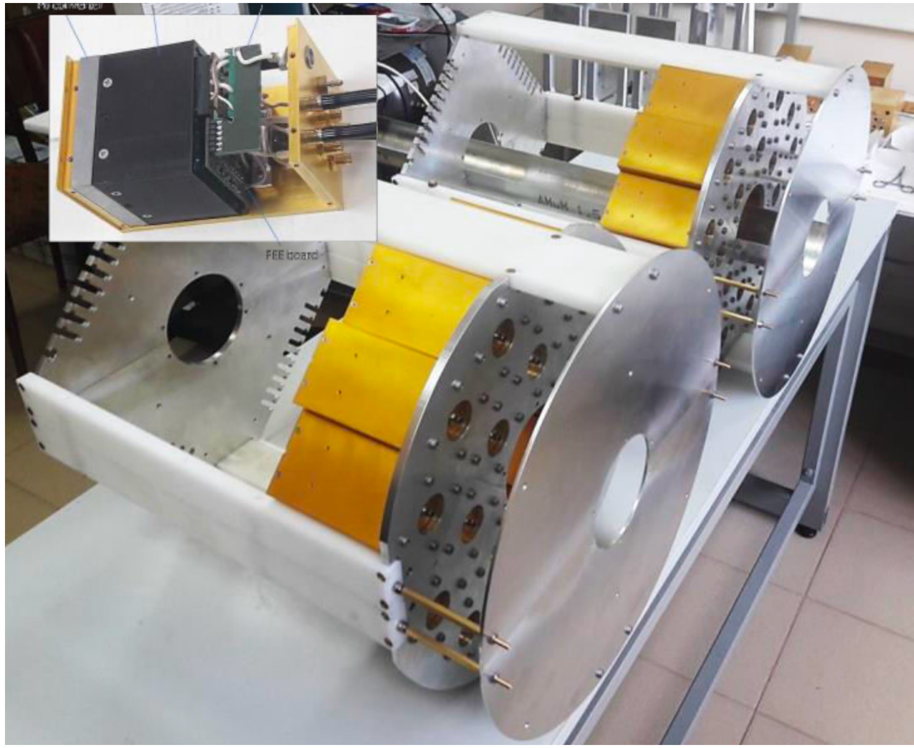

- Cherenkov modules, mechanics for installation in container with the beam pipe are available and ready for installation

MPD physics program

G. Feofilov, P. Parfenov

Global observables
- Total event multiplicity
- Total event energy
- Centrality determination
- Total cross-section measurement
- Event plane measurement at all rapidities
- Spectator measurement

V. Kolesnikov, Xianglei Zhu

Spectra of light flavor and hypernuclei
- Light flavor spectra
- Hyperons and hypernuclei
- Total particle yields and yield ratios
- Kinematic and chemical properties of the event
- Mapping QCD Phase Diag.

K. Mikhailov, A. Taranenko

Correlations and Fluctuations
- Collective flow for hadrons
- Vorticity, Λ polarization
- E-by-E fluctuation of multiplicity, momentum and conserved quantities
- Femtoscopy
- Forward-Backward corr.
- Jet-like correlations

D. Peresunko, Chi Yang

Electromagnetic probes
- Electromagnetic calorimeter meas.
- Photons in ECAL and central barrel
- Low mass dilepton spectra in-medium modification of resonances and intermediate mass region

Wangmei Zha, A. Zinchenko

Heavy flavor
- Study of open charm production
- Charmonium with ECAL and central barrel
- Charmed meson through secondary vertices in ITS and HF electrons
- Explore production at charm threshold

Charged identified hadron production

0-5% central AuAu@9 GeV (PHSD), 5 M events

Phys.Part.Nucl. 53 (2022) 2, 203-206

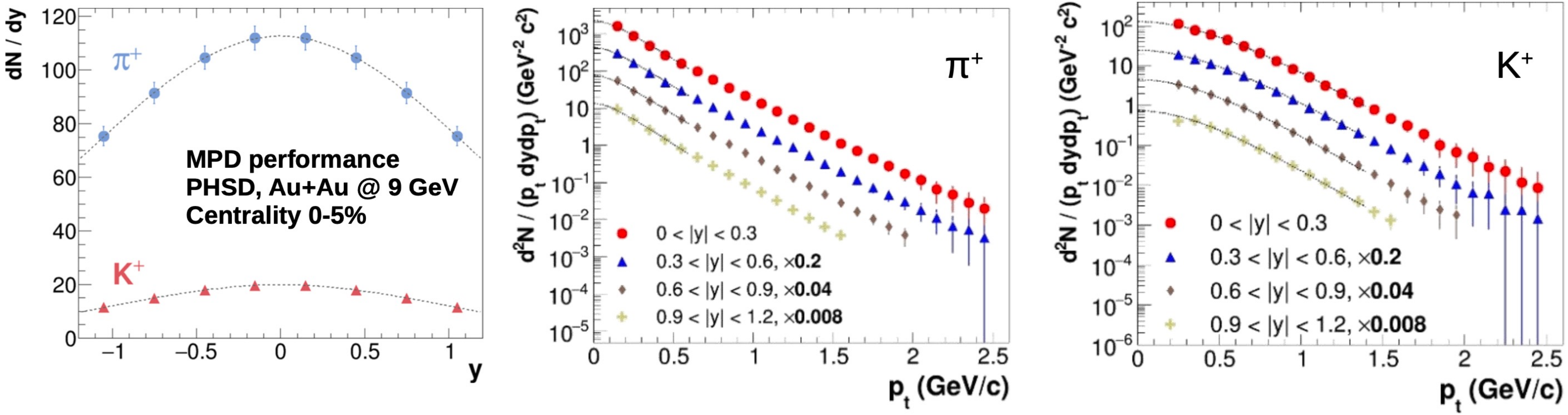

- Probe freeze-out conditions, collective expansion, hadronization mechanisms, strangeness production (“horn” for K/π), parton energy loss, etc. with particles of different masses, quark contents/counts
- Charged hadrons: large (~70% of π/K/p) and uniform acceptance + excellent PID capabilities of TPC and TOF down to p_T~0.1 GeV/c

Neutral identified hadron production

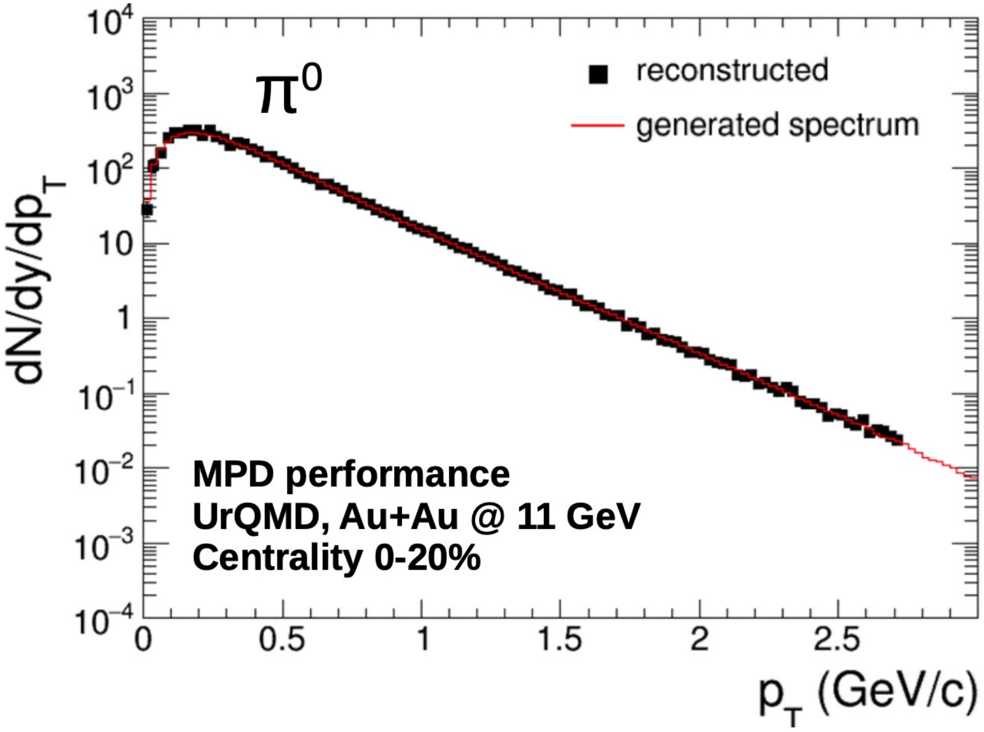

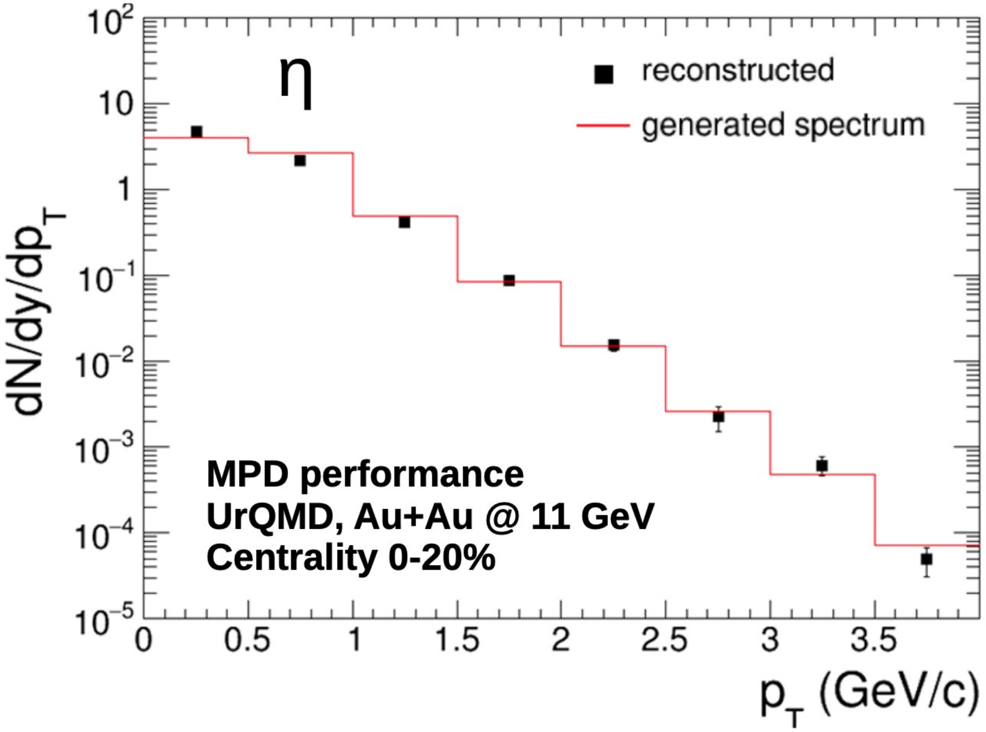

- MPD will be able to measure differential production spectra, integrated yields and $\langle p_T \rangle$, particle ratios, multiplicity distributions for a variety of identified hadrons ($\pi, K, \eta, \omega, \rho$, …)
- Neutral mesons ($\pi^0, K_S, \eta, \omega, \eta'$) : ECAL reconstruction + photon conversion method (PCM)
- Will be helpful to extend p_T ranges of charged particle measurements and assess systematics

Hyperon production

Acta Phys. Pol. B Proc. Suppl. 14, 529 (2021)

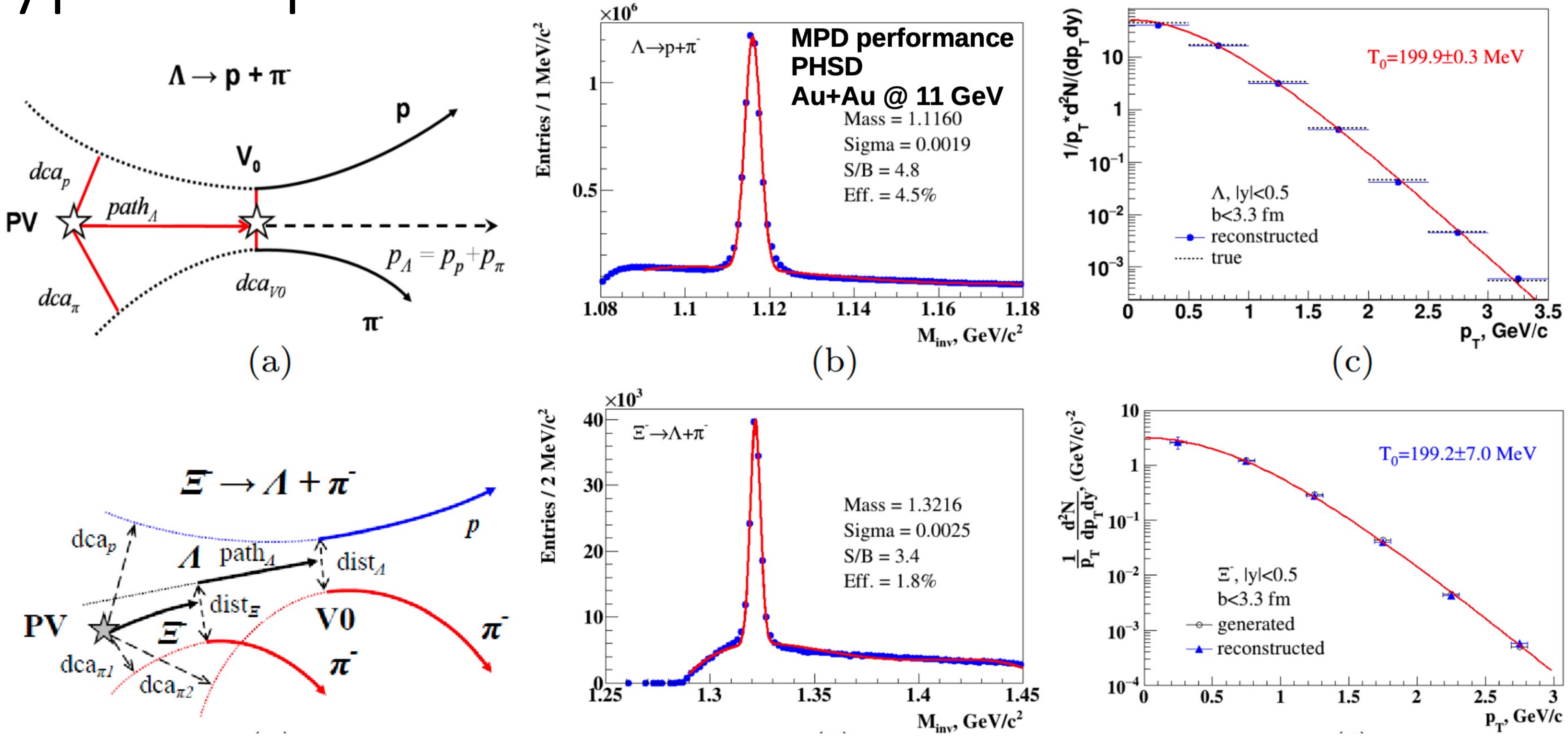

- Strangeness enhancement is considered to be a signature of the QGP formation with no consensus on the dominant mechanisms of strangeness enhancement – precise measurements are needed in pp, pA, AA
- Strange baryons can be reconstructed with a good level of significance (S/B ratios) with PID using TPC+TOF and different topology selections

Hypernuclei production

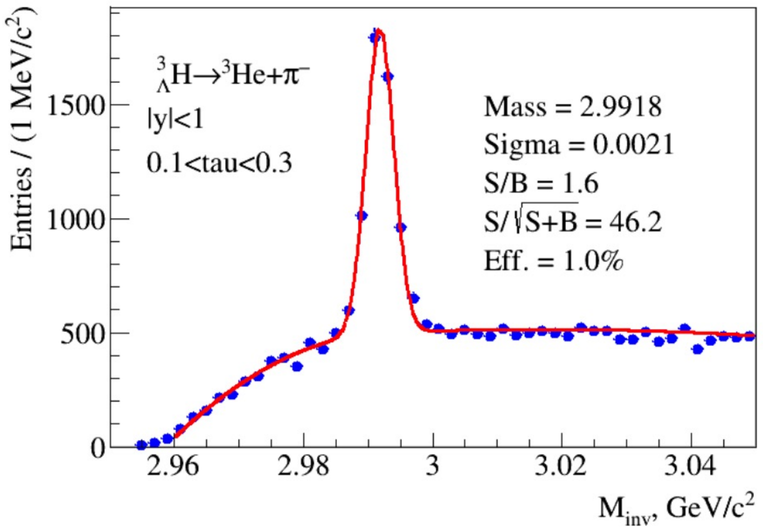

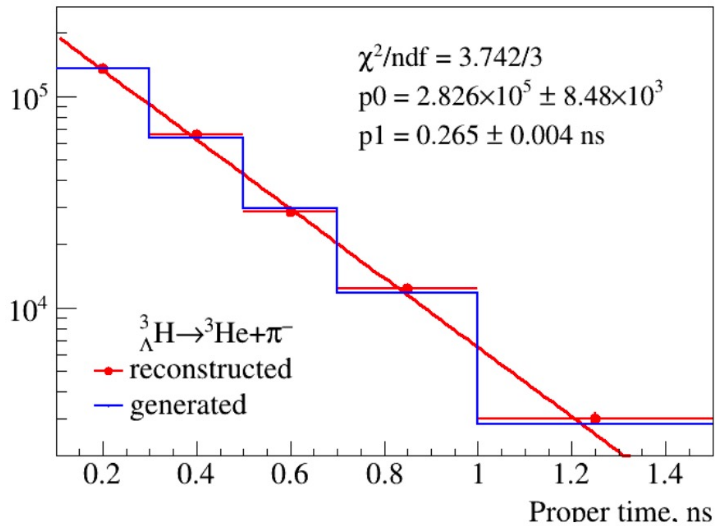

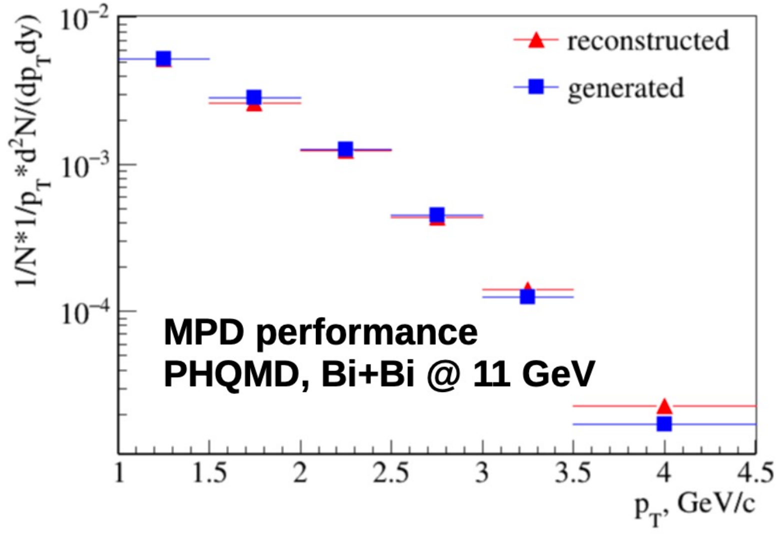

- Hypernuclei measurements may shed light on their production mechanism (statistical hadronisation, coalescence)
- Statistical models predict enchanced hypernuclei production at NICA energies – more hypernuclei are available for measurements
- Yields and lifetimes from the models are well reproduced in MPD performance studies with 40M events for $^{3}_{\Lambda}H$

Resonance production

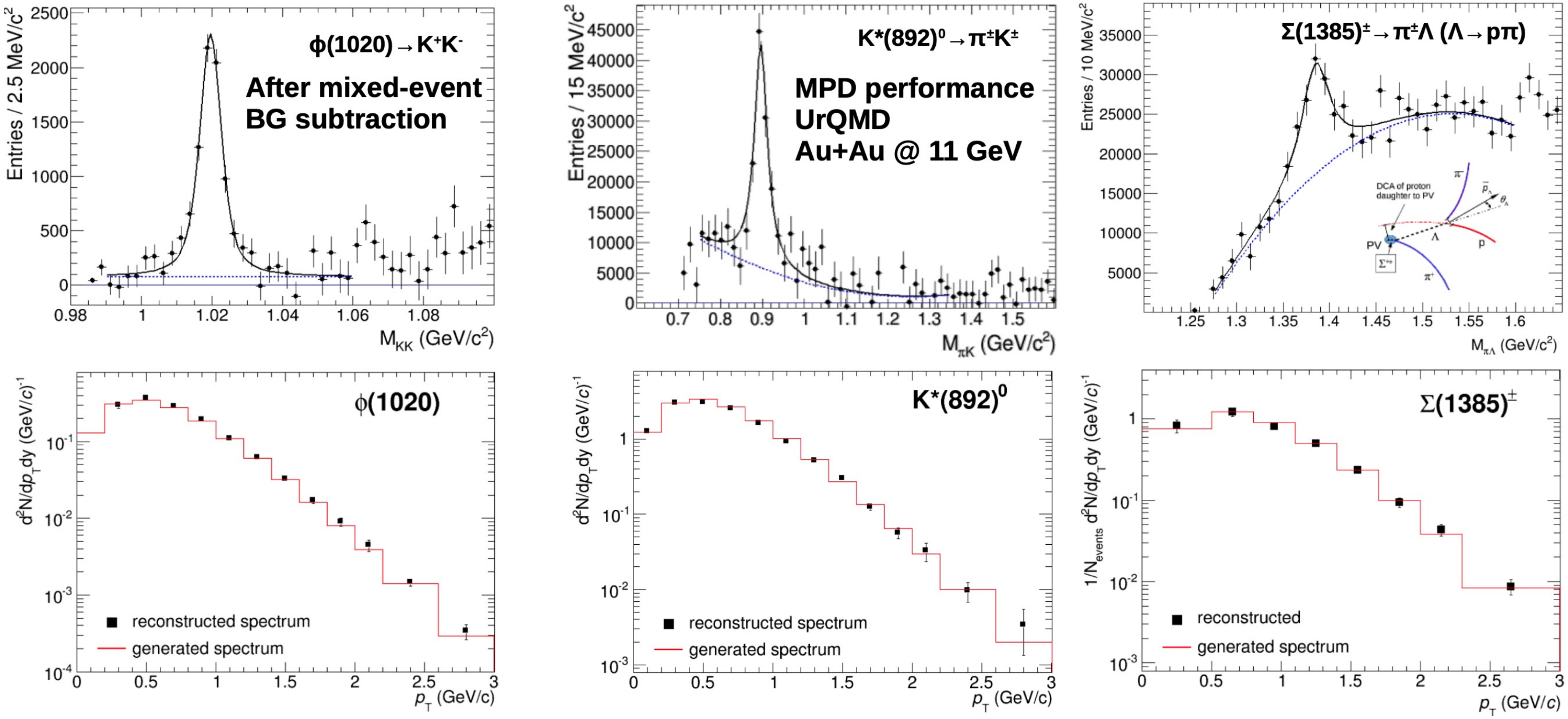

MPD is capable of resonance reconstruction using TPC and TOF for PID and selection based on the topology of the decay

First measurements are feasable with 10M events

Global polarization of Λ hyperon P_{Λ}

Eur.Phys.J.A 60 (2024) 4, 85

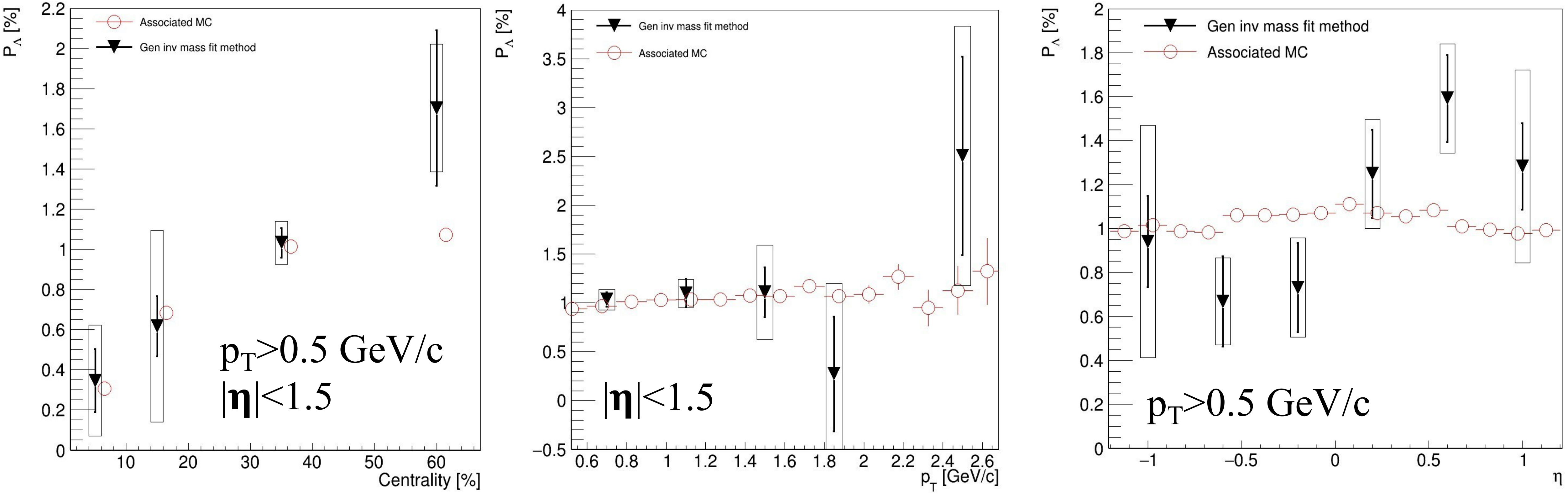

Good agreement with Associated MC

More statistics needed for differential (pT,**η**) measurements

Anisotropic flow of identified charged hadrons

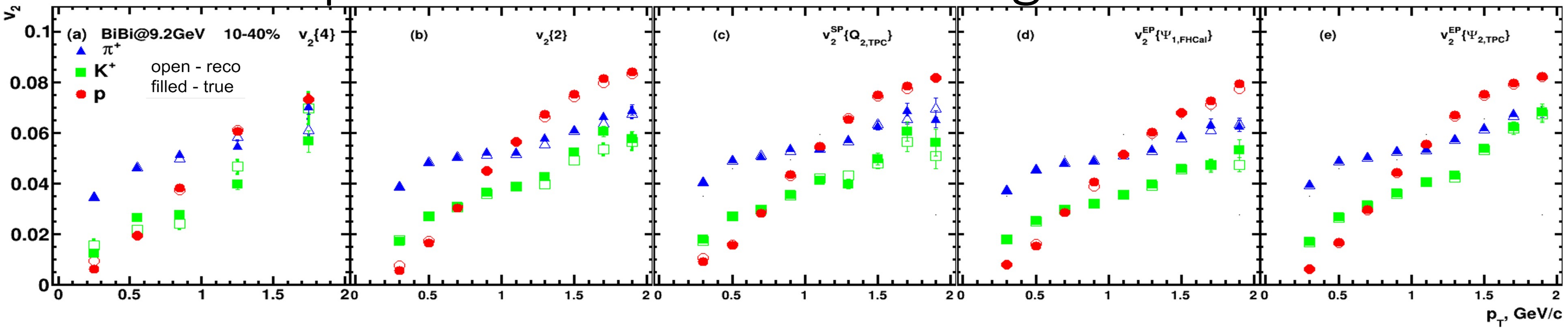

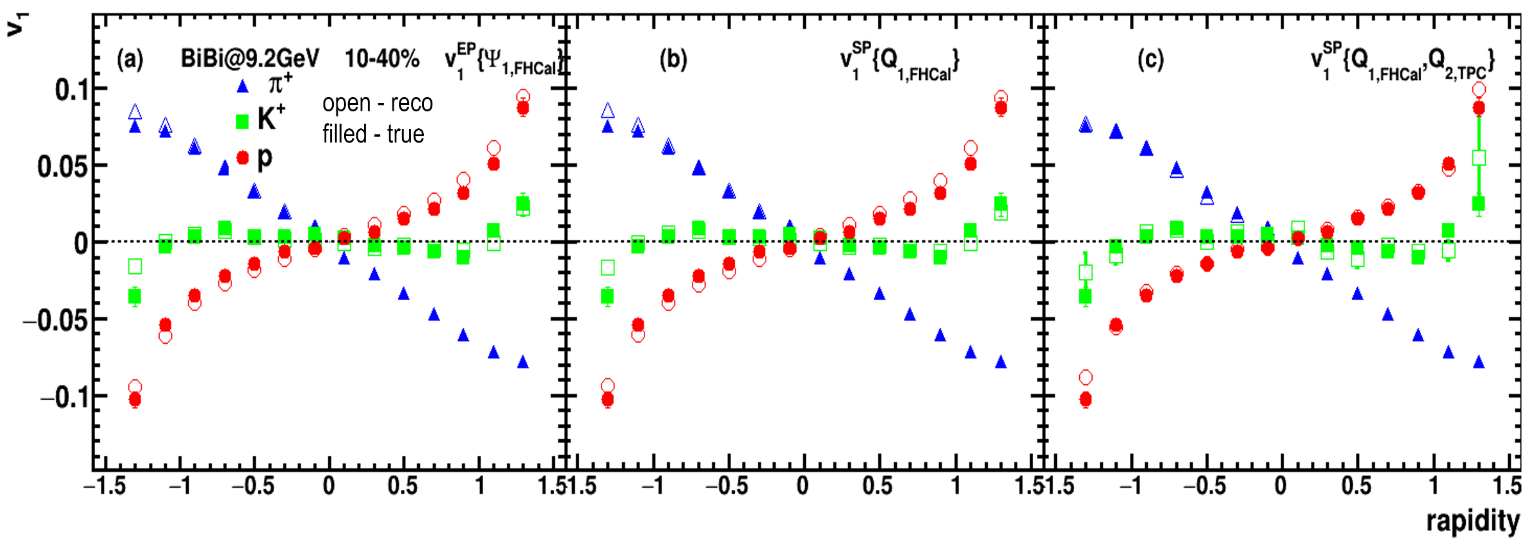

Good performance for v_1, v_2 using several methods for flow measurements (EP, SP, Q-Cumulants)

Good performance for flow measurements for all methods used (EP, SP, Q-cumulants)

Anisotropic flow of V0 particles

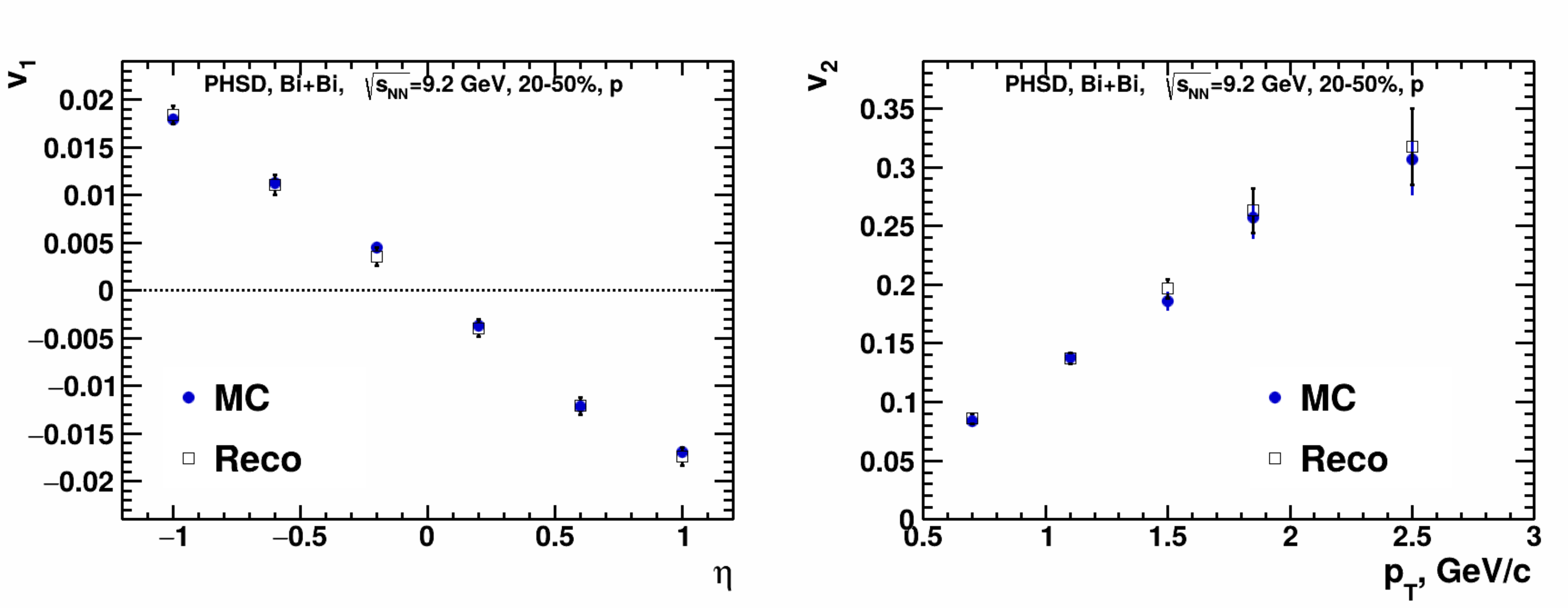

Good performance for v_1, v_2 using invariant mass fit and event plane methods

Anisotropic flow in MPD-FXT: $v_1(y)$

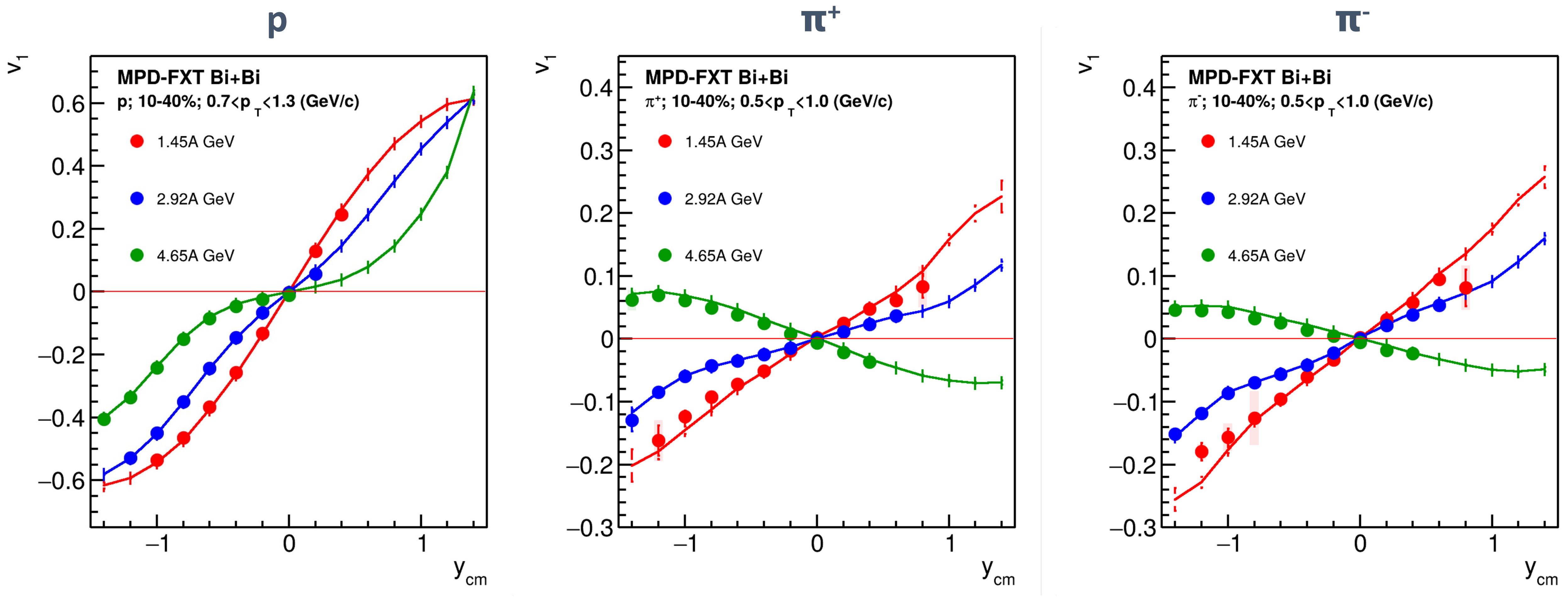

Good agreement with MC data

Anisotropic flow in MPD-FXT: $v_2(p_T)$

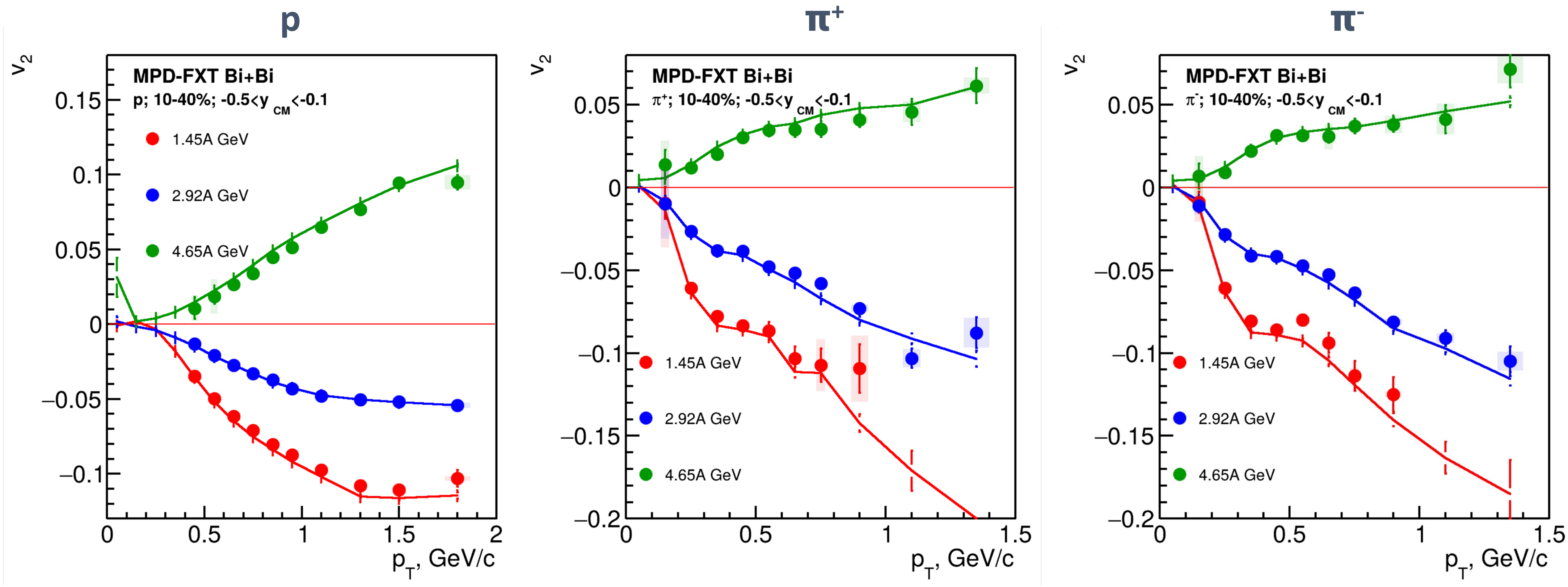

Good agreement with MC data

The BM@N and MPD-FXT experiments

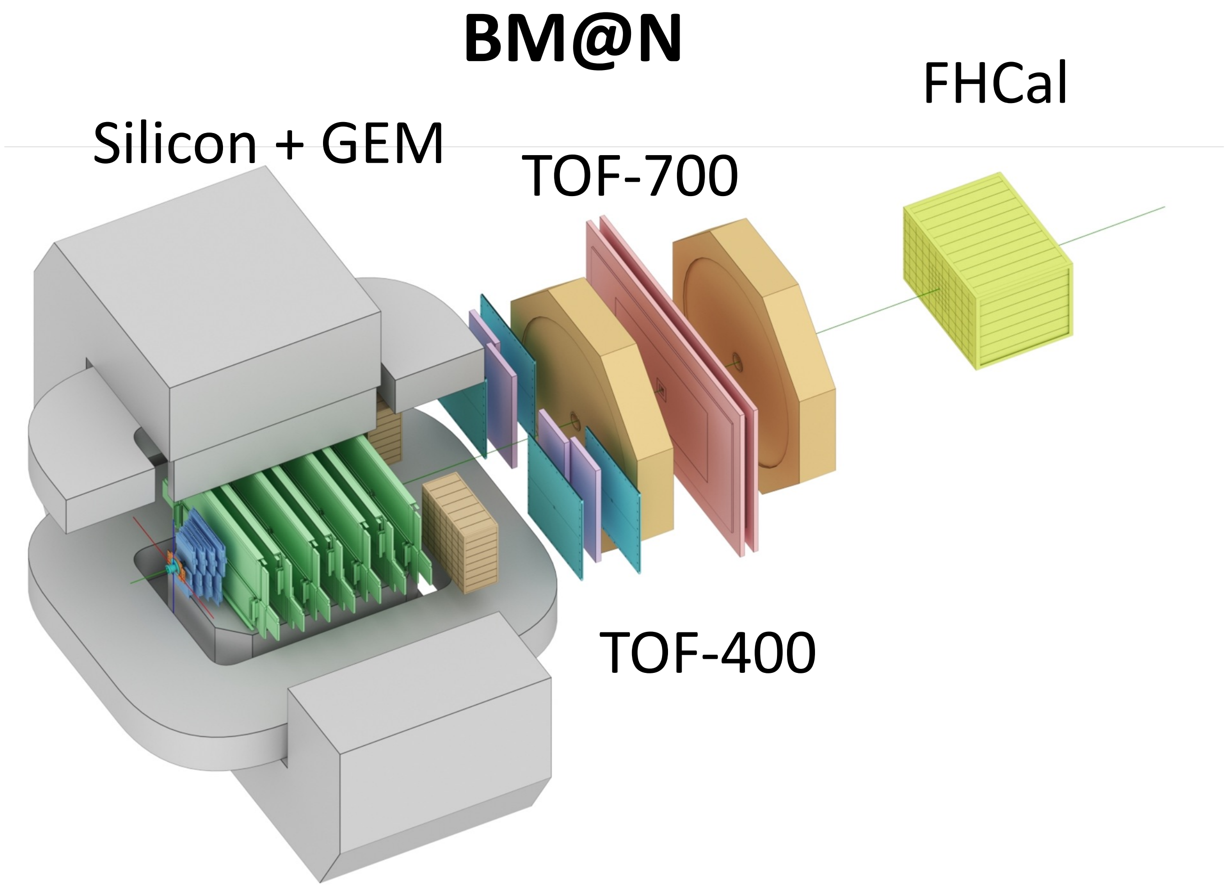

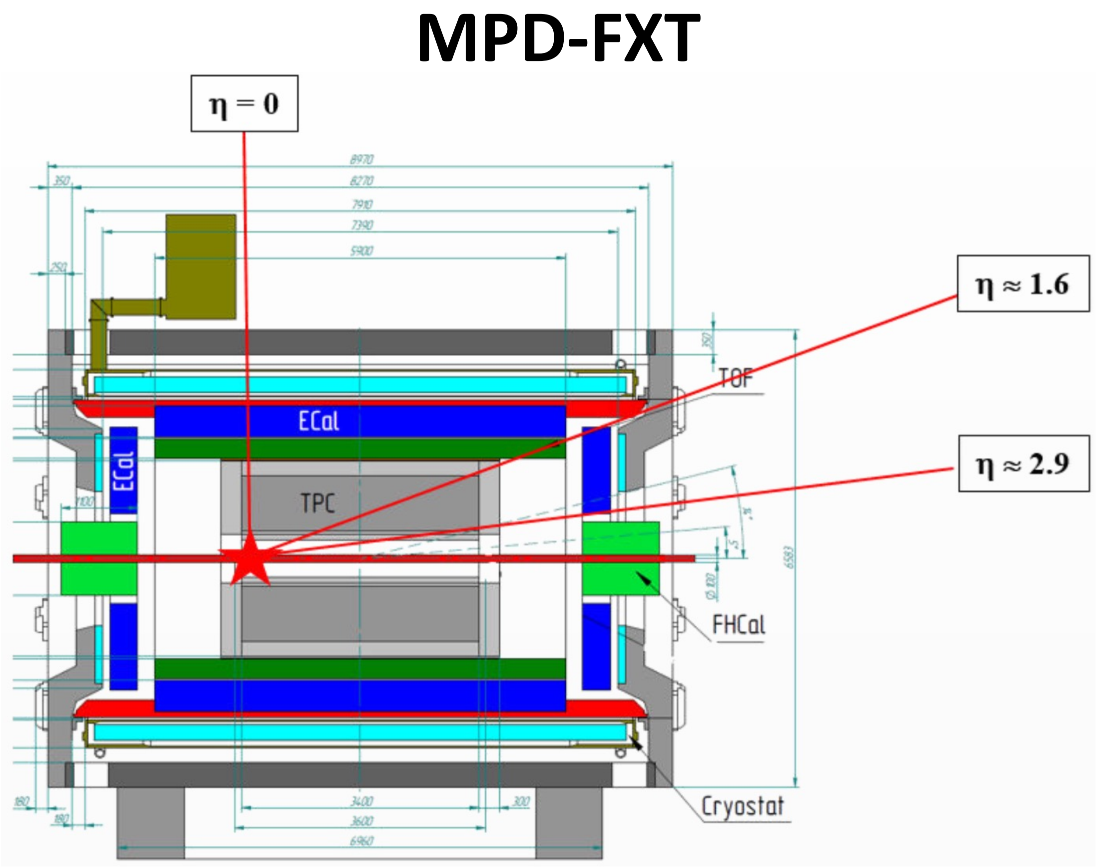

Detectors used for anisotropic flow measurements:

- **Tracking system:** FSD+GEM (BM@N); TPC (MPD-FXT)
- **PID:** TOF-400, TOF-700 (BM@N); TPC, TOF (MPD-FXT)
- **EP measurements:** FHCal (BM@N), FHCal (MPD-FXT)

Comparison with BM@N performance

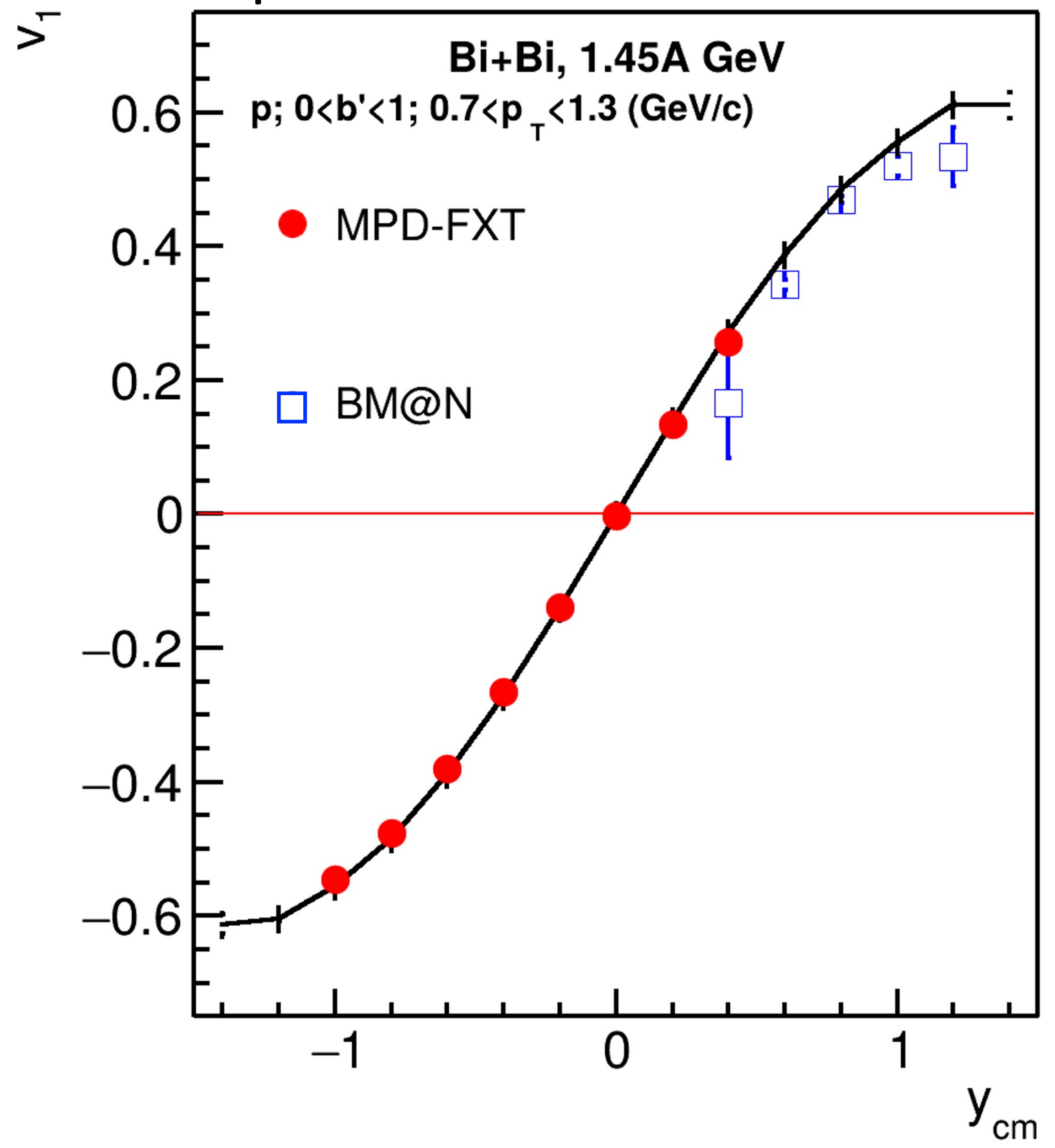

BM@N TOF system (TOF-400 and TOF-700) has poor midrapidity coverage at $\sqrt{s_{NN}}$ = 2.5 GeV

- One needs to check higher energies ($\sqrt{s_{NN}}$ = 3, 3.5 GeV)
- More statistics are required due to the effects of magnetic field in BM@N:
  - Only “yy” component of <uQ> and <QQ> correlation can be used

Despite the challenges, both MPD-FXT and BM@N can be used in v_n measurements:

- To widen rapidity coverage
- To perform a cross-check in the future

First results from the Xe run at BM@N

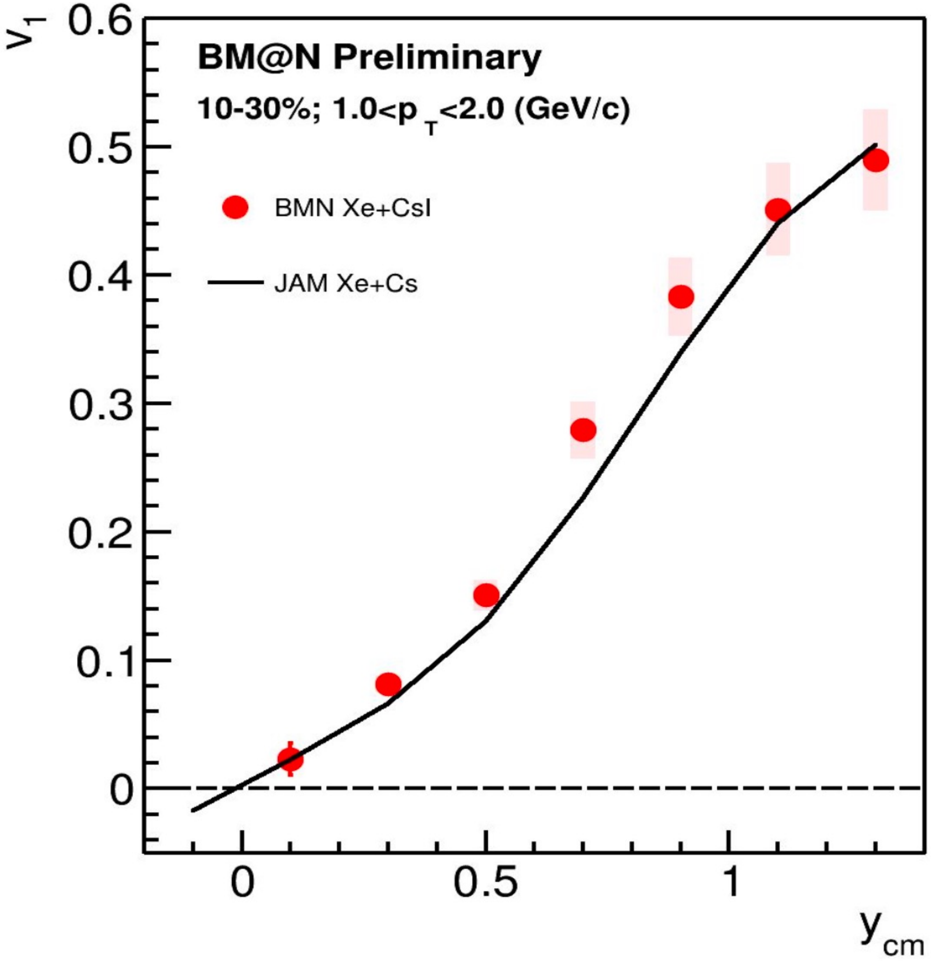

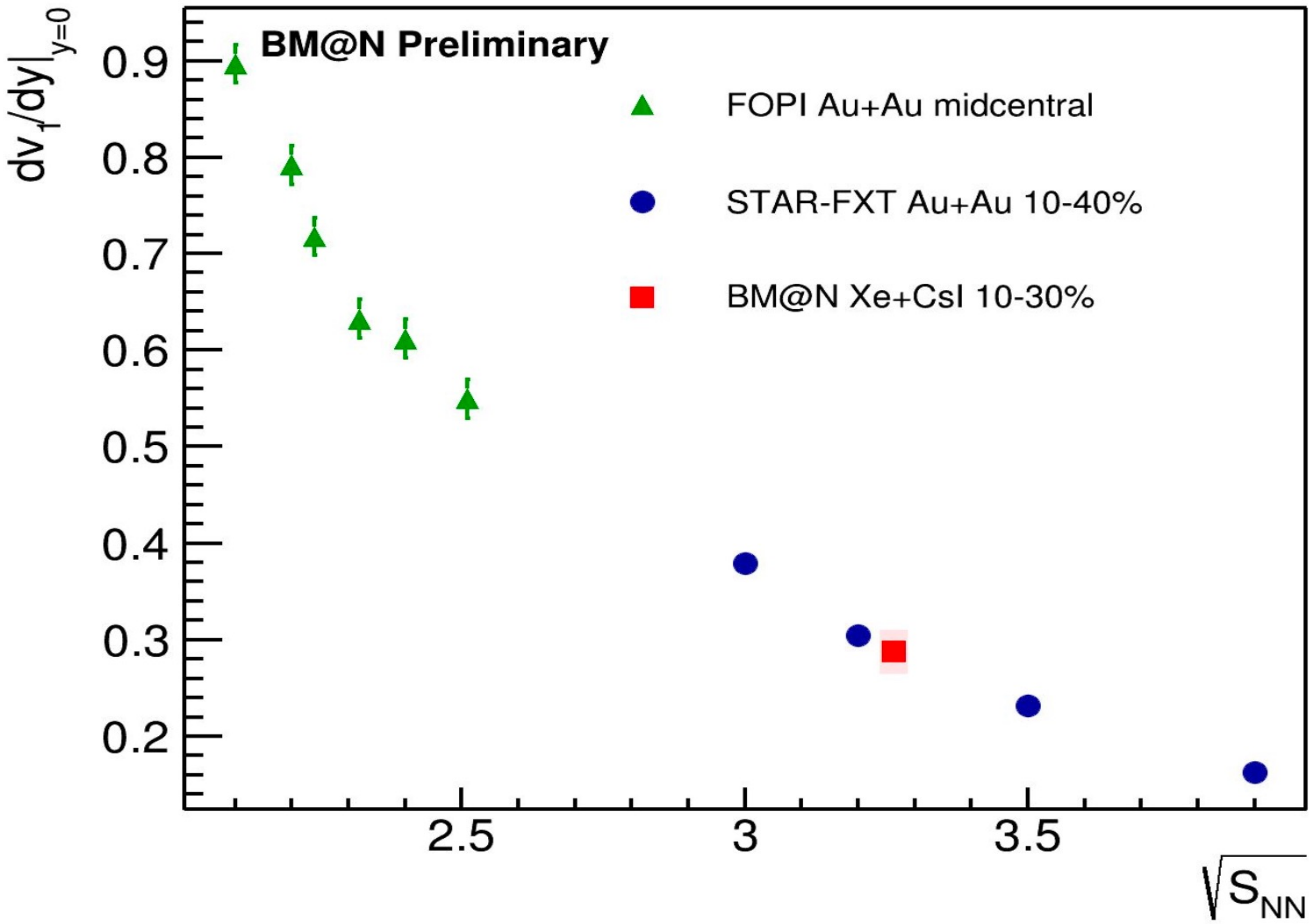

- **All analysis techniques and required corrections were tested with the BM@N experimental data**
- **JAM model with hard momentum-dependent EOS describes v1(y) dependence of protons reasonably well**
- **$dv_1/dy|_{y=0}$ from BM@N is in a good agreement with the world data**

First results from the Xe run at BM@N

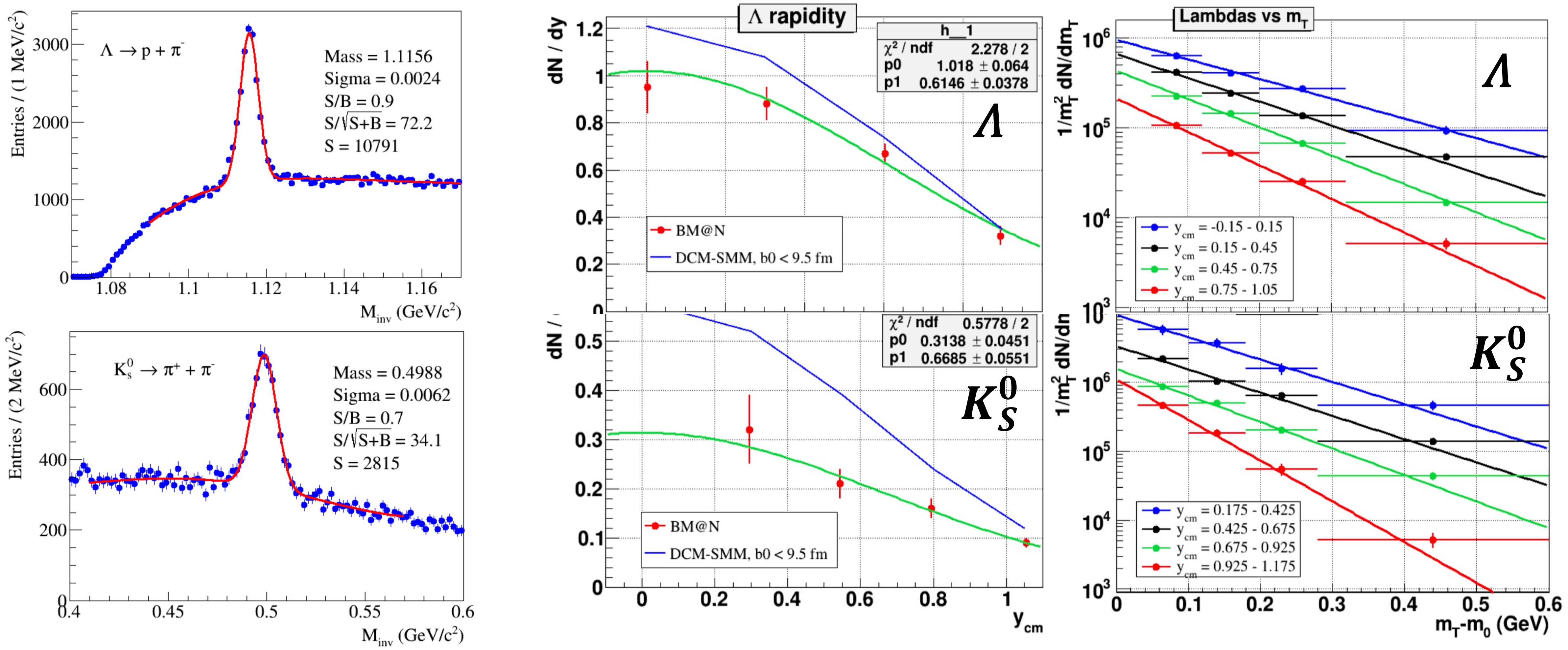

Procedure for Λ and K_S^0 measurements is implemented and tested – first results are ready

Next: analysis on the full statistics from the Xe run, anisotropic flow and global polarisation

Summary

Thank you for your attention!

- MPD collaboration is steadily coming to final integration of the detector and first data taking on the beams from NICA
- Physics program for the first years of MPD data taking is formulated and the first physics paper was published. Second paper under preparation.
- First operations of the MPD detector are expected at the end of 2025
- MPD will provide a unique opportunity for investigating properties of nuclear matter at maximal densities to map the QCD phase diagram, to search for phase transition and the Critical End Point

Backup

Collaboration activity

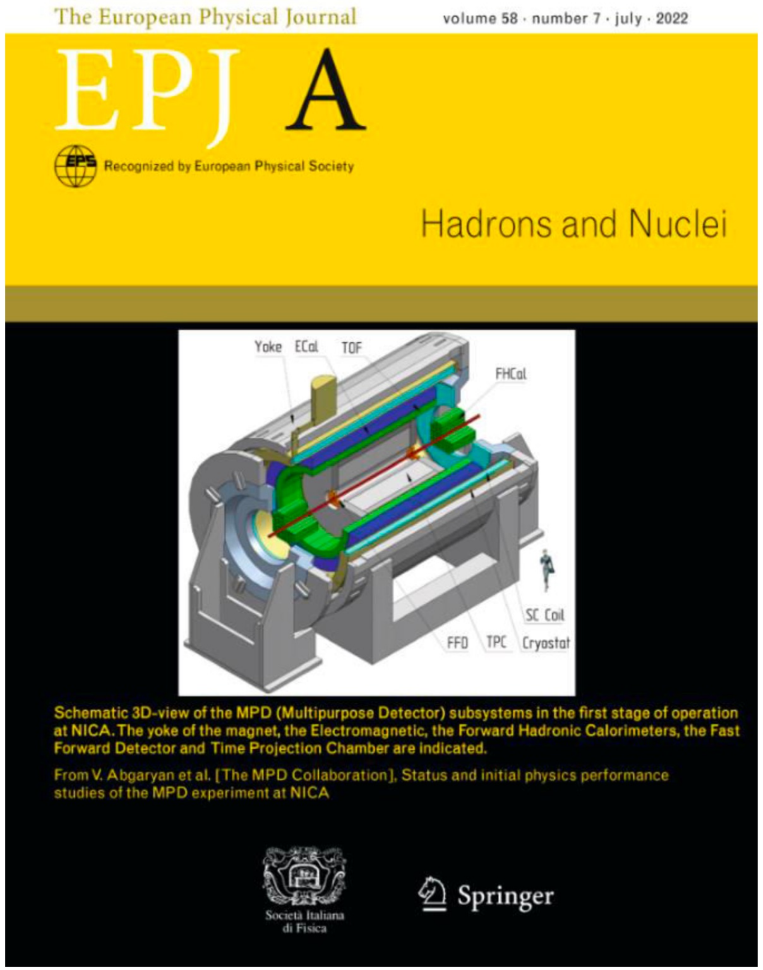

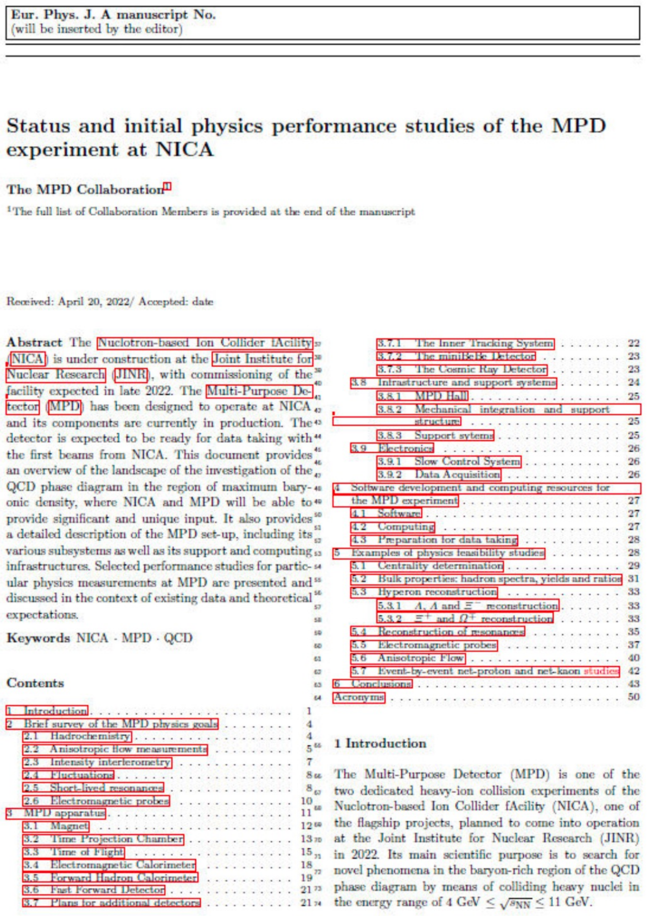

Eur. Phys. J. A manuscript No.
(will be inserted by the editor)

Status and initial physics performance studies of the MPD experiment at NICA

The MPD Collaboration[1]

[1]The full list of Collaboration Members is provided at the end of the manuscript

Received: April 20, 2022/ Accepted: date

Abstract The Nuclotron-based Ion Collider fAcility (NICA) is under construction at the Joint Institute for Nuclear Research (JINR), with commissioning of the facility expected in late 2022. The Multi-Purpose Detector (MPD) has been designed to operate at NICA and its components are currently in production. The detector is expected to be ready for data taking with the first beams from NICA. This document provides an overview of the landscape of the investigation of the QCD phase diagram in the region of maximum baryonic density, where NICA and MPD will be able to provide significant and unique input. It also provides a detailed description of the MPD set-up, including its various subsystems as well as its support and computing infrastructures. Selected performance studies for particular physics measurements at MPD are presented and discussed in the context of existing data and theoretical expectations.

Keywords NICA · MPD · QCD

Contents

1 Introduction . . . 1
2 Brief survey of the MPD physics goals . . . 4
2.1 Hadrochemistry . . . 4
2.2 Anisotropic flow measurements . . . 5
2.3 Intensity interferometry . . . 7
2.4 Fluctuations . . . 8
2.5 Short-lived resonances . . . 8
2.6 Electromagnetic probes . . . 10
3 MPD apparatus . . . 11
3.1 Magnet . . . 12
3.2 Time Projection Chamber . . . 13
3.3 Time of Flight . . . 15
3.4 Electromagnetic Calorimeter . . . 18
3.5 Forward Hadron Calorimeter . . . 19
3.6 Fast Forward Detector . . . 21
3.7 Plans for additional detectors . . . 21
3.7.1 The Inner Tracking System . . . 22
3.7.2 The miniBeBe Detector . . . 23
3.7.3 The Cosmic Ray Detector . . . 23
3.8 Infrastructure and support systems . . . 24
3.8.1 MPD Hall . . . 25
3.8.2 Mechanical integration and support structure . . . 25
3.8.3 Support sytems . . . 25
3.9 Electronics . . . 26
3.9.1 Slow Control System . . . 26
3.9.2 Data Acquisition . . . 26
4 Software development and computing resources for the MPD experiment . . . 27
4.1 Software . . . 27
4.2 Computing . . . 27
4.3 Preparation for data taking . . . 28
5 Examples of physics feasibility studies . . . 28
5.1 Centrality determination . . . 29
5.2 Bulk properties: hadron spectra, yields and ratios . . . 31
5.3 Hyperon reconstruction . . . 33
5.3.1 Λ, Λ and Ξ^- reconstruction . . . 33
5.3.2 Ξ^+ and Ω^+ reconstruction . . . 33
5.4 Reconstruction of resonances . . . 35
5.5 Electromagnetic probes . . . 37
5.6 Anisotropic Flow . . . 40
5.7 Event-by-event net-proton and net-kaon studies . . . 42
6 Conclusions . . . 43
Acronyms . . . 50

1 Introduction

The Multi-Purpose Detector (MPD) is one of the two dedicated heavy-ion collision experiments of the Nuclotron-based Ion Collider fAcility (NICA), one of the flagship projects, planned to come into operation at the Joint Institute for Nuclear Research (JINR) in 2022. Its main scientific purpose is to search for novel phenomena in the baryon-rich region of the QCD phase diagram by means of colliding heavy nuclei in the energy range of 4 GeV $\leq \sqrt{s_{NN}} \leq$ 11 GeV.

- First collaboration paper recently published EPJA (~ 50 pages): Eur.Phys.J.A 58 (2022) 7, 140
- Over 200 publications in total for hardware, software and physics studies
- Reports at all major conferences in the field
- Second collaboration paper is in progress

Anisotropic flow at Nuclotron-NICA energies

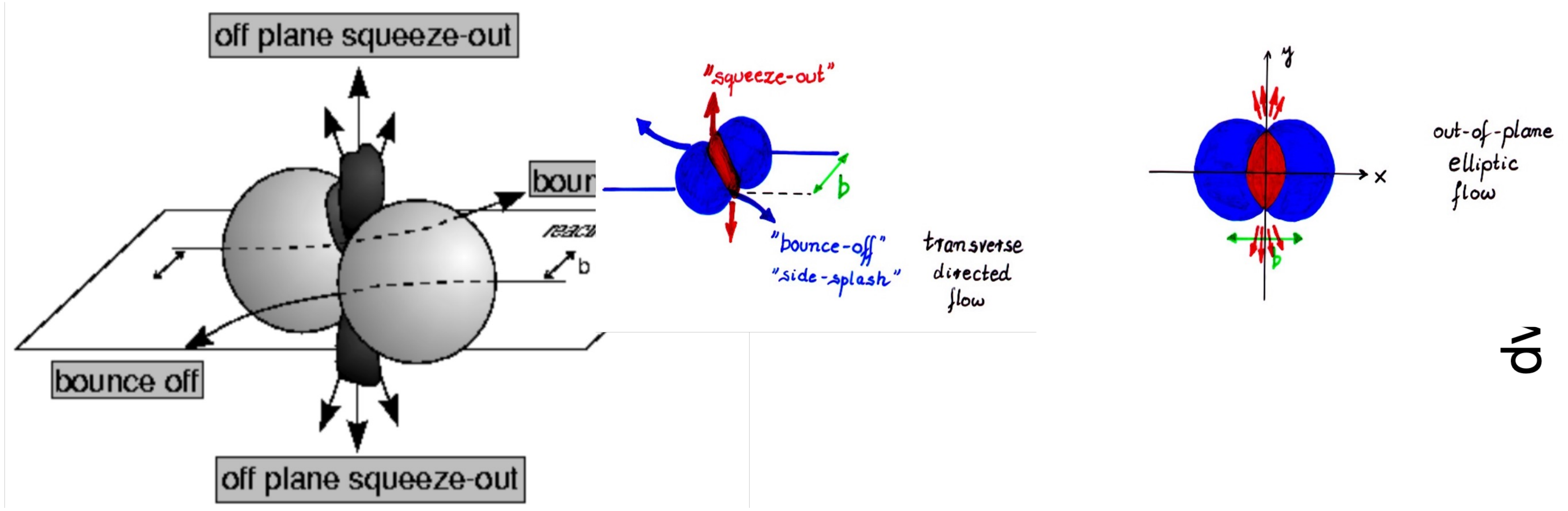

STAR, Phys.Lett.B 827 (2022) 137003

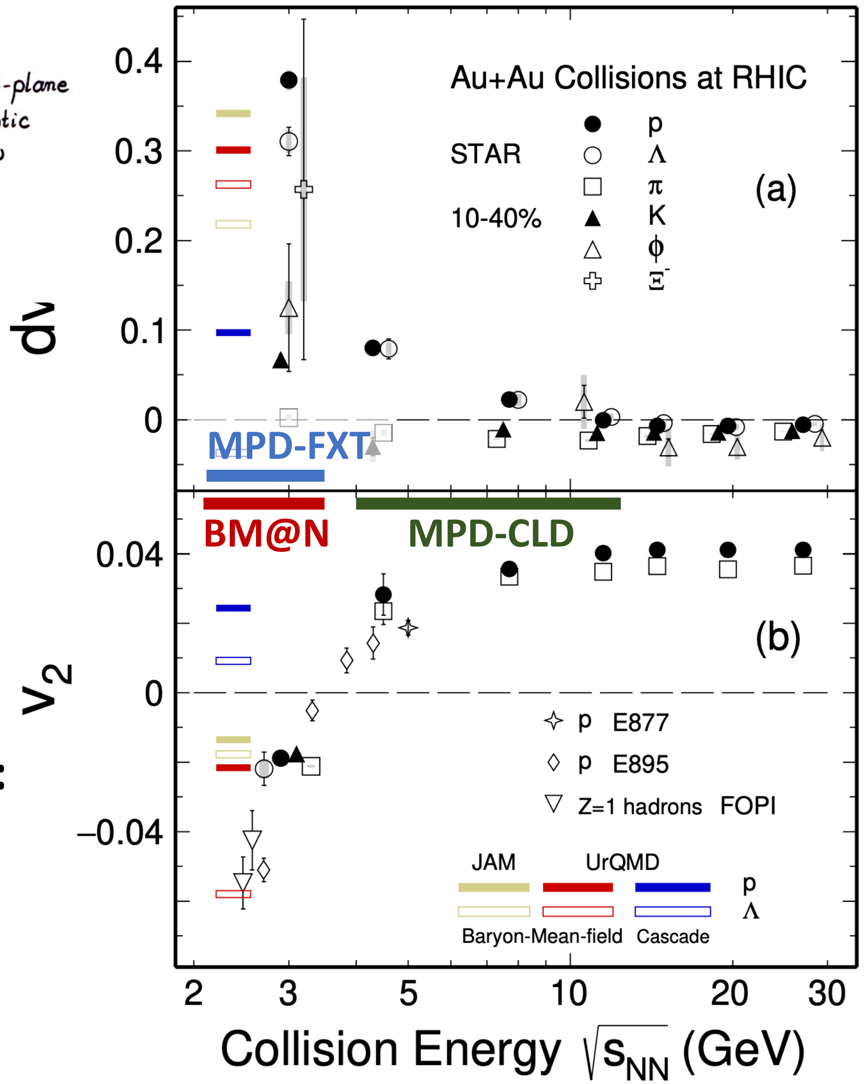

Strong energy dependence of dv_1/dy and v_2 at $\sqrt{s_{NN}}$=2-11 GeV

Anisotropic flow at Nuclotron-NICA energies is a delicate balance between:

I. The ability of pressure developed early in the reaction zone ($t_{exp} = R/c_s$)

II. The passage time for removal of the shadowing by spectators ($t_{pass} = 2R/\gamma_{CM}\beta_{CM}$)

Correlation between P_y and v_1

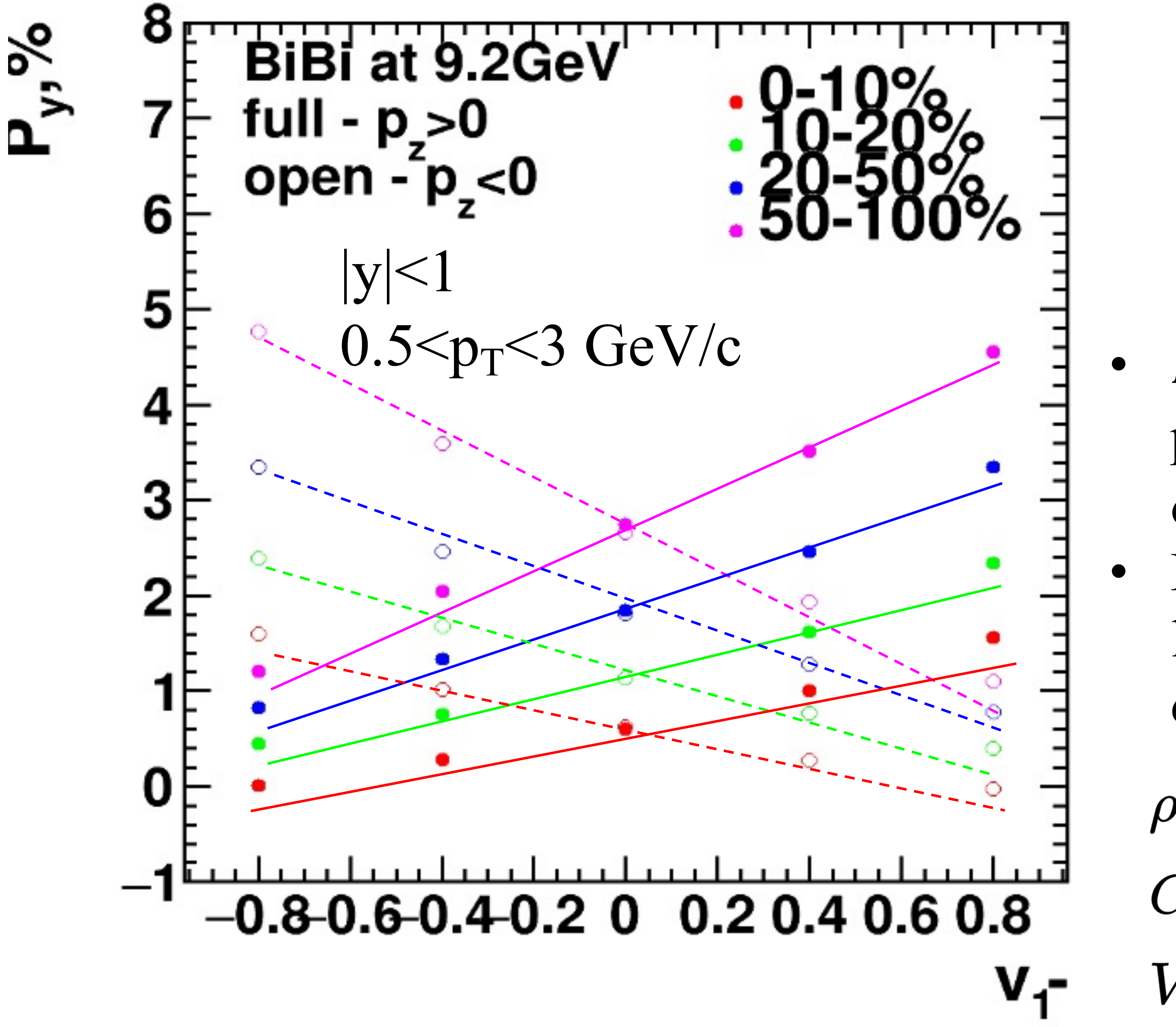

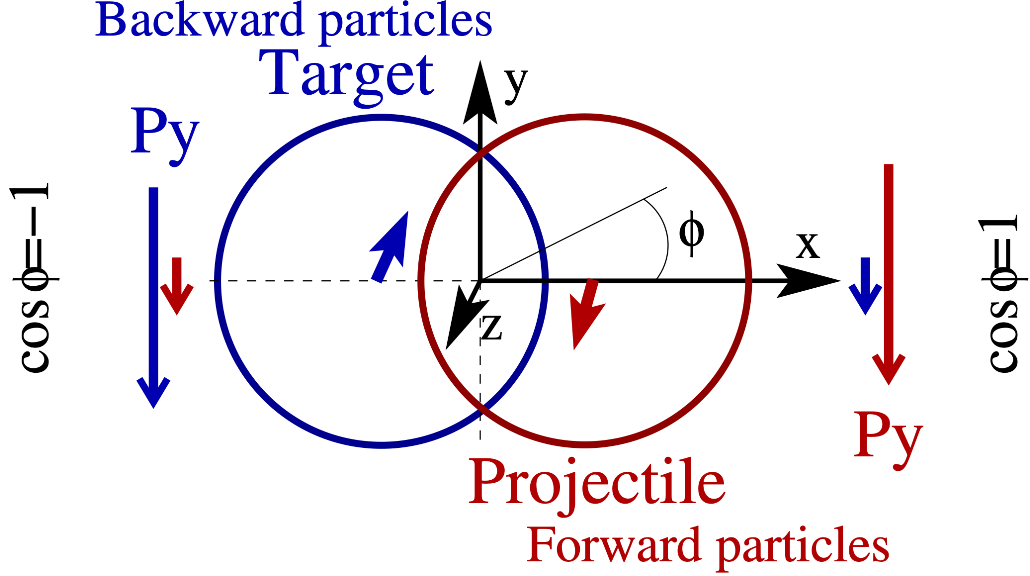

- P_y vs v_1 are correlated with reaction plane → P_y vs v_1 are correlated with each other
- Pearson correlation coefficient represent linear correlation between two sets of data from -1 to 1

$$\rho(X,Y) = \frac{Cov(X,Y)}{Var(X)Var(Y)}$$

$$Cov(X,Y) = \langle XY \rangle - \langle X \rangle \langle Y \rangle$$

$$Var(X) = \sqrt{\langle X^2 \rangle - \langle X \rangle^2}$$

Pearson correlation coefficient between P_y and v_1

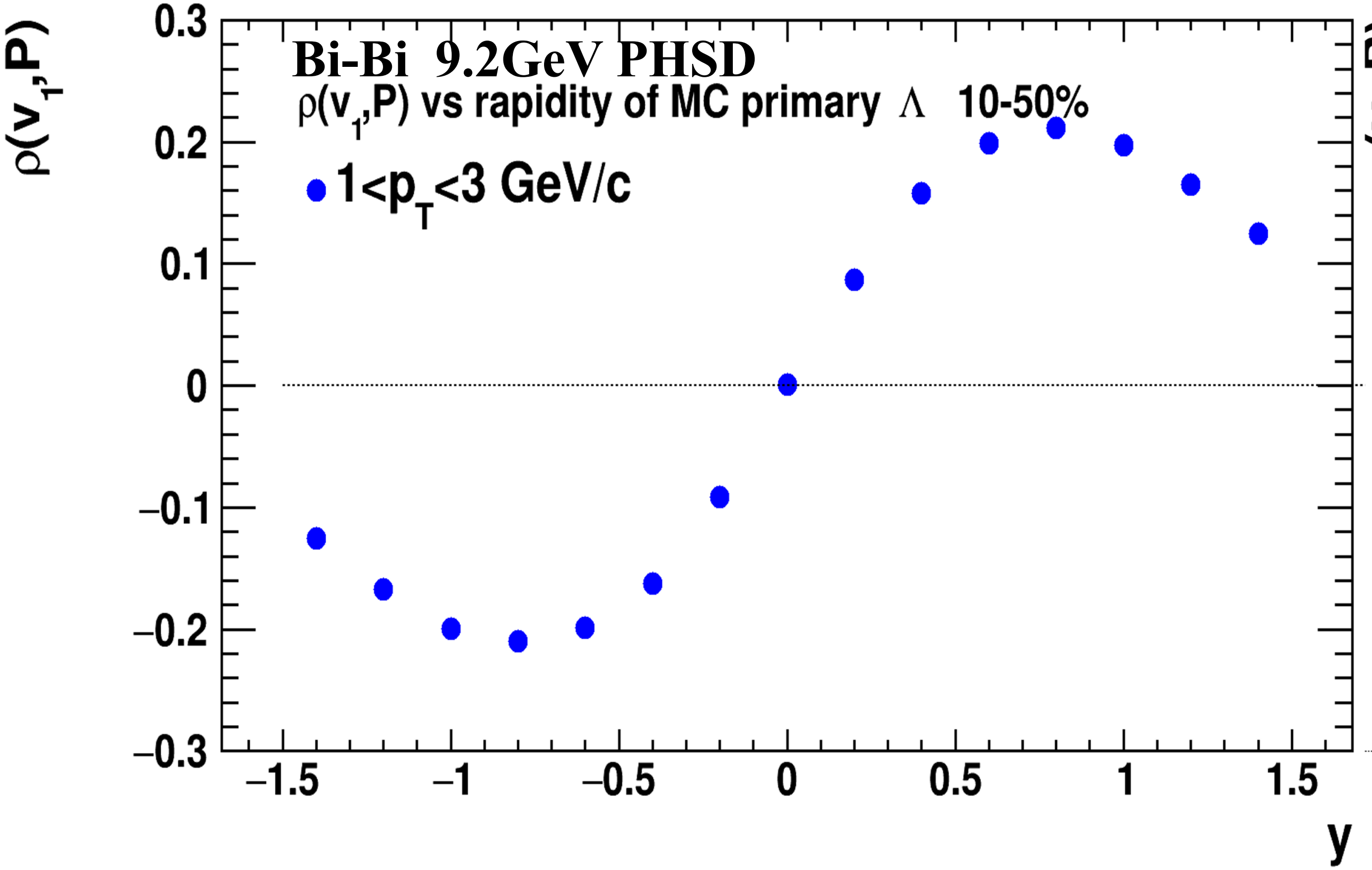

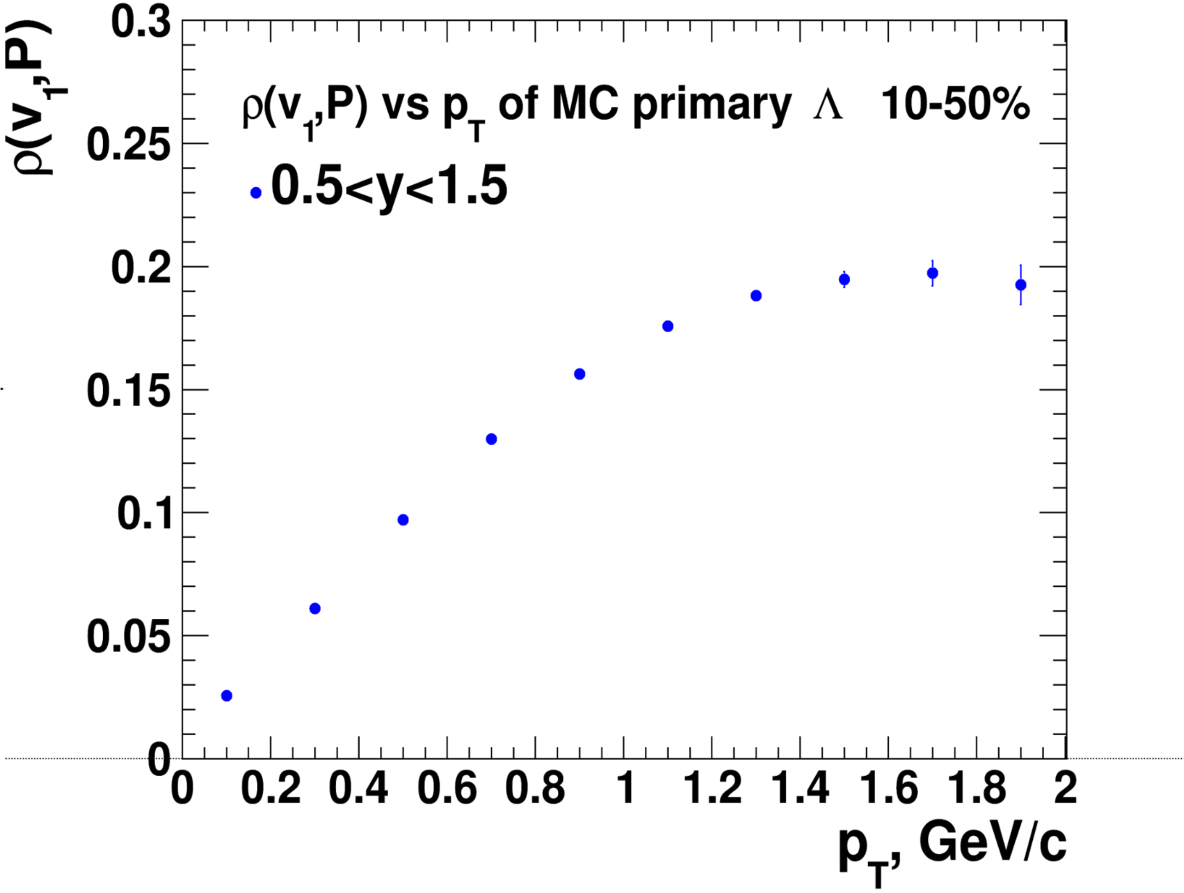

$$\rho(P, v_1) = \frac{\langle P v_1\rangle - \langle P\rangle\langle v_1\rangle}{(\sqrt{\langle v_1^2\rangle - \langle v_1\rangle^2})(\sqrt{\langle P^2\rangle - \langle P\rangle^2})}$$

- Non-zero linear correlation between P_y and v_1
- increasing with p_T
- highest for $0.5<y<1$

Elliptic flow at NICA energies: Models vs. Data comparison

Experimental data is taken from: *Phys.Rev.C* 103 (2021) 3, 034908

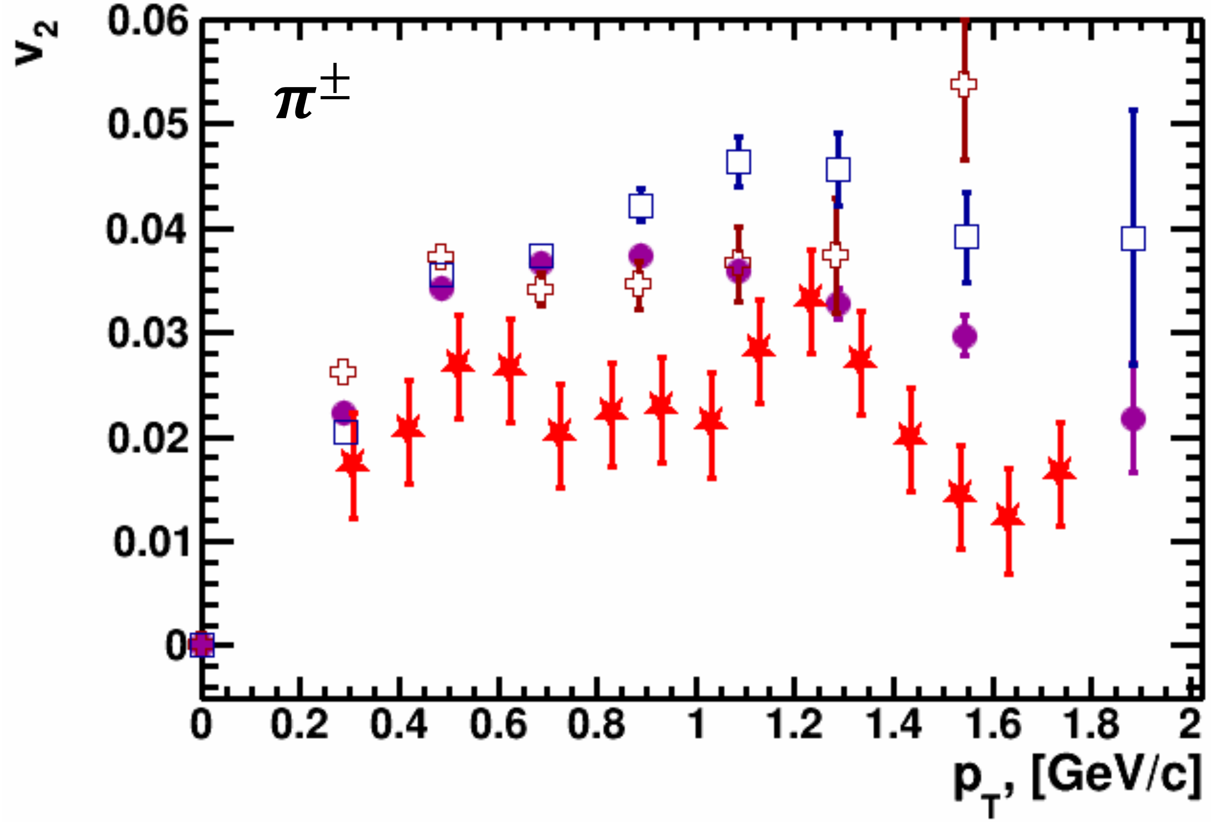

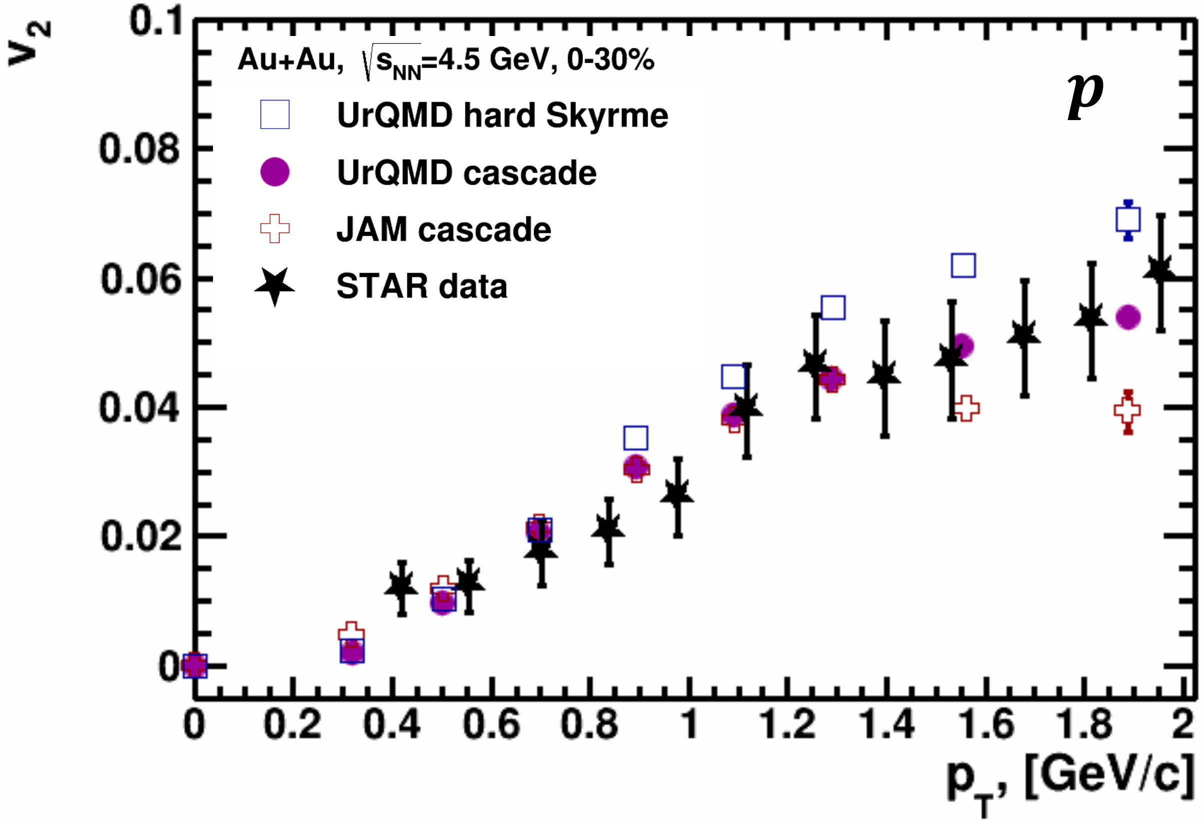

Pure String/Hadronic Cascade models give similar v_2 signal compared to STAR data for Au+Au $\sqrt{s_{NN}}$ =4.5 GeV

Symmetry energy in high-density region

X.X. Long, G.F. Wei, arXiv:2402.12912 (2024)

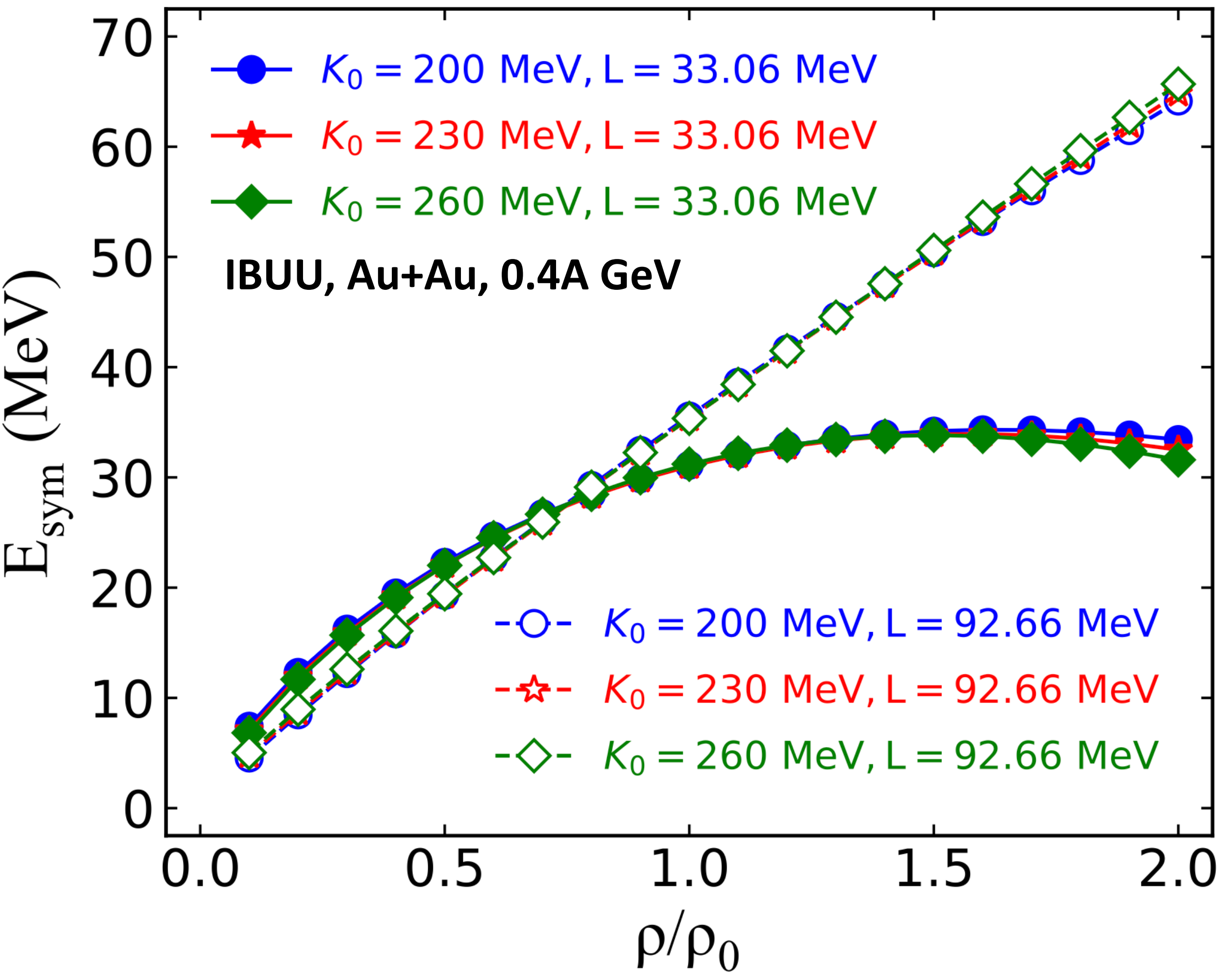

- Nuclotron-NICA density region:

$$\mathbf{2 \lesssim n_B/n_0 \lesssim 8}$$

- Symmetry energy E_{sym} has strong density dependence and can be described with its slope *L*:

$$L = 3\rho \frac{dE_{sym}(\rho)}{d\rho}$$

What observables can we use to extract information about *L*?

Using v_1^{np} to study L

X.X. Long, G.F. Wei, arXiv:2402.12912 (2024)

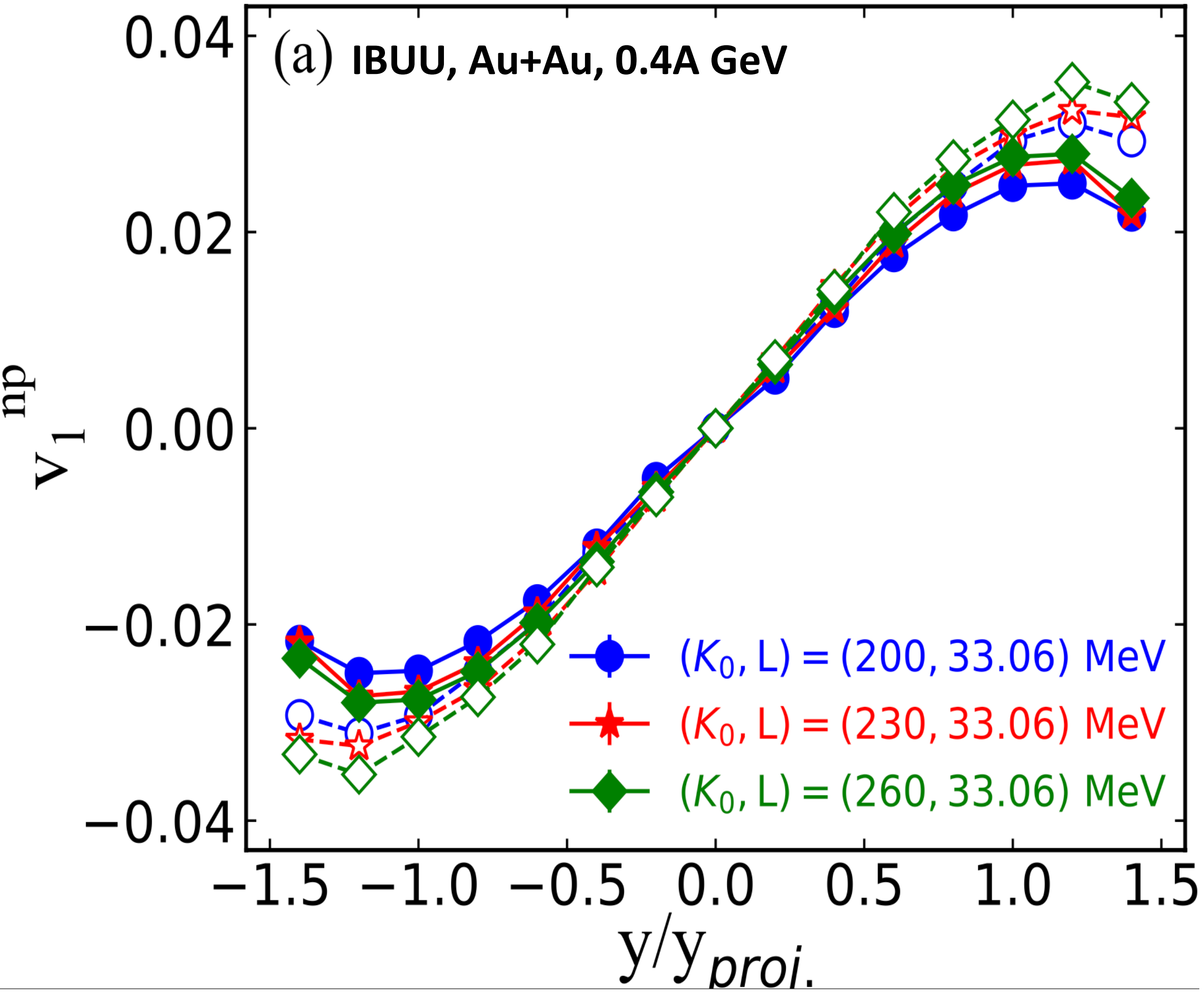

One can define free neutron-proton differential directed flow:

$$v_1^{np} = \frac{N_n(y)}{N(y)} \langle v_1^n(y) \rangle - \frac{N_p(y)}{N(y)} \langle v_1^p(y) \rangle$$

- v_1^{np} sensitive to both K_0 and L which may lead to ambigous interpretation
  - More observables might be necessary for robust study of L

Using $dN/dy\,(n,p)$, $dN/dE_{kin}(n,p)$ to study L

X.X. Long, G.F. Wei, arXiv:2402.12912 (2024)

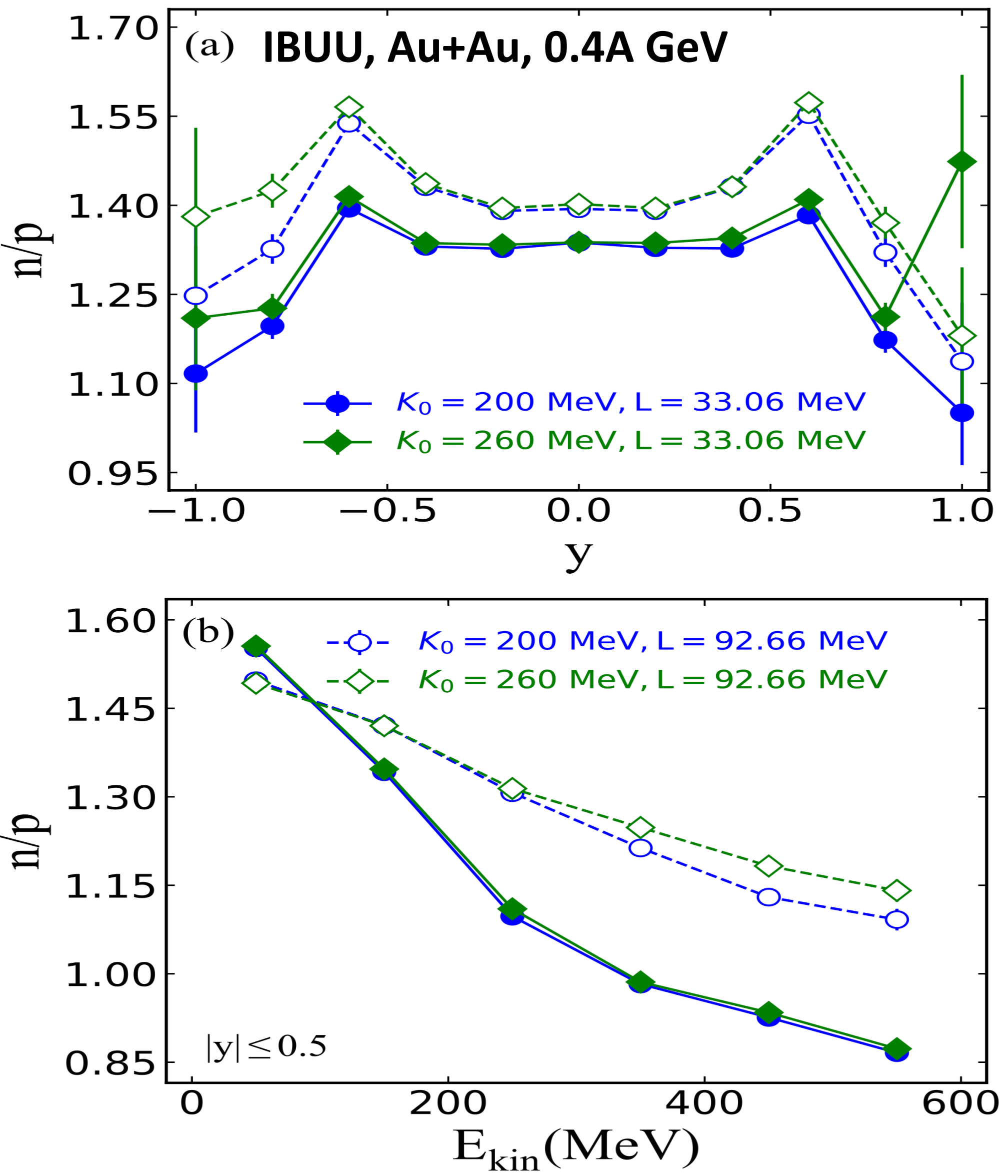

Rapidity and kinetic energy distributions of n/p ratios can be used to study L

- n/p ratios show strong dependence on L and significantly weaker dependence on K_0
- n/p ratios require less statistics than anisotropic flow measurements

Using $dN/dE_{kin}(\pi^+, \pi^-)$ to study L

X.X. Long, G.F. Wei, arXiv:2402.12912 (2024)

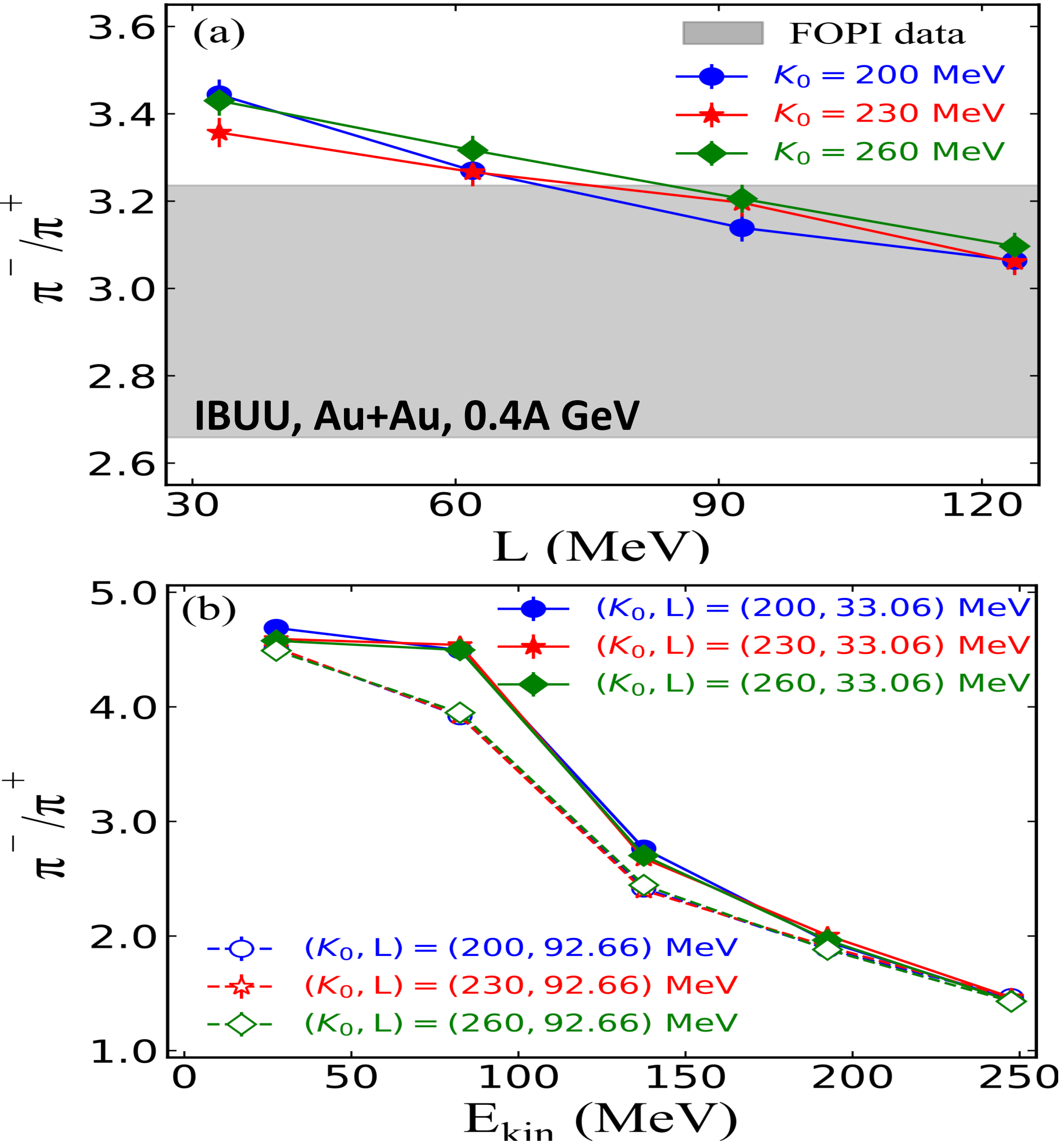

Rapidity and kinetic energy distributions of π^-/π^+ ratios can be used to study L

- Noticeable dependence on L and almost no sensitivity to K_0
- Requires less statistics than anisotropic flow measurements
- However, it might be a bit challenging to identify π^+ using TOF-400, TOF-700 near midrapidity at Nuclitron energies

MPD physics program

G. Feofilov, P. Parfenov

Global observables
- Total event multiplicity
- Total event energy
- Centrality determination
- Total cross-section measurement
- Event plane measurement at all rapidities
- Spectator measurement

V. Kolesnikov, Xianglei Zhu

Spectra of light flavor and hypernuclei
- Light flavor spectra
- Hyperons and hypernuclei
- Total particle yields and yield ratios
- Kinematic and chemical properties of the event
- Mapping QCD Phase Diag.

K. Mikhailov, A. Taranenko

Correlations and Fluctuations
- Collective flow for hadrons
- Vorticity, Λ polarization
- E-by-E fluctuation of multiplicity, momentum and conserved quantities
- Femtoscopy
- Forward-Backward corr.
- Jet-like correlations

D. Peresunko, Chi Yang

Electromagnetic probes
- Electromagnetic calorimeter meas.
- Photons in ECAL and central barrel
- Low mass dilepton spectra in-medium modification of resonances and intermediate mass region

Wangmei Zha, A. Zinchenko

Heavy flavor
- Study of open charm production
- Charmonium with ECAL and central barrel
- Charmed meson through secondary vertices in ITS and HF electrons
- Explore production at charm threshold

Methods for v_n measurements in MPD-CLD

- **Sub-event 2-particle Q-cumulants v2{2}:**

Δη=0.1 is applied between 2 sub-events A, B to suppress non-flow

$$Q_n = \sum_{i=1}^{M} e^{in\phi} \qquad \langle 2\rangle_{a|b} = \frac{Q_{n_a} Q^*_{n,b}}{M_a M_b} \qquad v_2\{2\} = \sqrt{\langle\langle 2\rangle\rangle_{a|b}}$$

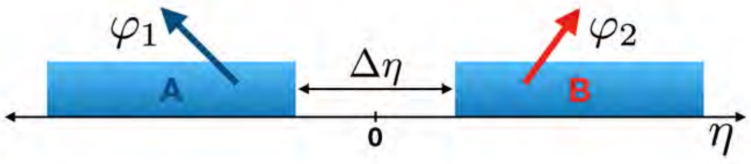

- **4-particle Q-cumulants v2{4}**

$$\langle 2\rangle = \frac{|Q_n|^2 - M}{M(M-1)} \qquad v_2\{4\} = \sqrt[4]{2\langle\langle 2\rangle\rangle^2 - \langle\langle 4\rangle\rangle}$$

$$\langle 4\rangle = \frac{|Q_n|^4 + |Q_{2n}|^2 - 2\Re[Q_{2n}Q^*_n Q^*_n] - 4(M-2)|Q_n|^2 - 2M(M-3)}{M(M-1)(M-2)(M-3)}$$

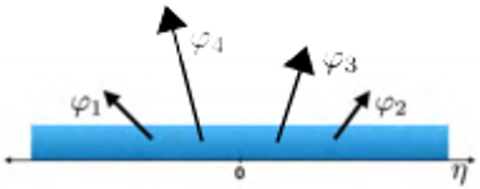

- **Event plane method:** Δη=0.1

$$Q_{n,x} = \sum_i w_i \cos(n\phi_i) \qquad Q_{n,y} = \sum_i w_i \sin(n\phi_i)$$

$$\Psi_n^{EP} = \frac{1}{n}\tan^{-1}\left(\frac{Q_{n,y}}{Q_{n,x}}\right) \qquad v_n = \frac{\langle \cos[n(\phi - \Psi_n^{EP})]\rangle}{\sqrt{\langle \cos[n(\Psi_{n,a} - \Psi_{n,b})]\rangle}}$$

Here: ω_i - $p_{T,i}$ transverse momentum of the i-th track in the TPC

φ_i - azimuthal angle of the i-th track in the TPC

Ψ_n- event plane angles

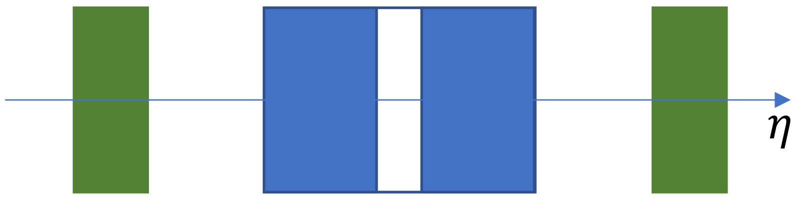

Method's details described in PRC 83 (2011), 044913 , EP method: Phys.Rev.C 77 (2008) 034904

Λ selection in MpdRoot framework

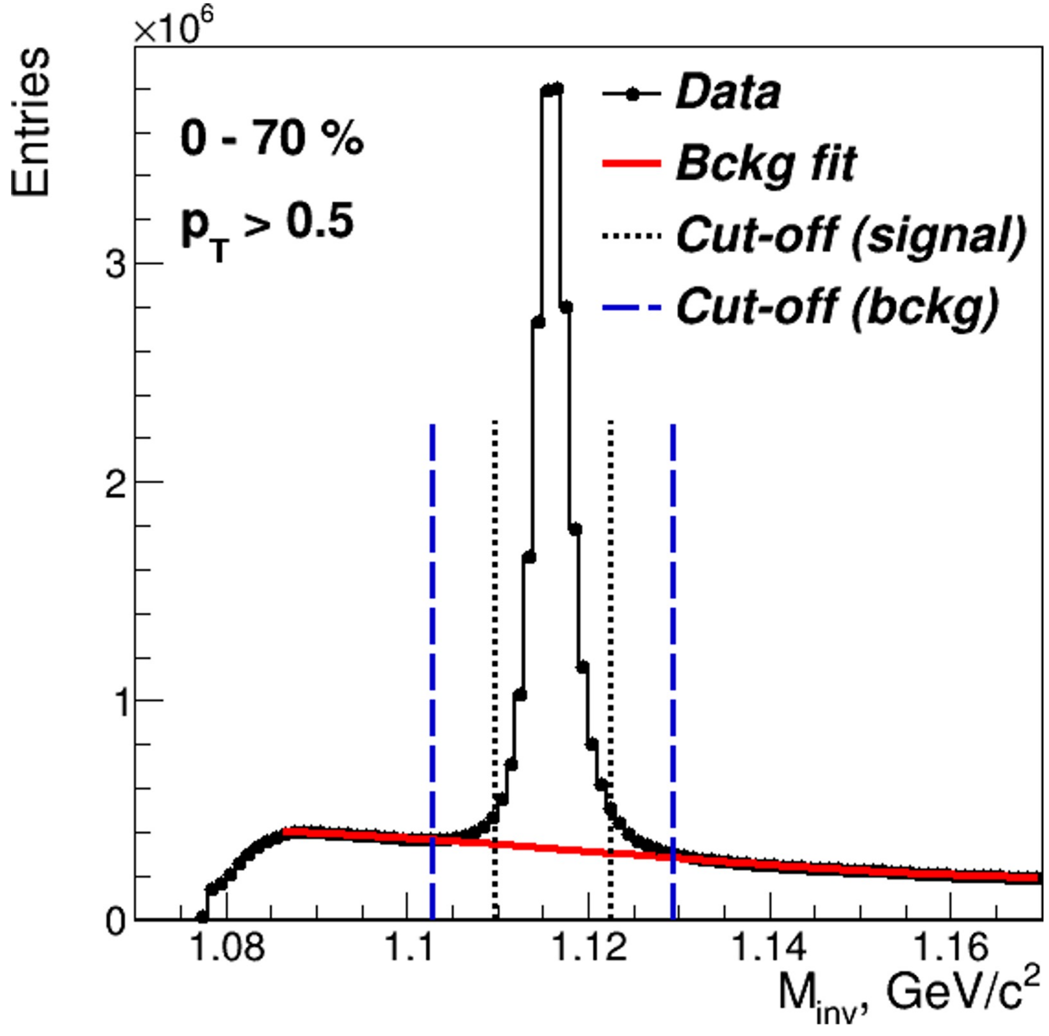

Fitting procedure (sideband method):

- Global fit (Gauss + Legendre polynomials)
- Background fit in sidebands (± 7σ)
- Signal Cut-off: <M>± 3σ
- Λ selection criteria:
  - «ω»-selection (1 parameter)
  - «χ»-selection (5 parameters)

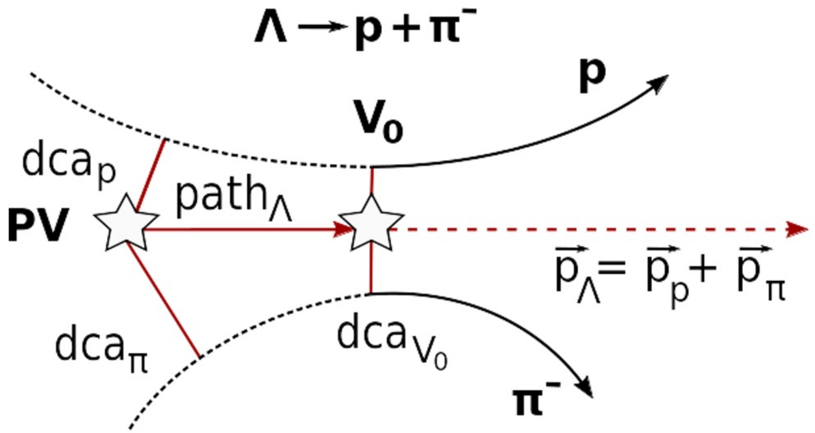

$$\omega_2 = \ln \frac{\sqrt{\chi_\pi^2 \chi_p^2}}{\chi_\Lambda^2 + \chi_{V_0}^2}$$

Anisotropic flow of V0 particles

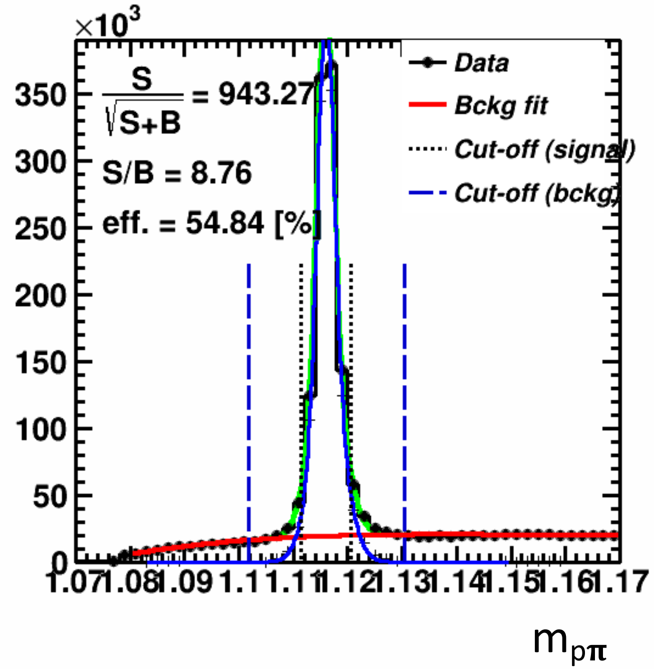

Differential flow can be defined using the following fit:

$$v_n^{SB}(m_{inv}) = v_n^S \frac{N^S(m_{inv})}{N^{SB}(m_{inv})} + v_n^B(m_{inv}) \frac{N^B(m_{inv})}{N^{SB}(m_{inv})}$$

where:

- v_n^S - signal anisotropic flow (set as a parameter in the fit)
- $v_n^B(m_{inv})$ - background flow (set as polynomial function)
- $N^{SB}(m_{inv})$ - m_{inv} distribution (signal + background)
- $N^S(m_{inv})$ - m_{inv} signal distribution
- $N^B(m_{inv})$ - m_{inv} background distribution

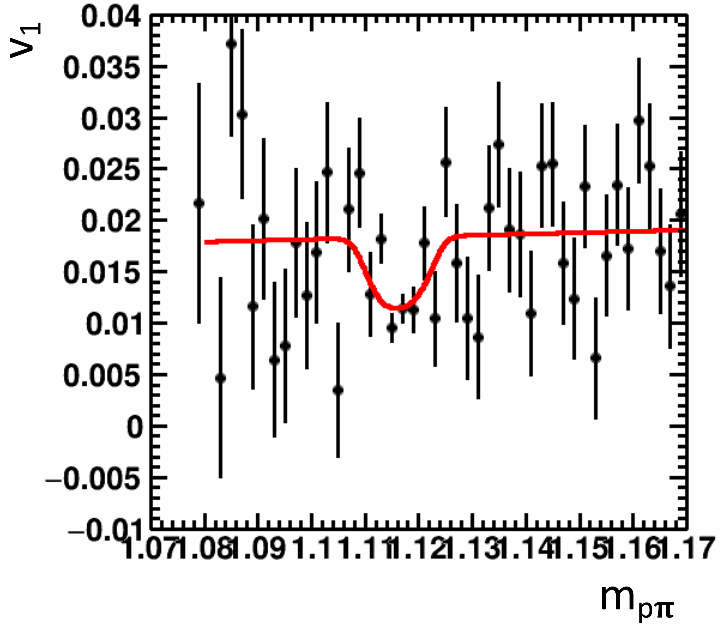

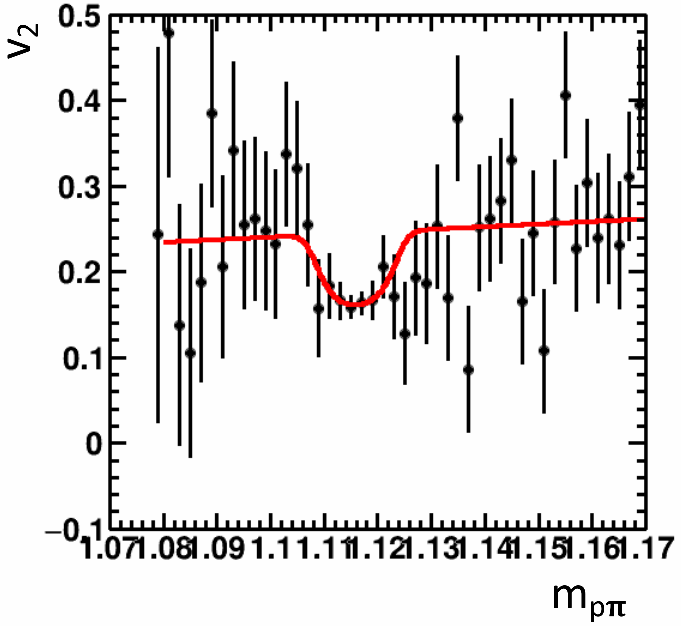

Flow vectors for MPD-FXT case

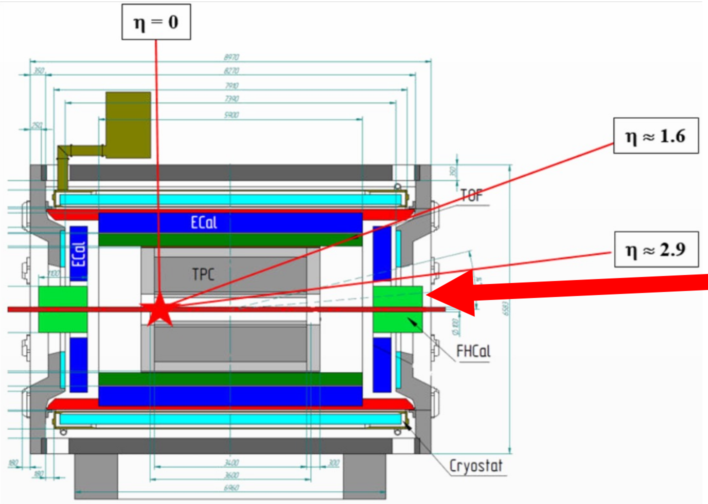

Modules of FHCal divided into 3 groups

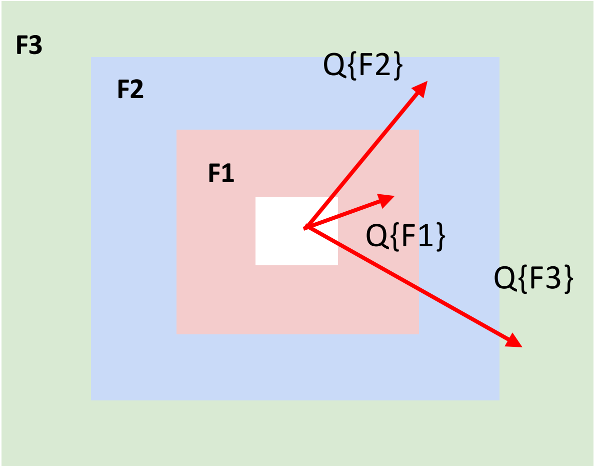

From momentum of each measured particle define a u_n-vector in transverse plane:

$$u_n = e^{in\phi}$$

where ϕ is the azimuthal angle

Sum over a group of u_n-vectors in one event forms Q_n-vector:

$$Q_n = \frac{\sum_{k=1}^{N} w_n^k u_n^k}{\sum_{k=1}^{N} w_n^k} = |Q_n| e^{in\Psi_n^{EP}}$$

Ψ_n^{EP} is the event plane angle

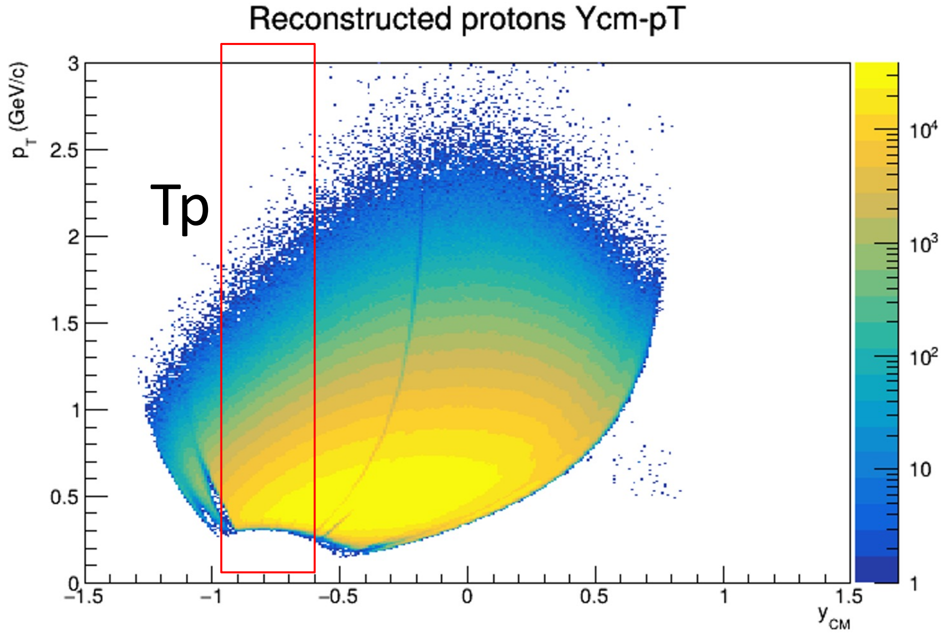

Additional subevents from tracks not pointing at FHCal:
Tp: p; -1.0<y<-0.6;

Flow methods for v_n calculation

Tested in HADES: M Mamaev et al 2020 PPNuclei 53, 277–281
M Mamaev et al 2020 J. Phys.: Conf. Ser. 1690 012122

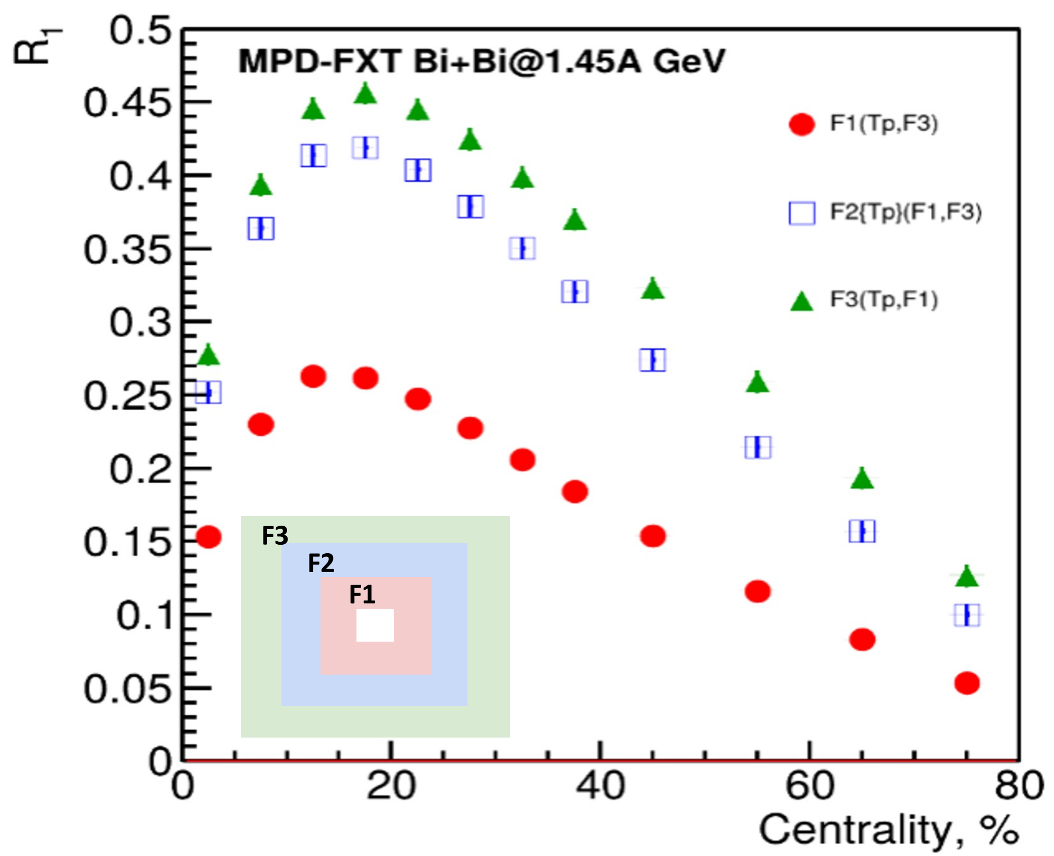

Scalar product (SP) method:

$$v_1 = \frac{\langle u_1 Q_1^{F1} \rangle}{R_1^{F1}} \qquad v_2 = \frac{\langle u_2 Q_1^{F1} Q_1^{F3} \rangle}{R_1^{F1} R_1^{F3}}$$

Where R_1 is the resolution correction factor

$$R_1^{F1} = \langle \cos(\Psi_1^{F1} - \Psi_1^{RP}) \rangle$$

Symbol “F2(F1,F3)” means R_1 calculated via (3S resolution):

$$R_1^{F2(F1,F3)} = \frac{\sqrt{\langle Q_1^{F2} Q_1^{F1} \rangle \langle Q_1^{F2} Q_1^{F3} \rangle}}{\sqrt{\langle Q_1^{F1} Q_1^{F3} \rangle}}$$

Symbol “F2{Tp}(F1,F3)” means R_1 calculated via (4S resolution):

$$R_1^{F2\{Tp\}(F1,F3)} = \langle Q_1^{F2} Q_1^{Tp} \rangle \frac{\sqrt{\langle Q_1^{F1} Q_1^{F3} \rangle}}{\sqrt{\langle Q_1^{Tp} Q_1^{F1} \rangle \langle Q_1^{Tp} Q_1^{F3} \rangle}}$$

P_H measurements: inv. mass fit method

- Use invariant mass distribution
- Calculate Sig/All, Bg/All ratios
- Fit <sin($\mathbf{\Psi}_{EP}$ - φ_p^*)> as a function of inv. mass:

$$P^{SB}(m_{inv},p_T) = P^S(p_T)\frac{N^S(m_{inv},p_T)}{N^{SB}(m_{inv},p_T)} + P^B(m_{inv},p_T)\frac{N^B(m_{inv},p_T)}{N^{SB}(m_{inv},p_T)}$$

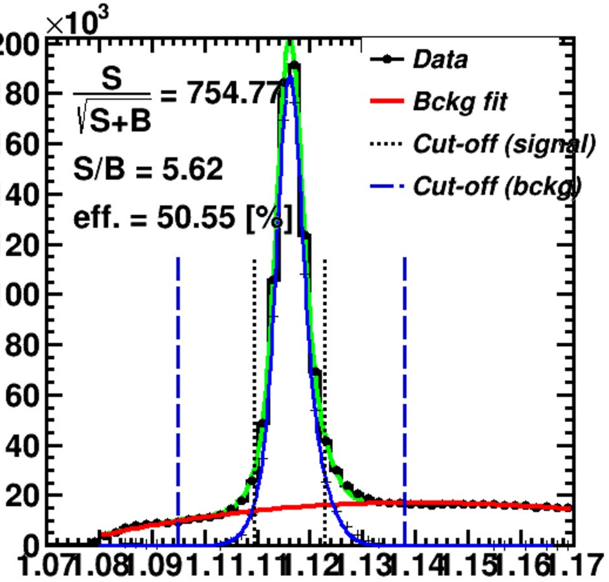

- Use $P^S(p_T)$ = <sin($\mathbf{\Psi}_{RP}$ - φ_p^*)>^{sig} to find P_H^{true} using fit:

$$\frac{8}{\pi\alpha_\Lambda}\frac{1}{R_{EP}^{(1)}}\langle\sin(\Psi_1 - \phi_p^\star)\rangle^{sig} = \overline{P_\Lambda}^{true} + cv_1\sin(\phi_\Lambda - \phi_p^\star)$$

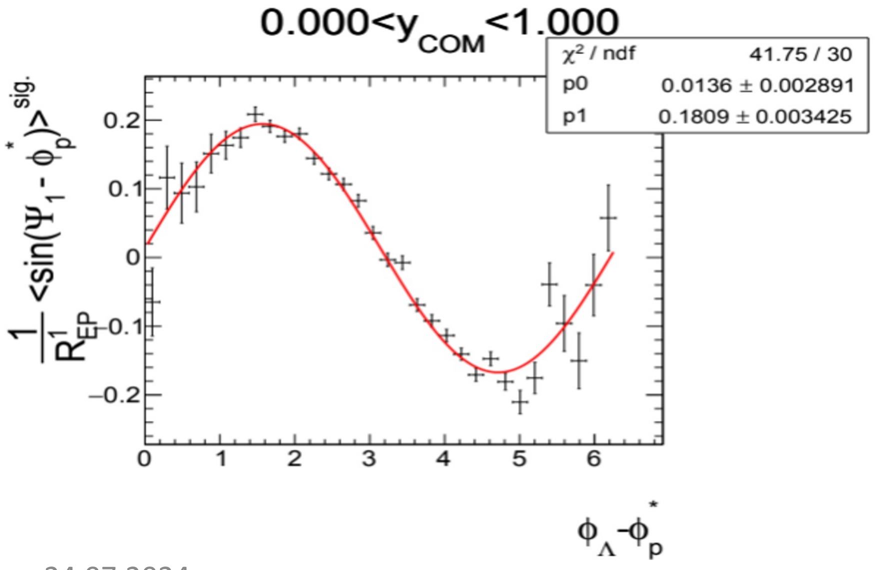

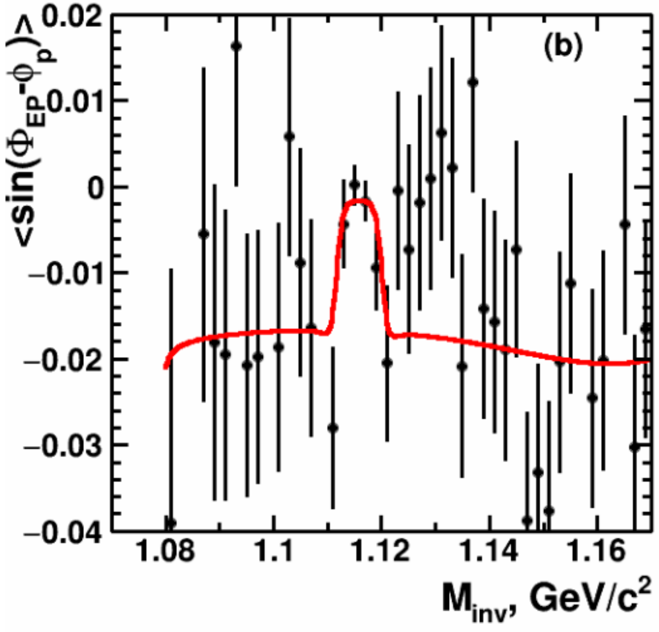

Last fit corrects effects of directed flow and acceptance contributions to P_H

Sensitivity of the collective flow to the EOS

A. Sorensen et. al., Prog.Part.Nucl.Phys. 134 (2024) 104080

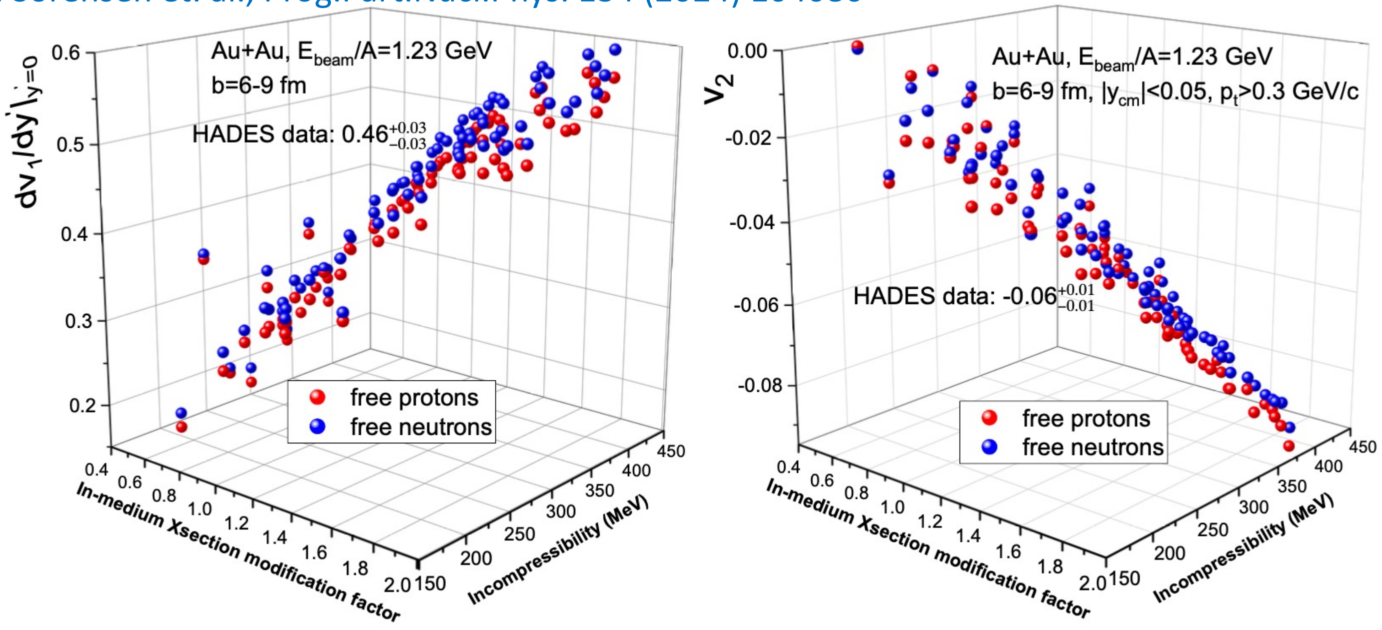

A. Sorensen et. al., Prog.Part.Nucl.Phys. 134 (2024) 104080

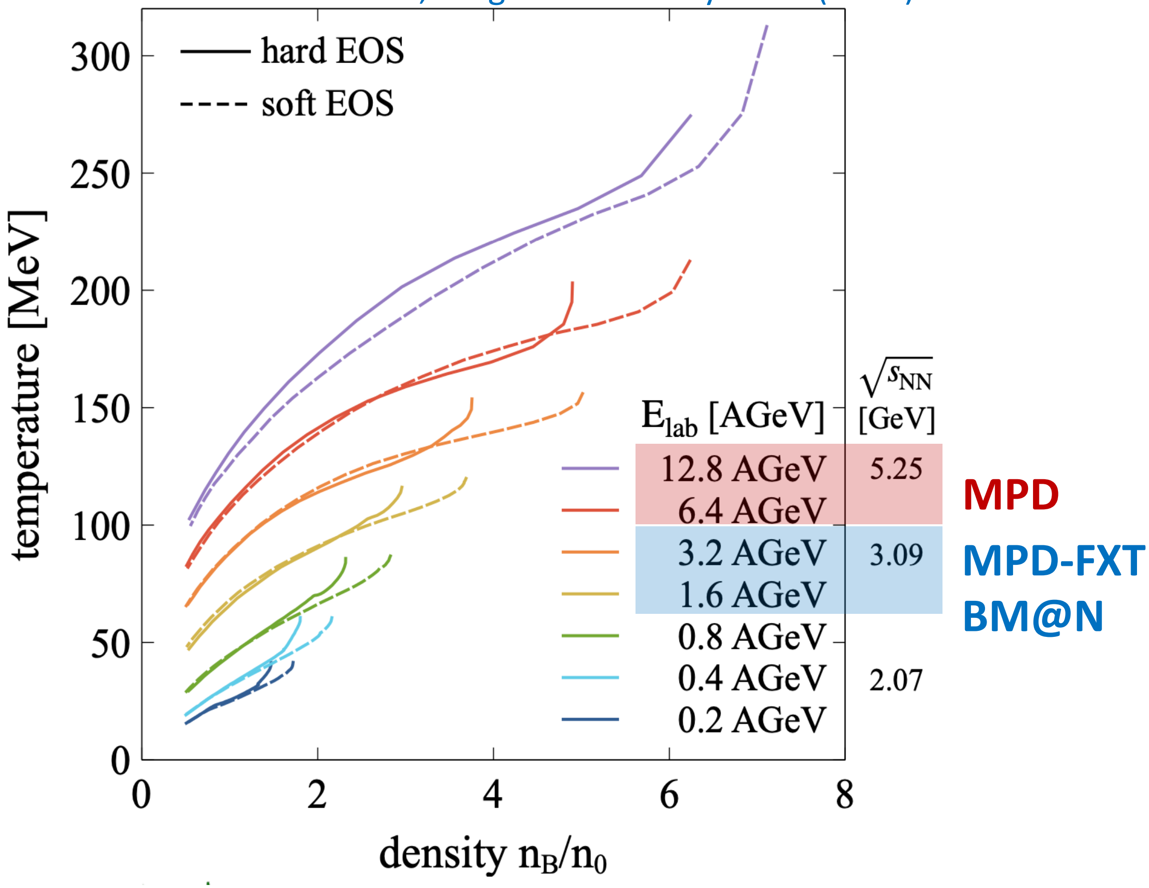

Incompressibility K_0:
parameter which specifies the behavior of EOS in the given baryon densities $K_0 = K_0(n_B)$

Models with flexible EOS for different (K_0, n_B) are required

Nuclotron-NICA coverage in terms of density: $2 \lesssim n_B/n_0 \lesssim 8$

Sensitivity of the collective flow to the EOS

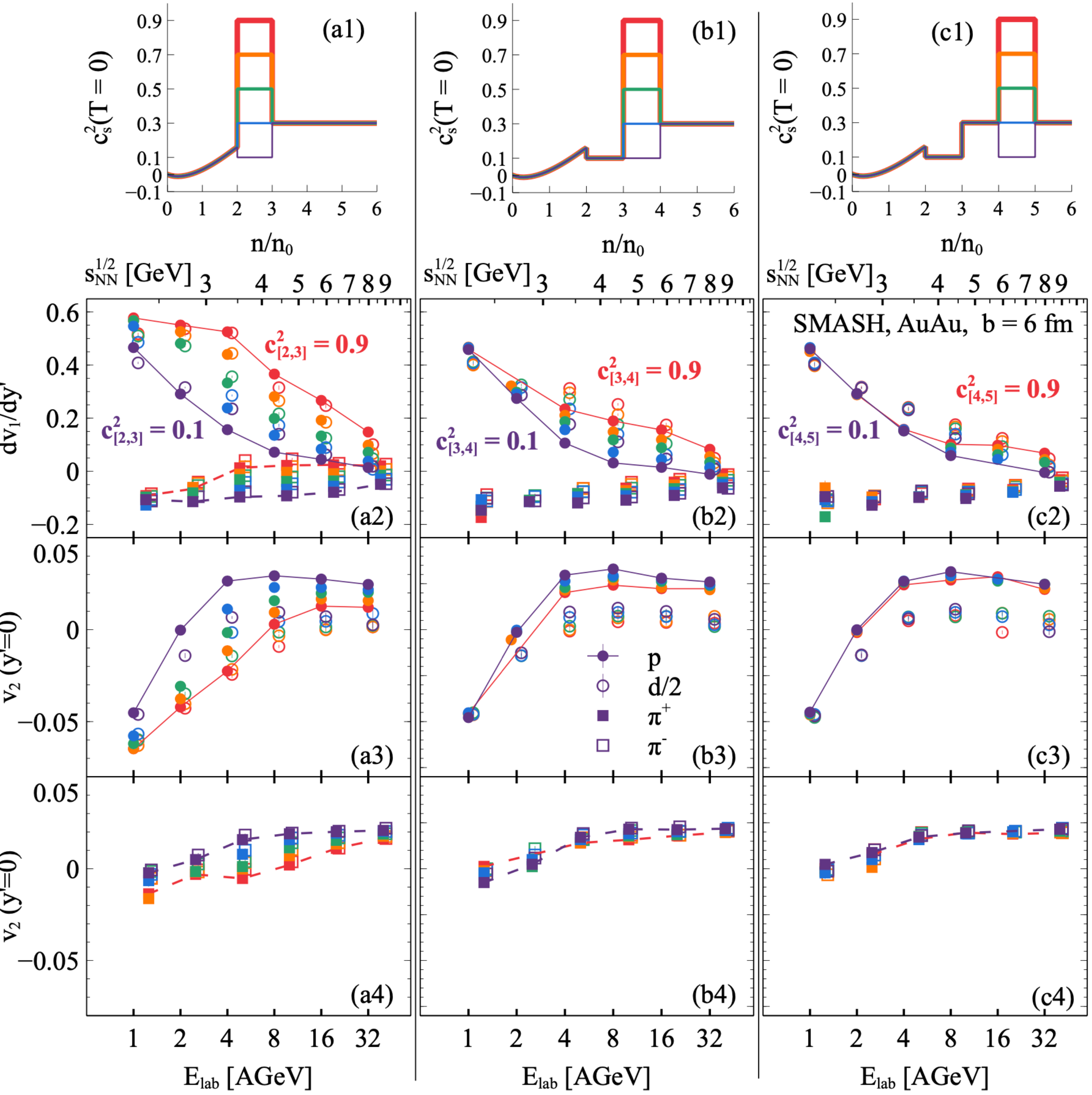

A. Sorensen et. al., Prog.Part.Nucl.Phys. 134 (2024) 104080

- SMASH model with flexible EOS was used to test the sensitivity of the v_n to changes of EOS in a specific density range n/n_0:
    - $\mathbf{2 < n_B/n_0 < 3}$: dv_1/dy' and v_2 of pions, protons and deuterons are very sensitive to the EOS
    - $\mathbf{3 < n_B/n_0 < 4}$: dv_1/dy' and v_2 of protons and deuterons are sensitive to the EOS
    - $\mathbf{4 < n_B/n_0 < 5}$: weak sensitivity to the EOS

The most precise constraints can be achieved from the flow of identified hadrons (*π*±,*K*±,*p*,…) and light nuclei (*d*,*t*,…)

$v_n(y)$ in Au+Au $\sqrt{s_{NN}}$=2.4 GeV: cascade models

P. Parfenov, Particles 5, no.4, 561-579 (2022)

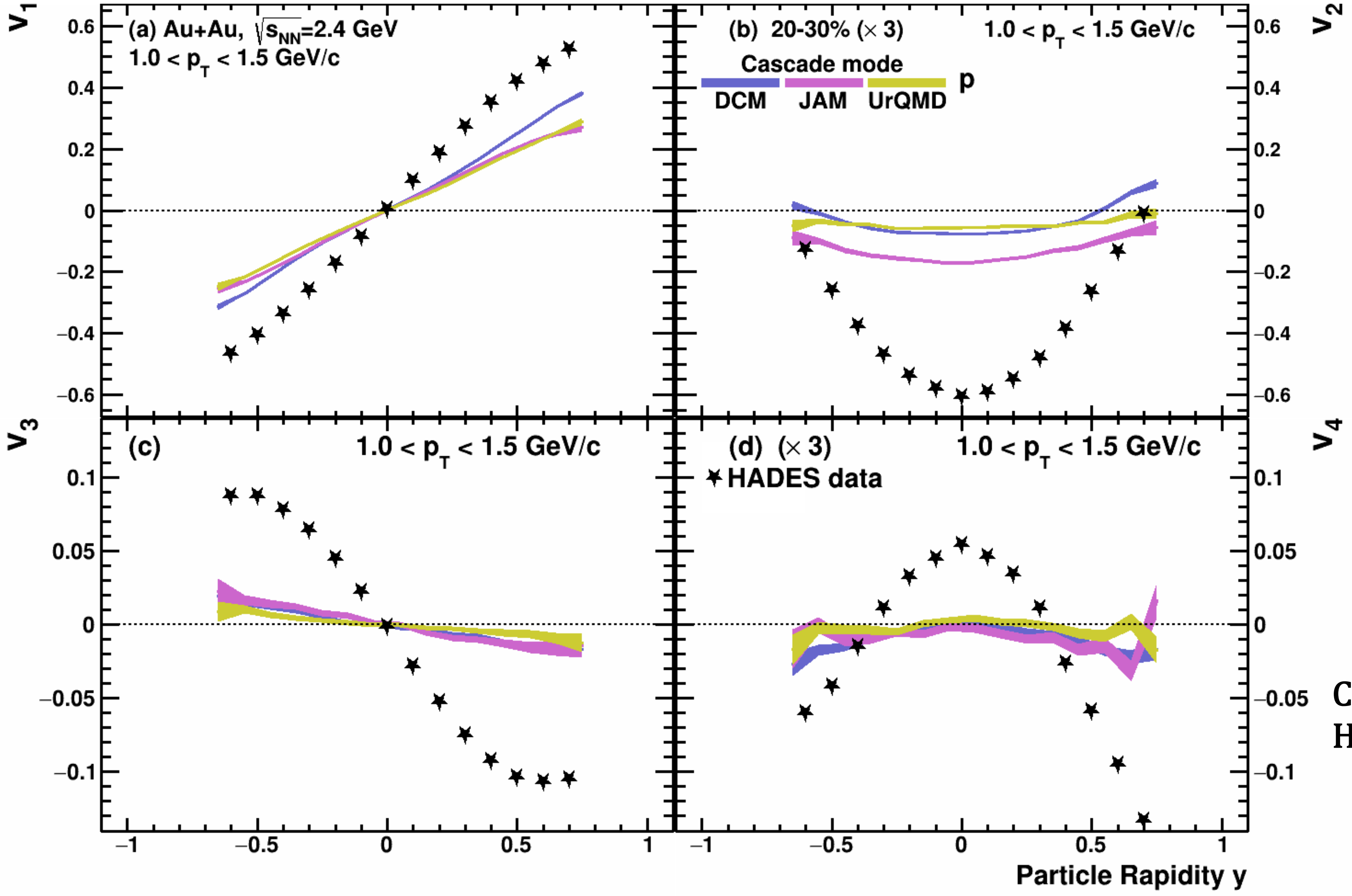

Kinematic cuts:
$V_{1,3}(y)$: 1.0 < pT < 1.5 GeV/c
$V_{2,4}(y)$: 1.0 < pT < 1.5 GeV/c

Cascade models fail to reproduce HADES experimental data

$v_n(y)$ in Au+Au $\sqrt{s_{NN}}$=2.4 GeV: models vs. HADES data

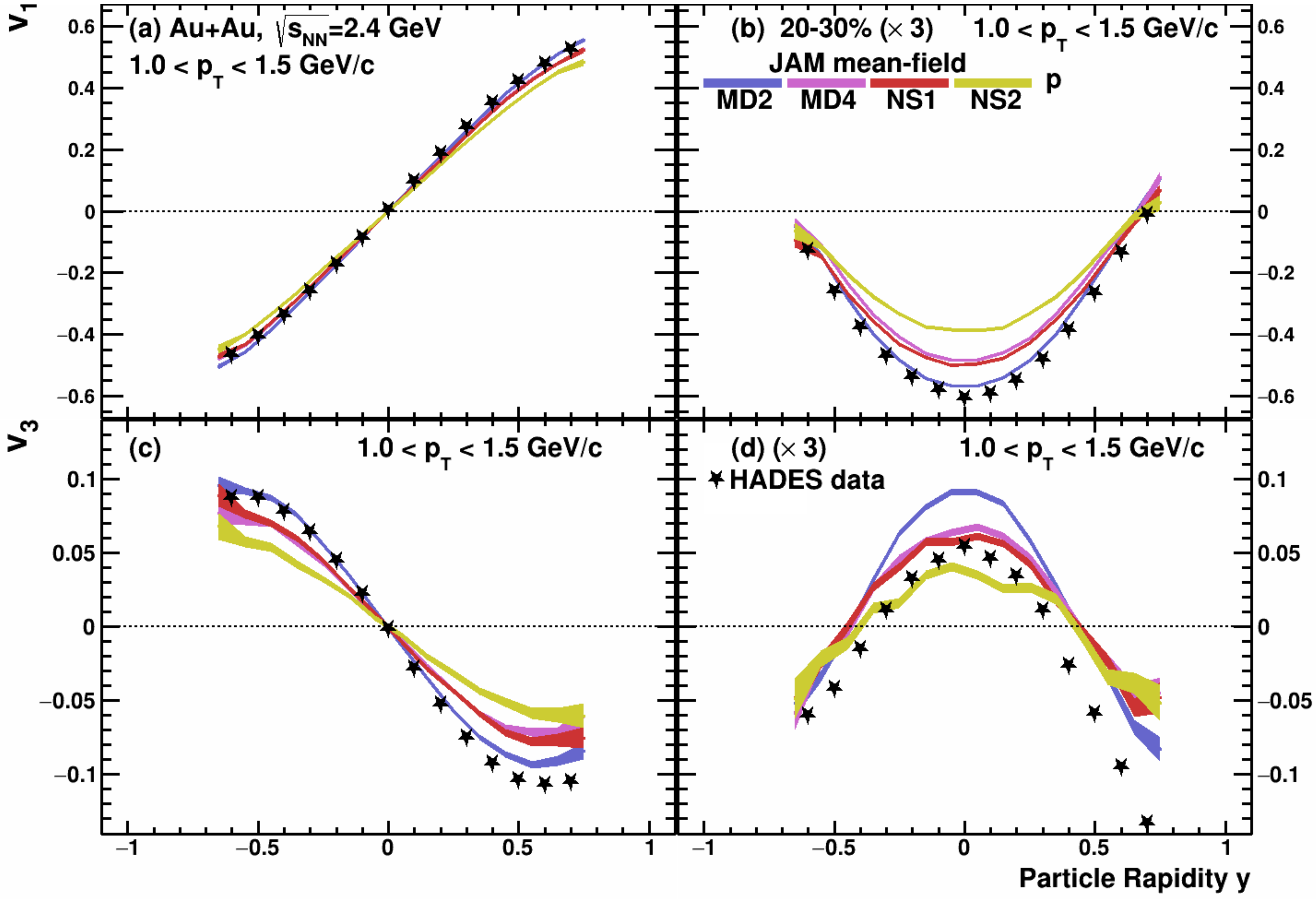

P. Parfenov, Particles 5, no.4, 561-579 (2022)

Kinematic cuts:
$V_{1,3}(y)$: 1.0 < pT < 1.5 GeV/c
$V_{2,4}(y)$: 1.0 < pT < 1.5 GeV/c

Good agreement for $v_n(y)$
Higher harmonics are more sensitive to different EOS than v_1

$v_n(y)$ in Au+Au $\sqrt{s_{NN}}$=2.4 GeV: models vs. HADES data

HADES, Eur. Phys. J. A 59 (2023) 4, 80

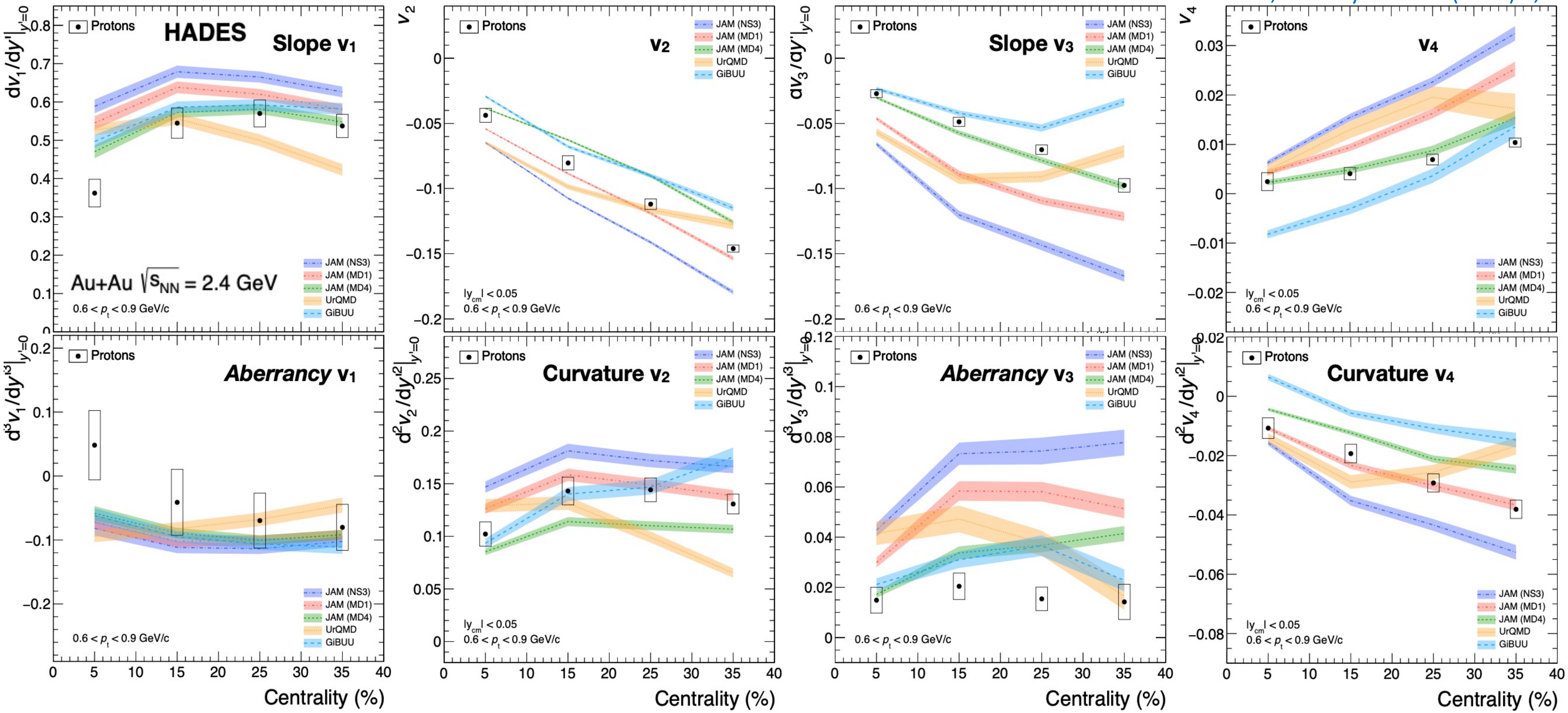

Overall trend reasonably well described, but no model works everywhere

$v_{1,2}(y)$ in Au+Au $\sqrt{s_{NN}}$=3 GeV: model vs. STAR data

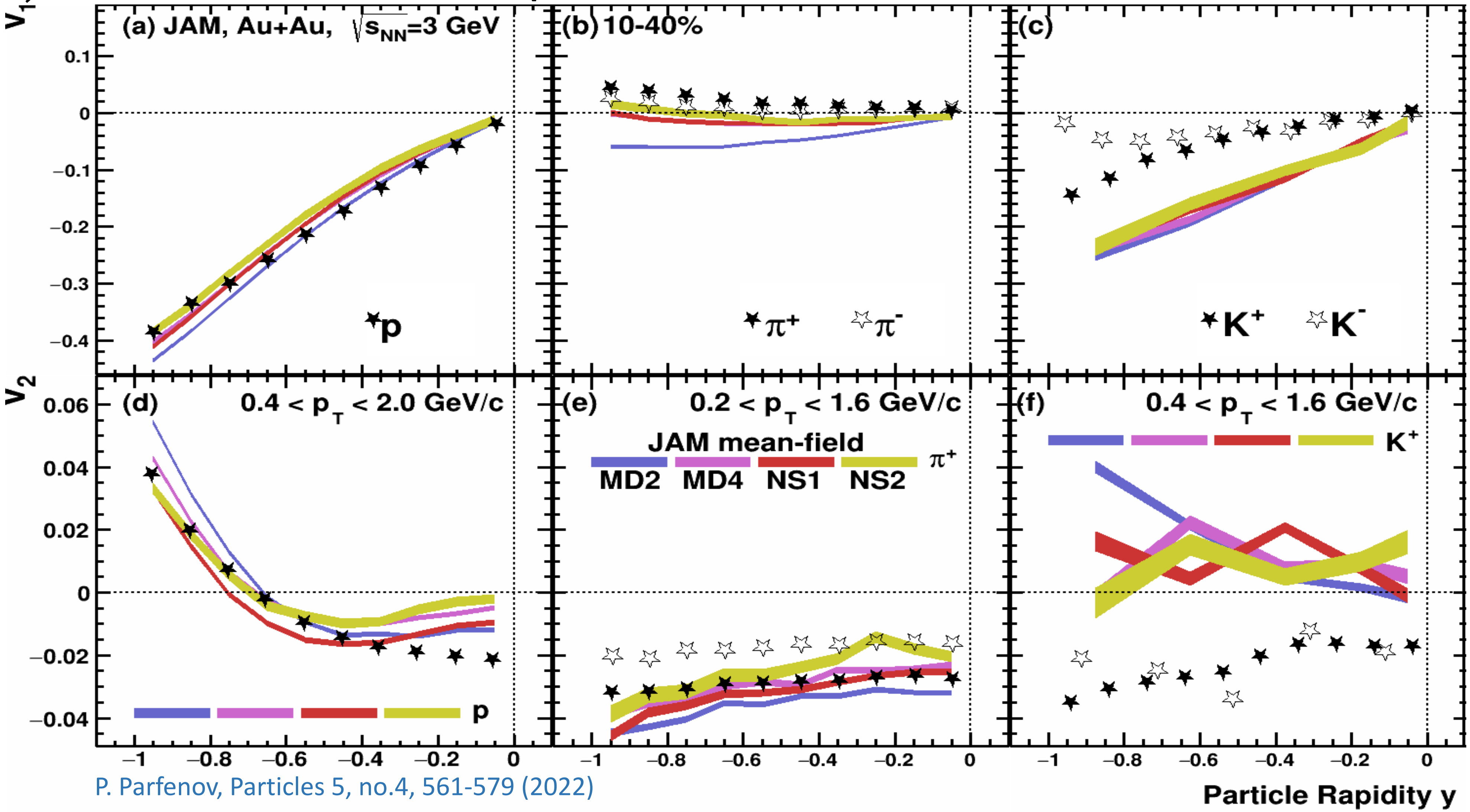

P. Parfenov, Particles 5, no.4, 561-579 (2022)

Models do not describe all particle species equally well

v_1, v_2 of protons are described by JAM, UrQMD (hard EOS) and SMASH (hard EOS with softening at higher densities)

v_2 transition from out-of-plane to in-plane

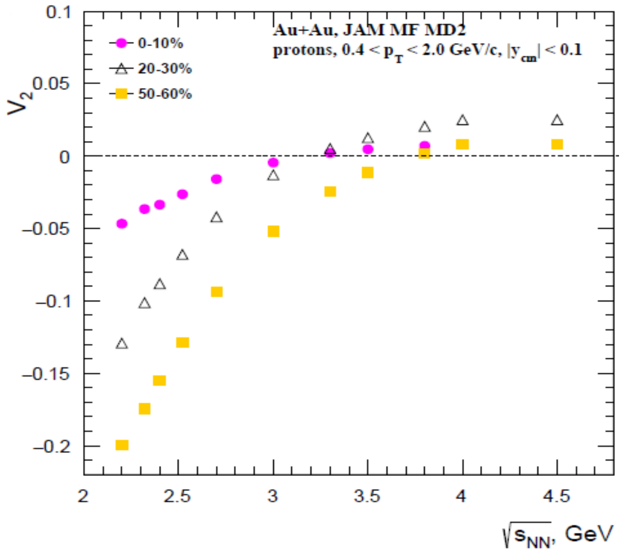

P. Parfenov, Particles 5, no.4, 561-579 (2022)

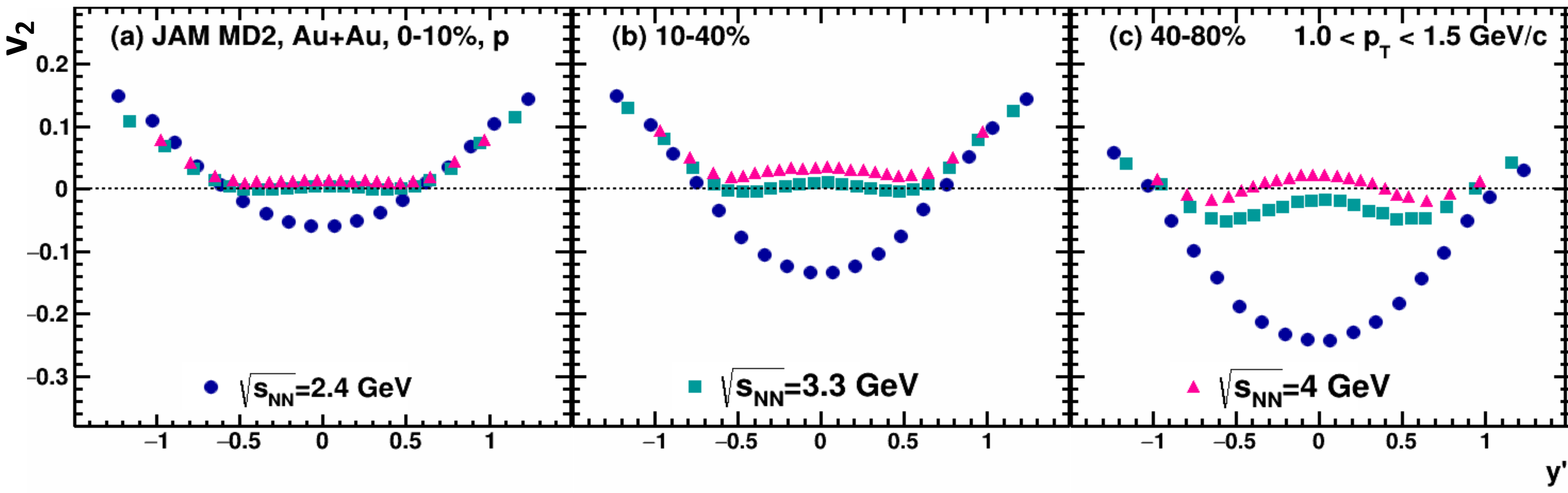

Results from QM 2023

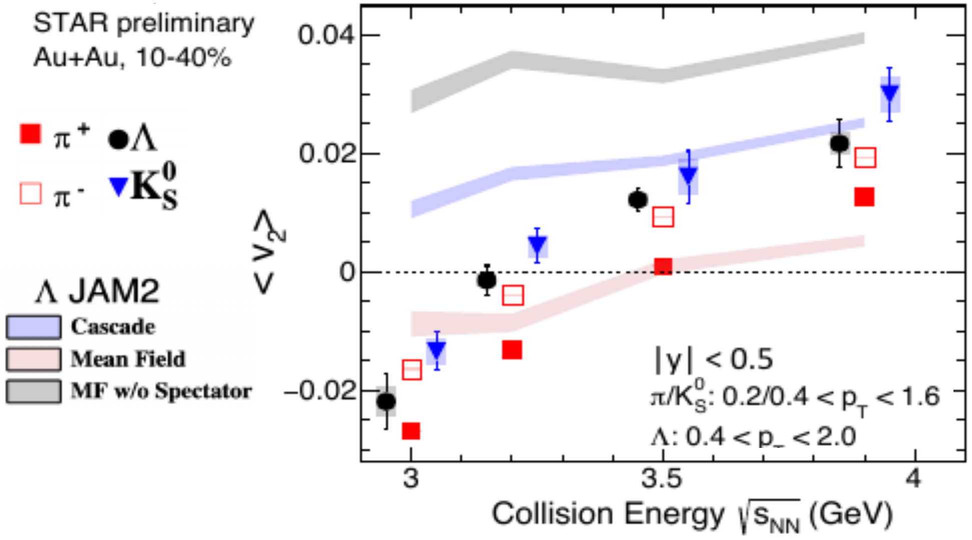

Transition of v_2 from out-of-plane to in-plane can be a good tool to constrain models and extract information about EOS

- $v_2 \approx 0$ in midrapirity at $\sqrt{s_{NN}}$=3.3 GeV for central and mid-central collisions for protons
- $v_2 < 0$ for peripheral collisions
- Models can not reproduce v_2 of $\pi^{\pm}$, $K^{\pm}$, $K^0{}_S$, Λ

Transition from out-of-plane to in-plane depends on centrality, rapidity and particle species

Event-wise flow correlations

B. Kardan, EMMI Workshop 2024

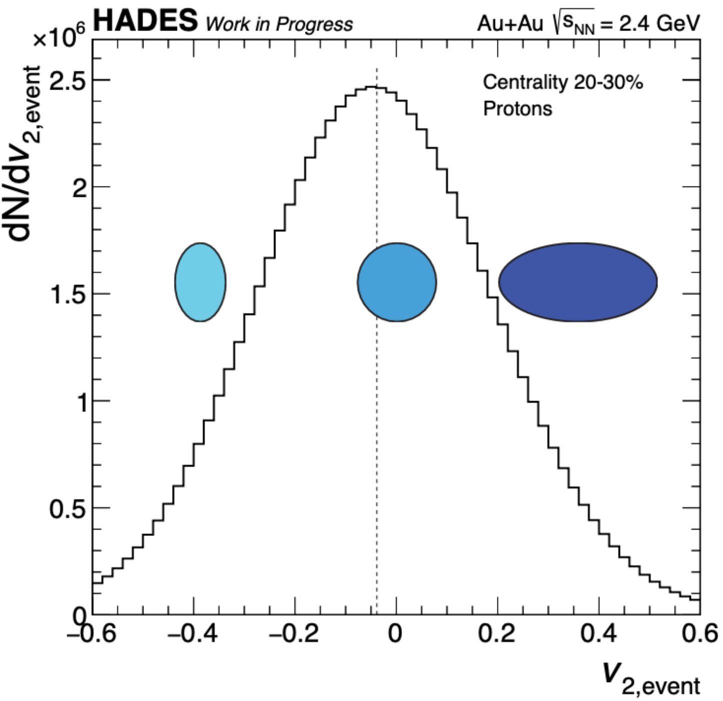

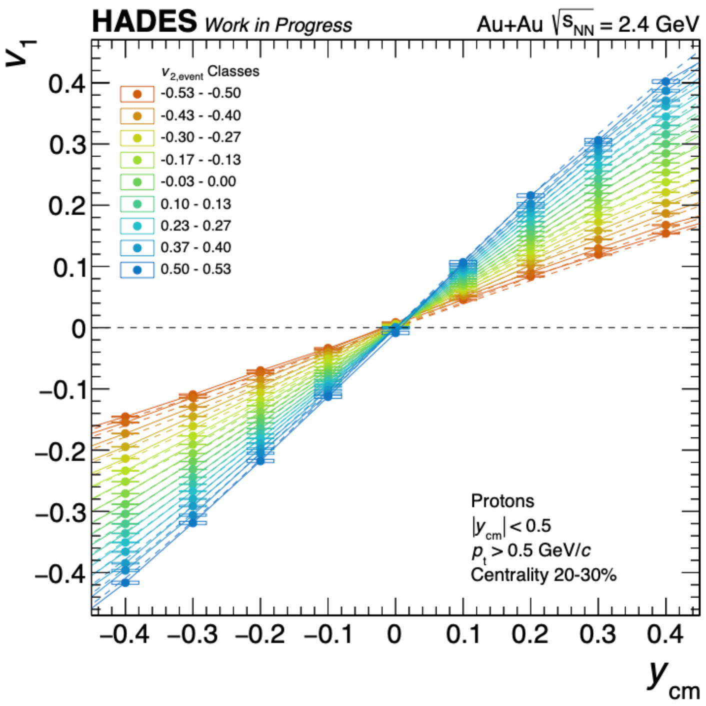

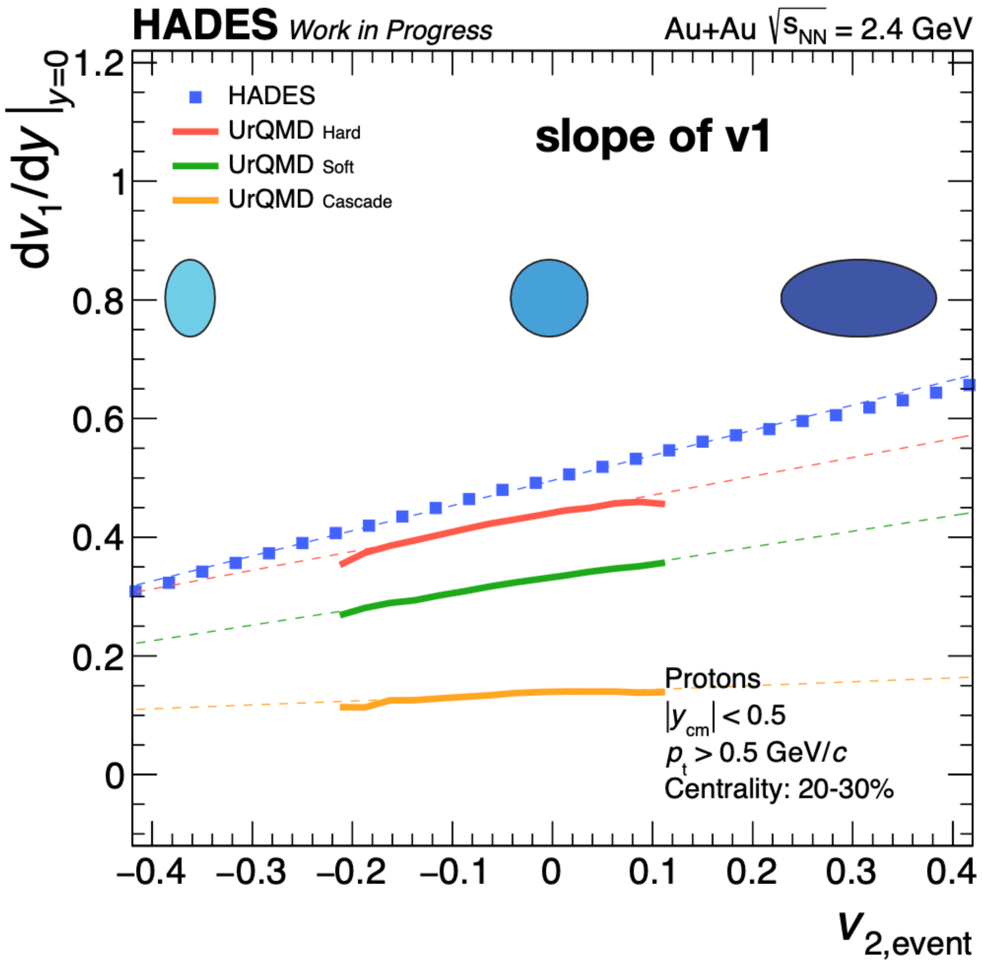

- Events can be characterized based on the event-wise magnitude of the elliptic flow $v_{2,event}$
- UrQMD can not discribe $dv_1/dy|_{y=0}$ of protons as a function of $v_{2,event}$
- Strong sensitivity to the EOS

Event-wise flow correlations

B. Kardan, EMMI Workshop 2024

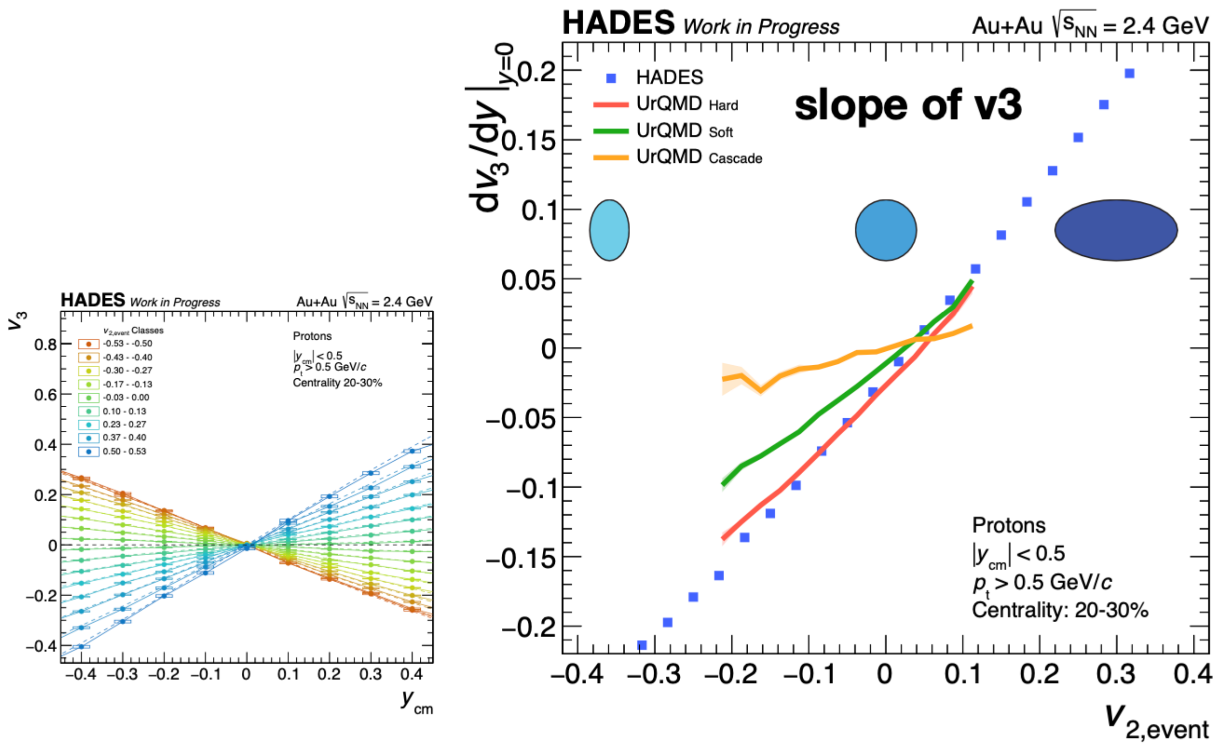

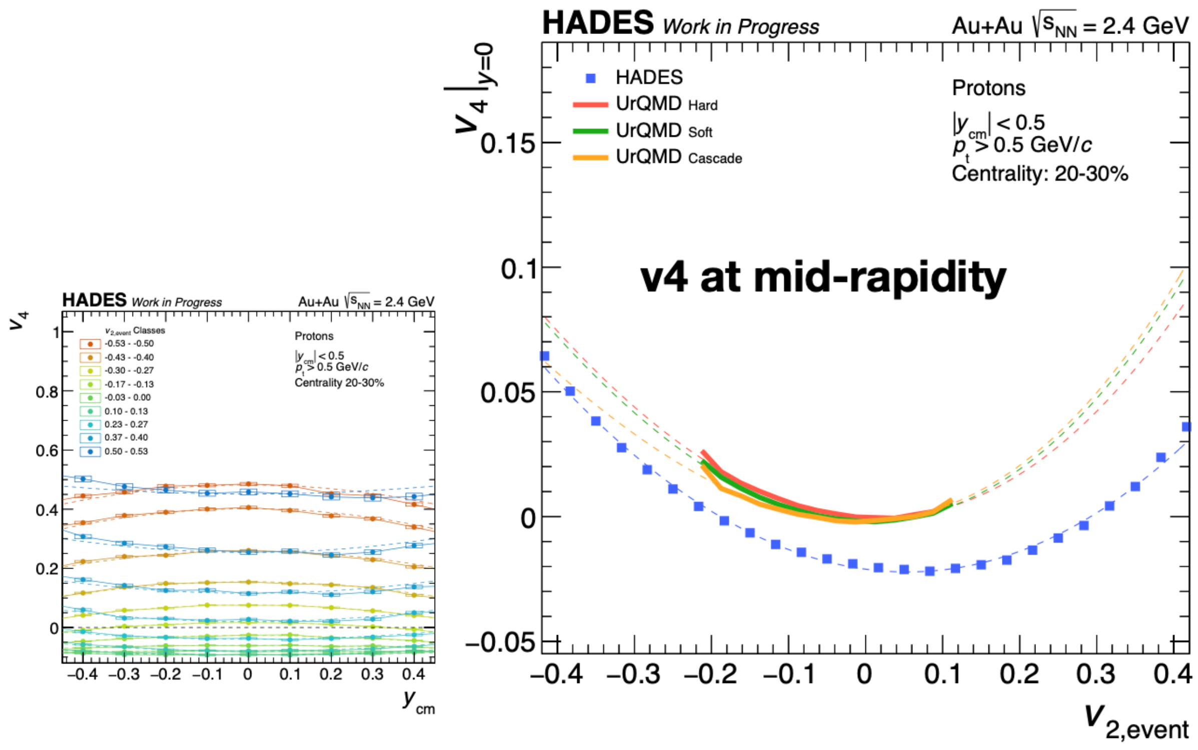

$dv_3/dy|_{y=0}$ of protons as a function of $v_{2,event}$ shows strong sensitivity to EoS

Models overestimate v_4 of protons as a function of $v_{2,event}$ compared to the HADES data

Mean-field models do not reproduce experimental data on the event-wise flow correlations of protons

New STAR results from BES-II

Results from QM 2023

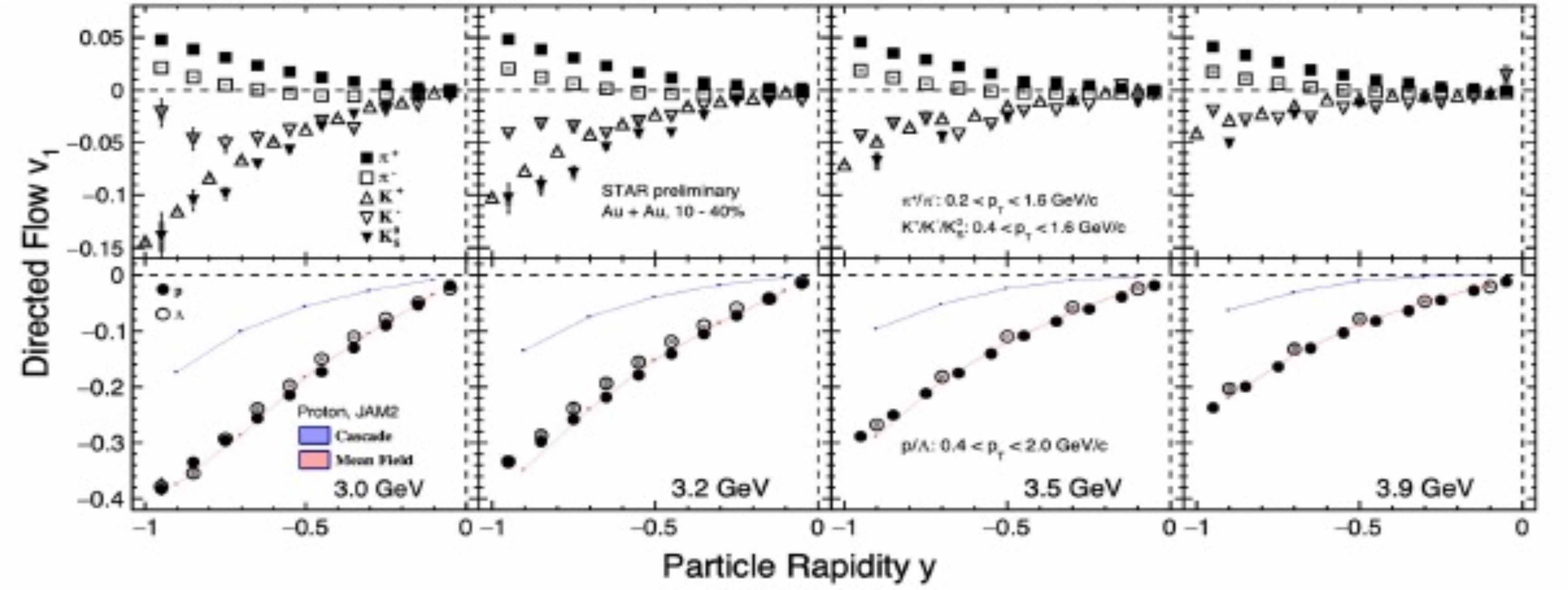

New preliminary results from STAR BES-II were presented at QM-2023 for Au+Au at $\sqrt{s_{NN}}$=3, 3.2, 3.5, 3.9 GeV

Feasibility studies: centralized analysis framework

Physics feasibility studies are done using centralized large-scale MC productions
Requirements for the analysis framework:

- Consistency of approaches and results across the collaboration – robust crosscheck of the analysis
- Ability to easily implement analysis in the framework – modular structure of the software, code standartization
- Easy data storage and reduced number of I/O operations – execution of the modules in one sequence

Solution: Analysis Train

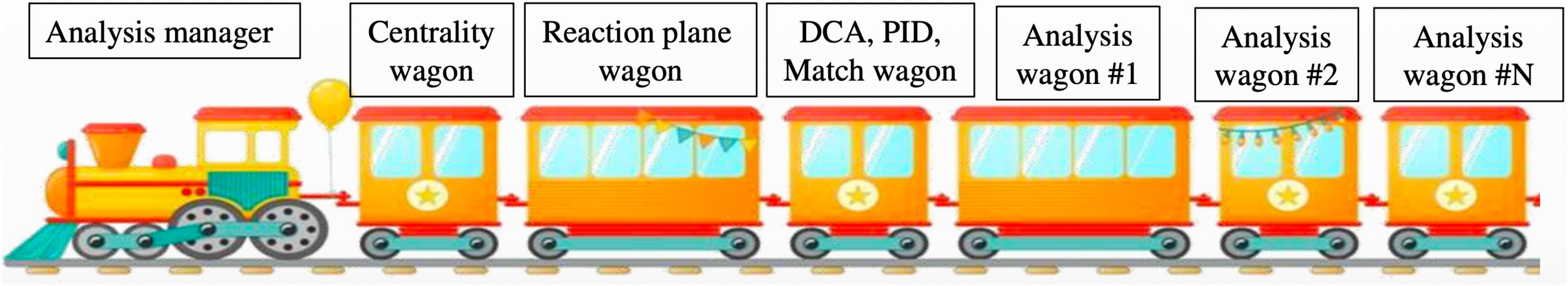

- First Analysis Train runs started in September 2023 – regular runs on request
- Continuous development:
  - Improvements to the current analysis wagons (improved PID parameters)
  - Implementation of the new wagons

Analysis Train became a new standard for physics (feasibility) studies in MPD

v_n at Nuclotron-NICA energies

P. DANIELEWICZ, R. LACEY, W. LYNCH
10.1126/science.1078070

v_1 suggests soft EoS | v_2 suggests hard EoS

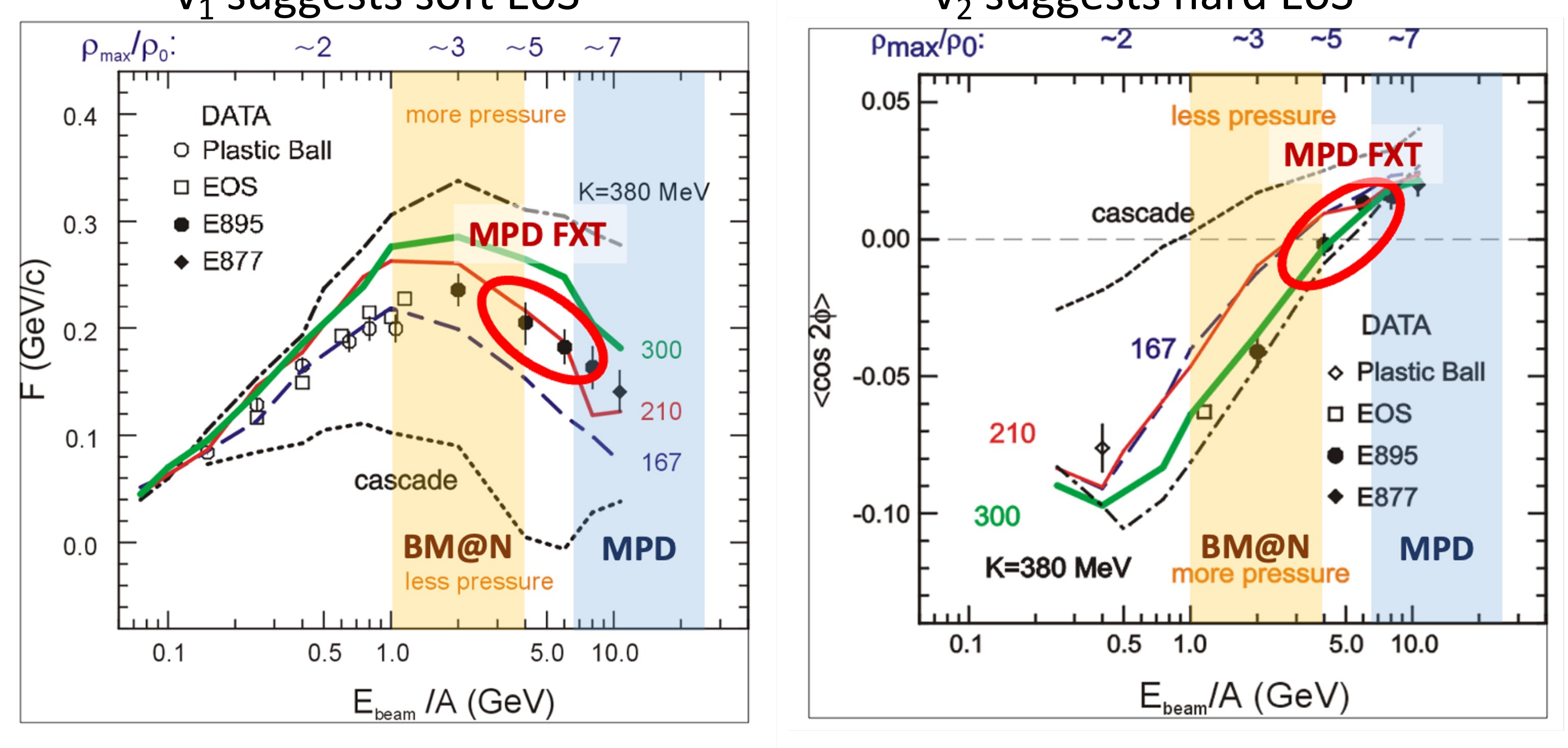

- **v_n results from the E895 experiment are ambiguous:**
  - v_1 suggests EoS and v_2 suggests hard EoS
- **Additional experimental data are required to address such discrepancies**

The Bayesian inversion method (Γ-fit)

Relation between multiplicity N_{ch} and impact parameter b is defined by

the fluctuation kernel:

$$P(N_{ch}|c_b) = \frac{1}{\Gamma(k(c_b))\theta^k} N_{ch}^{k(c_b)-1} e^{-n/\theta} \qquad \frac{\sigma^2}{\langle N_{ch} \rangle} = \theta \simeq const,\ k = \frac{\langle N_{ch} \rangle}{\theta}$$

$c_b = \int_0^b P(b')db'$ – centrality based on impact parameter

Mean multiplicity as a function of c_b can be defined as follows:

$$\langle N_{ch} \rangle = N_{knee} \exp\left(\sum_{j=1}^{3} a_j c_b^j \right)$$

N_{knee}, θ, a_j - 5 parameters

Fit function for N_{ch} distribution:

$$P(N_{ch}) = \int_0^1 P(N_{ch}|c_b)dc_b$$

b-distribution for a given N_{ch} range:

$$P(b|n_1 < N_{ch} < n_2) = P(b) \frac{\int_{n_1}^{n_2} P(N_{ch}|b)dN_{ch}}{\int_{n_1}^{n_2} P(N_{ch})dN_{ch}}$$

2 main steps of the method:

Fit experimental (model) distribution with P(N)

↓

Construct P(b|E) using Bayes’ theorem: P(b|N) = P(b)P(N|b)/P(N)

Centrality determination: multiplicity fit

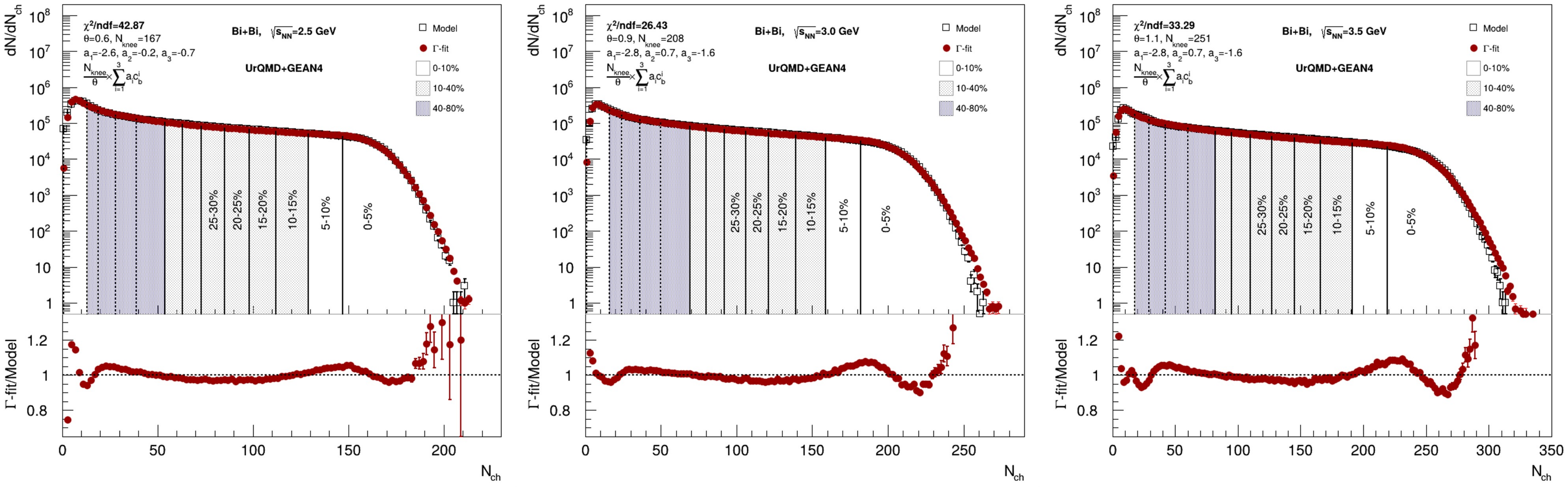

Cuts on tracks:

- Nhits>16
- $0 < \eta < 2$

Good agreement between fit and data

Multiplicity-based centrality determination (Γ-fit) was used

PID procedure

W. Blum, W. Riegler, L. Rolandi, Particle Detection with Drift Chambers (2nd ed.), Springer, Verlag (2008)

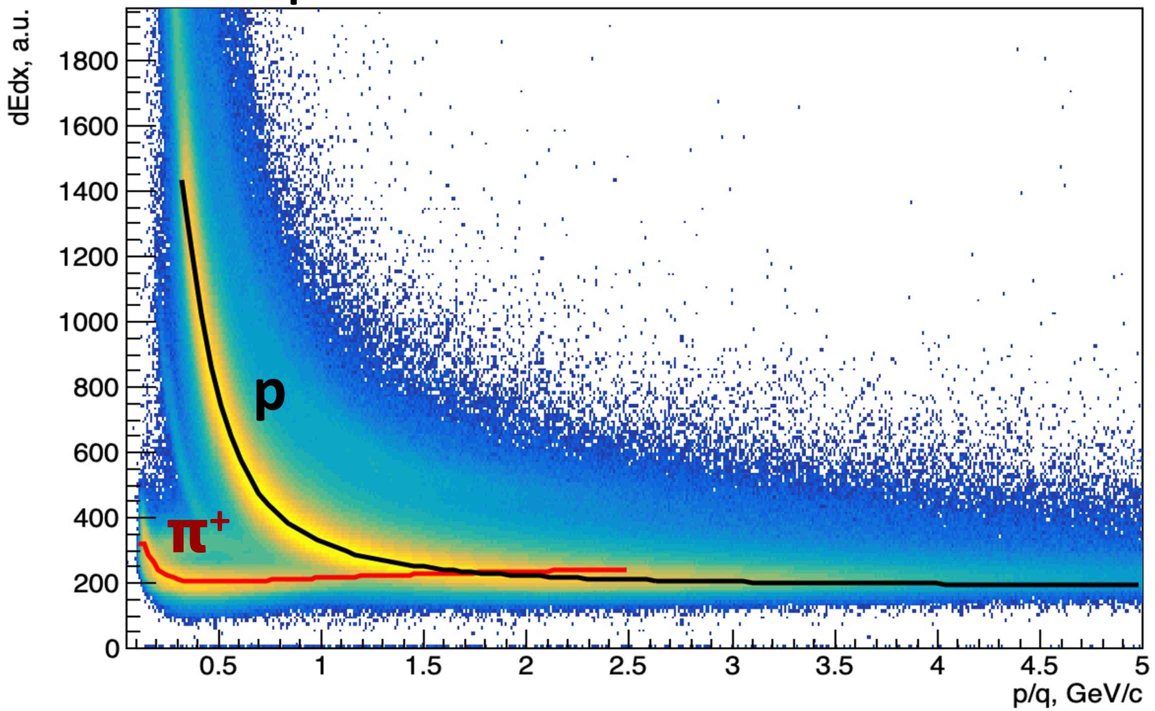

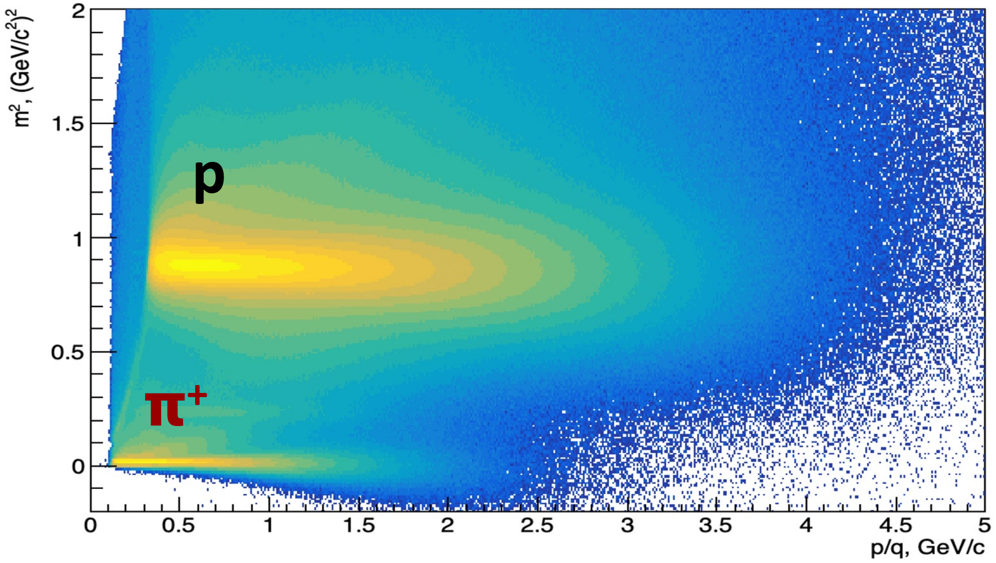

Fit dE/dx distributions with Bethe-Bloch parametrization:

$$f(\beta\gamma) = \frac{p_1}{\beta^{p_4}}\left(p_2 - \beta^{p_4} - \ln\left(p_3 + \frac{1}{(\beta\gamma)^{p_5}}\right)\right)$$

$$\beta^2 = \frac{p^2}{m^2+p^2}, \beta\gamma = \frac{p}{m}$$

p_i - fit parameters

Fit *(dE/dx - f(βγ))/f(βγ)* with gaus in the slices of p/q and get σ_p(dE/dx)

Fit m^2 with gaus in the slices of p/q and get $\sigma_p(m^2)$

(dE/dx,m)→(x,y) coordinates for PID:

$$x_p = \frac{(dE/dx)^{meas} - (dE/dx)_p^{fit}}{(dE/dx)_p^{fit}\sigma_p^{dE/dx}}, \ y_p = \frac{m^2 - m_p^2}{\sigma_p^{m^2}}$$

PID procedure: Results

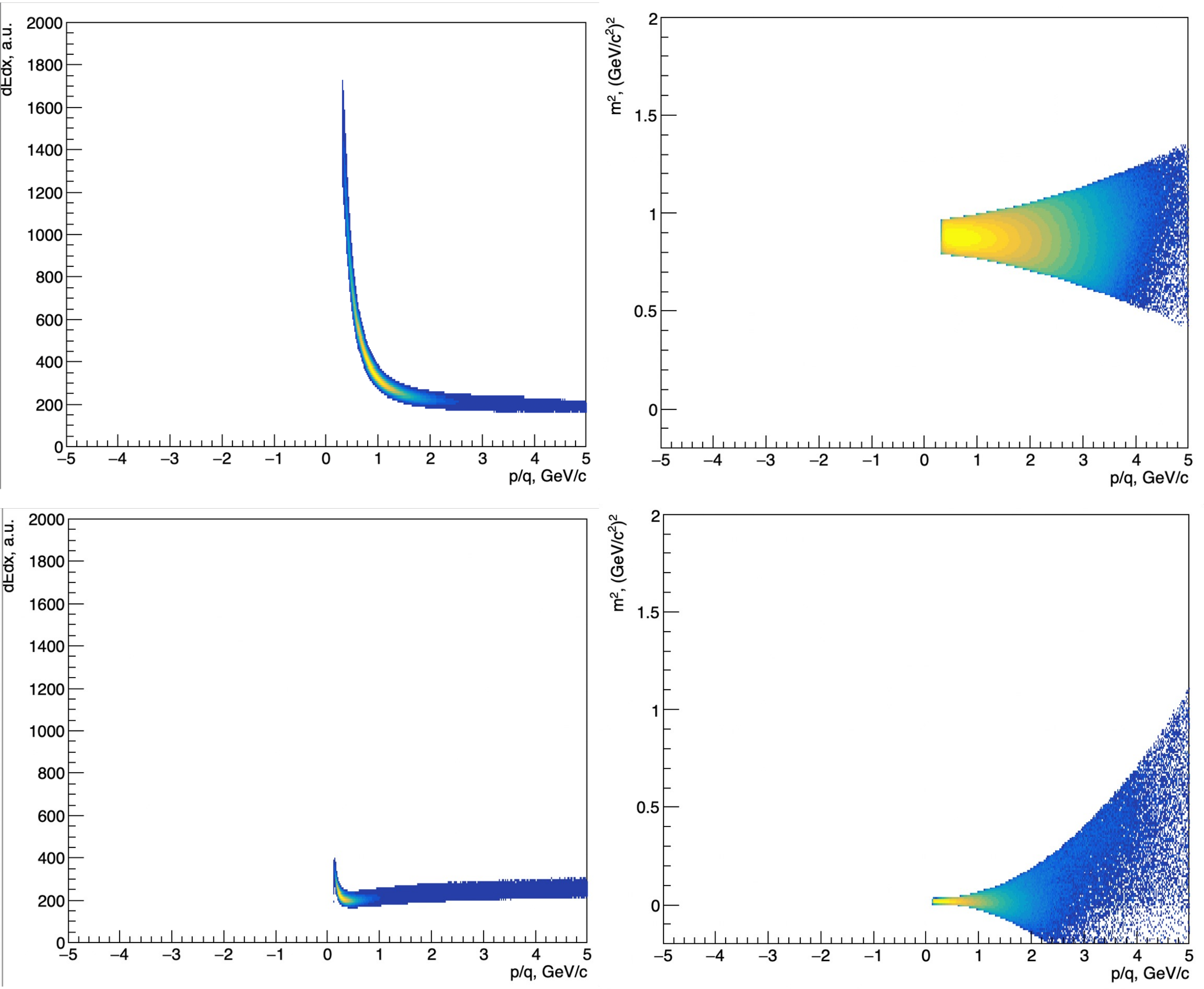

$$x_p = \frac{(dE/dx)^{meas} - (dE/dx)_p^{fit}}{(dE/dx)_p^{fit}\sigma_p^{dE/dx}}$$

$$y_p = \frac{m^2 - m_p^2}{\sigma_p^{m^2}}$$

Protons:

$$\sqrt{x_p^2 + y_p^2} < 2, \sqrt{x_\pi^2 + y_\pi^2} > 3$$

Pions (π^+):

$$\sqrt{x_\pi^2 + y_\pi^2} < 2, \sqrt{x_p^2 + y_p^2} > 3$$

Pions (π^-):

charge<0

(y-pt) distribution, efficiency and δpt

$$\text{eff} = \frac{\frac{dN}{dydp_T}(\text{reco})}{\frac{dN}{dydp_T}(\text{sim})}$$

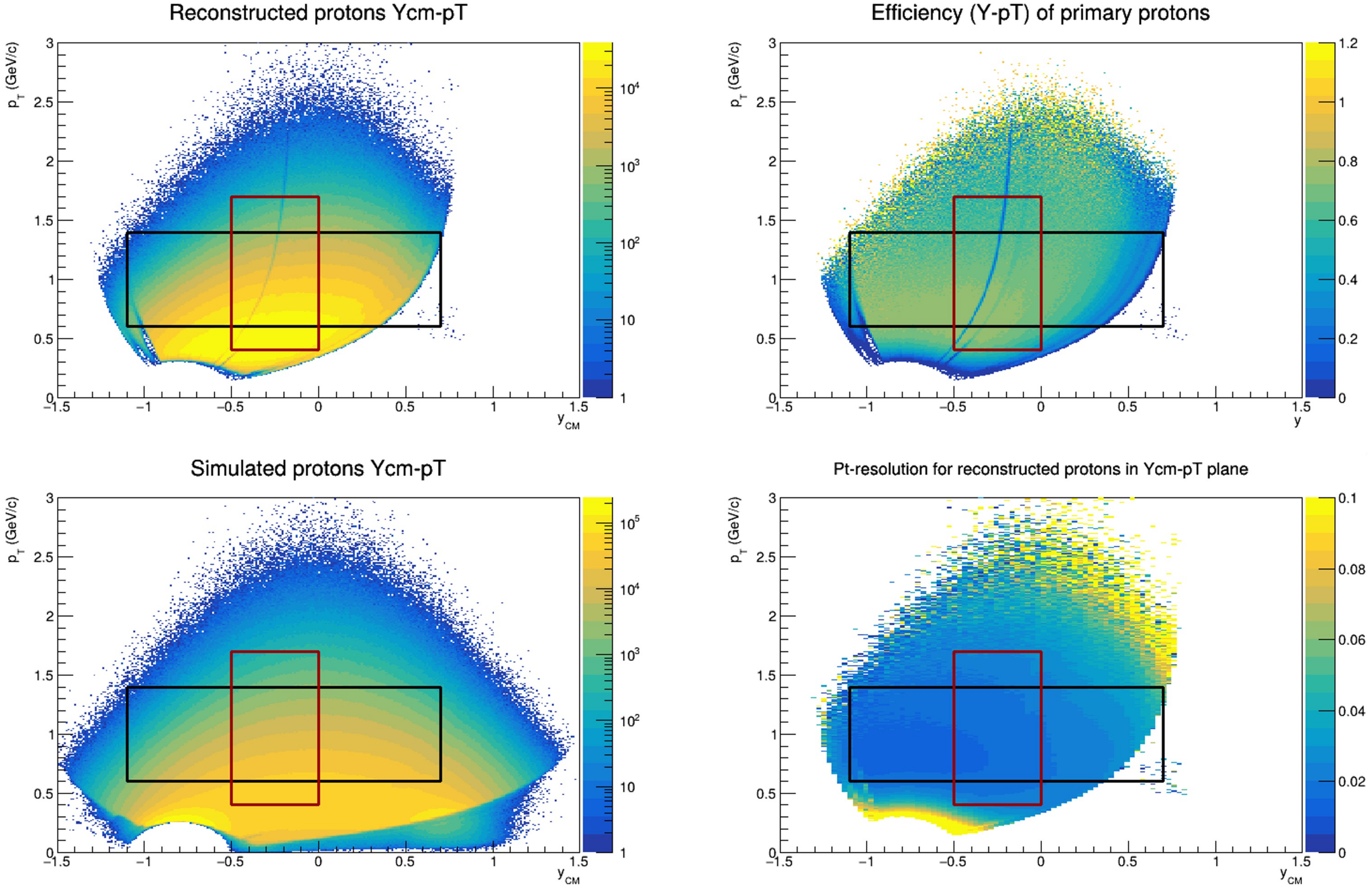

$$\Delta p_T = \frac{|p_T^{\text{reco}} - p_T^{\text{mc}}|}{p_T^{\text{mc}}}$$

Bi+Bi $\sqrt{s_{NN}}$=2.5 GeV

Cuts for reco tracks:

- Nhits>27
- DCA< 1 cm
- PID (TPC+TOF)
- Primary (DCA<1 cm

Cuts for sim particles:

- PID (pdg code)
- Primary (motherId)

Black box: acceptance window for $v_n(y)$

Red box: acceptance window

V0 selection: PFSimple

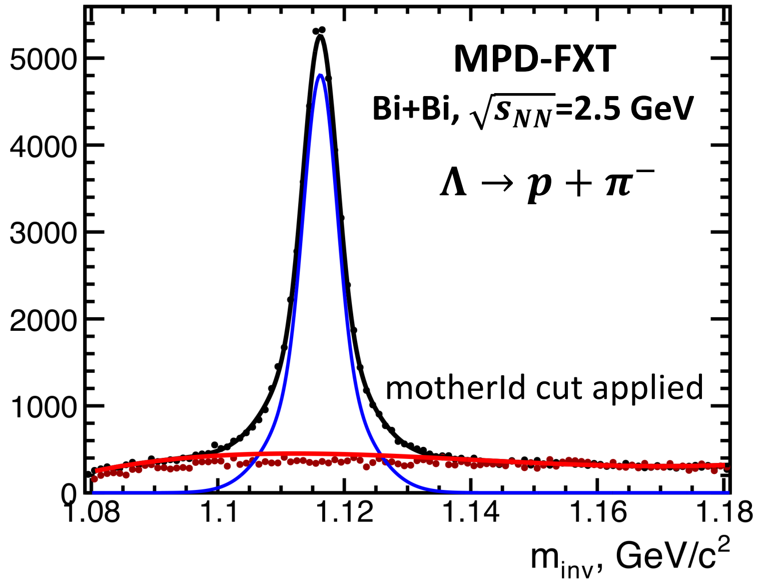

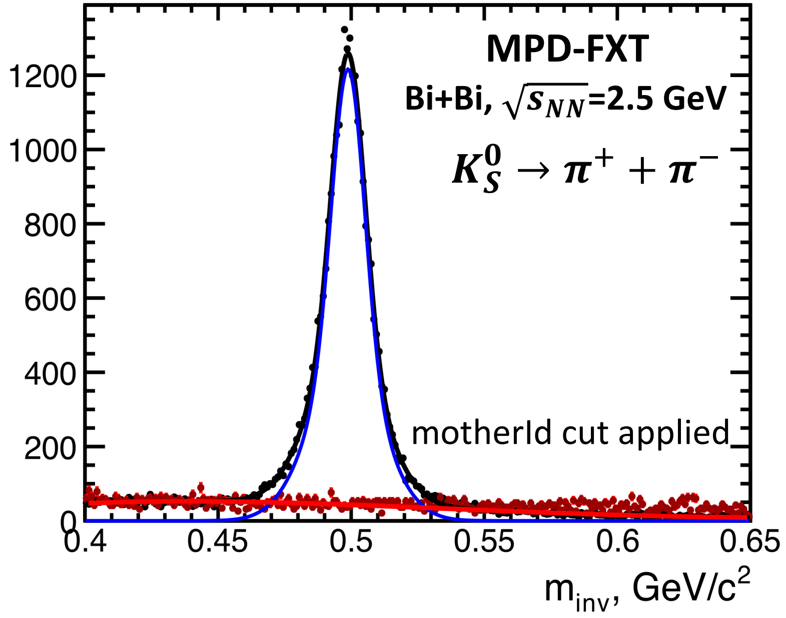

PFSimple: interface for the KFParticle package

KFParticle: package developed for complete reconstruction of short-lived particles

- Successfully used in many experiments
- Based on the Kalman filter mathematics
- Independent in the sense of experimental setup (collider, fixed target)

First tests for Λ, K_S^0 from the MPD-FXT production are ready:

- Basic topological cuts:

$$\chi^2_{topo} < 50, \chi^2_{geo} < 50, L > 3\ cm, \frac{L}{dL} > 5\ cm$$

- Signal extraction: sideband fits, rotation background were tested

PFSimple is already available as a module in the cvmfs

Flow measurements in MPD-CLD: evFlowEP wagon

Wagon #1 | Wagon #2 | Wagon #3

AnalysisManager → evCentrality → evPlane → evFlowEP → `Results`

AnalysisManager → `MpdAnalysisEvent event`

evCentrality → `event.getCentrTPC()`

evPlane → `Get event plane angles from FHCal/TPC`

Directed flow:

$$v_1 = \frac{<cos(\phi - \Psi_1^{EP})>}{Res(\Psi_1)}$$

Elliptic flow:

$$v_2(\Psi_2) = \frac{<cos[2(\phi - \Psi_2^{EP})]>}{Res(\Psi_2)} \qquad v_2(\Psi_1) = \frac{<cos[2(\phi - \Psi_{1,FHCal}^{EP})]>}{Res(\Psi_1)}$$

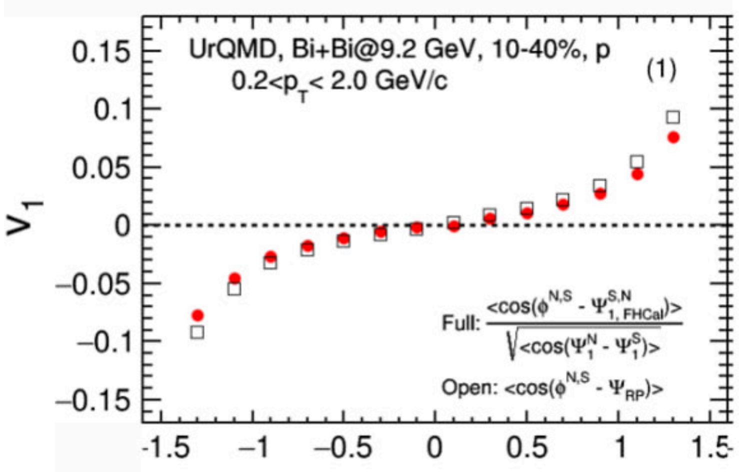

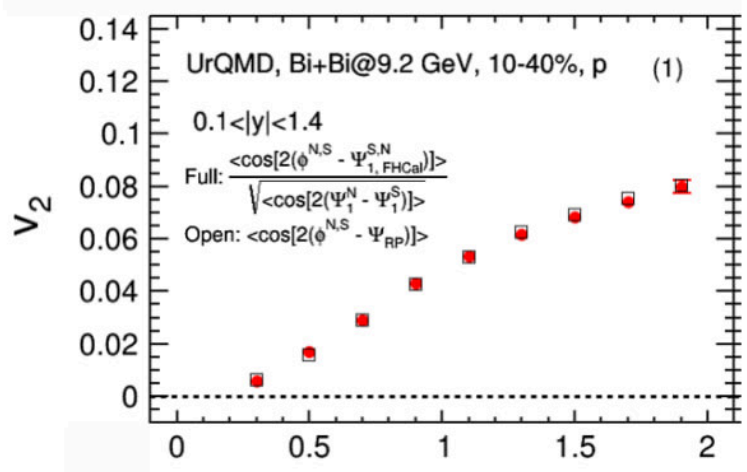

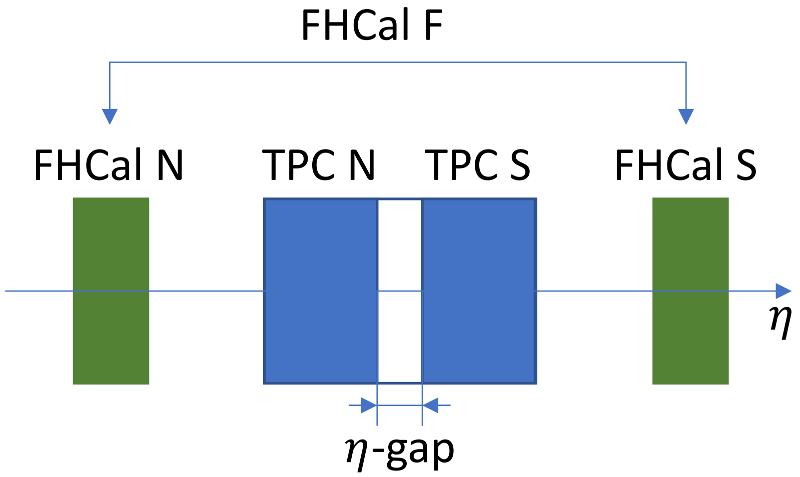

First results from the Xe run at BM@N

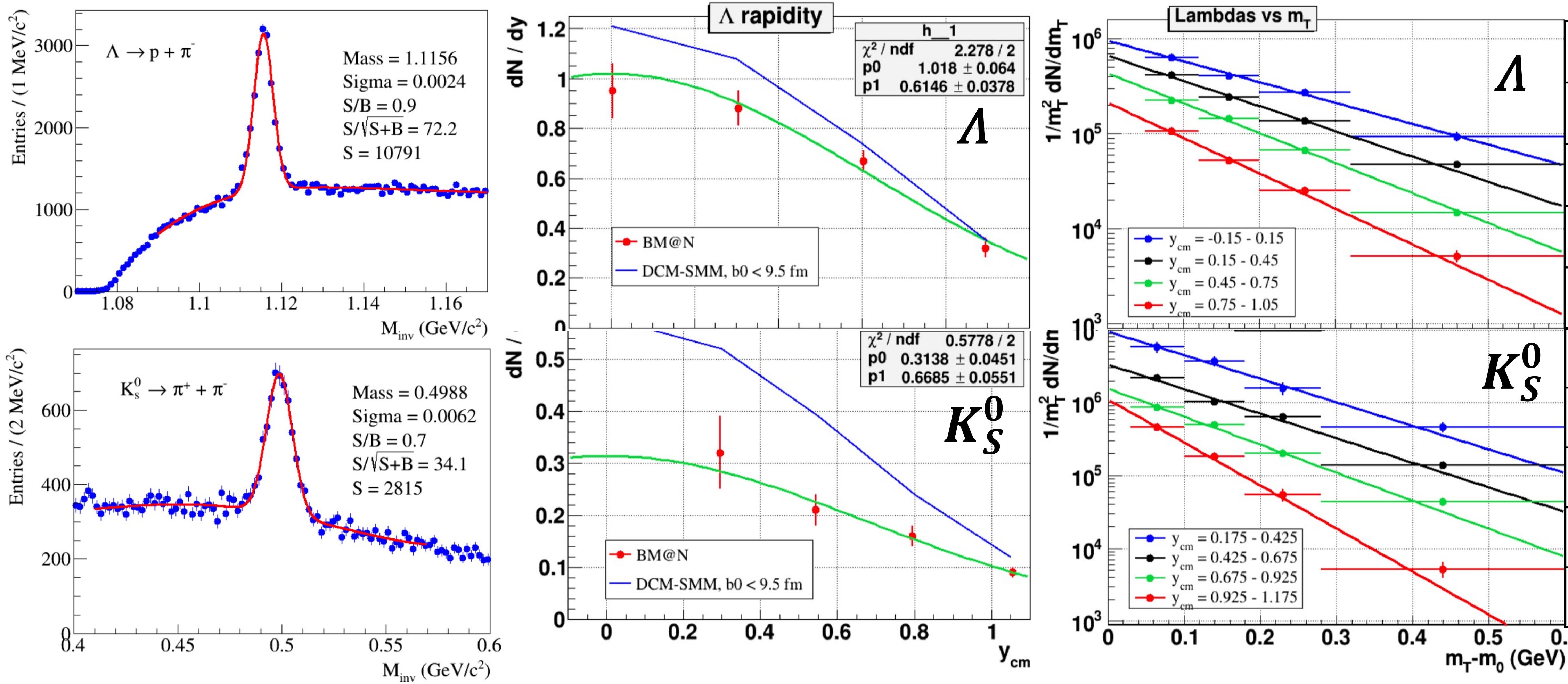

T_{eff}, MeV
198±12
164±7
138±4
117±6

T_{eff}, MeV
146±7
158±8
149±8
163±13

Procedure for Λ and K_S^0 measurements is implemented and tested – first results are ready

Next: analysis on the full statistics from the Xe run, anisotropic flow and global polarisation